1988

Coal Desulfurization Using Pyrite Conversion Through Dielectric Heating

Daniel C. Cleaveland

Eastern Illinois University

This research is a product of the graduate program in Chemistry at Eastern Illinois University. Find out more about the program.

THESIS REPRODUCTION CERTIFICATE

TO: Graduate Degree Candidates who have written formal theses.

SUBJECT: Permission to reproduce theses.

The University Library is receiving a number of requests from other institutions asking permission to reproduce dissertations for inclusion in their library holdings. Although no copyright laws are involved, we feel that professional courtesy demands that permission be obtained from the author before we allow theses to be copied.

Please sign one of the following statements:

Booth Library of Eastern Illinois University has my permission to lend my thesis to a reputable college or university for the purpose of copying it for inclusion in that institution's library or research holdings.

_2/29/88_____

Date   Author

I respectfully request Booth Library of Eastern Illinois University not allow my thesis be reproduced because _____ ____

_____

_____

_____   _____

Date   Author

m

COAL DESULFURIZATION USING PYRITE

CONVERSION THROUGH DIELECTRIC HEATING

<div align="center">(TITLE)</div>

<div align="center">BY</div>

<div align="center">Daniel C. Cleaveland</div>

THESIS

SUBMITTED IN PARTIAL FULFILLMENT OF THE REQUIREMENTS
FOR THE DEGREE OF

Master of Science in Chemistry

IN THE GRADUATE SCHOOL, EASTERN ILLINOIS UNIVERSITY
CHARLESTON, ILLINOIS

1988

<div align="center">YEAR</div>

I HEREBY RECOMMEND THIS THESIS BE ACCEPTED AS FULFILLING
THIS PART OF THE GRADUATE DEGREE CITED ABOVE

2/23/88

DATE

2/23/88

DATE

COAL DESULFURIZATION USING PYRITE CONVERSION

THROUGH DIELECTRIC HEATING

Thesis Approved

2/2 3/88

David H. Buchanan   Date

Feb 23, 1988

Jerry W. Ellis   Date

2-23-88

Giles L. Henderson   Date

2/23/88

Richard L. Keiter   Date

.   Thesis submitted to Eastern Illinois University for award of
Master of Science in Chemistry for research conducted, "Coal
Desulfurization using Pyrite Conversion Through Dielectric Heating",
by Daniel Cleaveland.

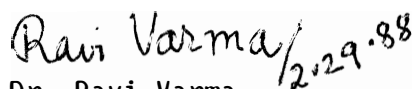Date Submitted February 23, 1988

Supervisers

Dr. David Buchanan

Dept. of Chemistry

Eastern Illinois University

Charleston, Ill

61920

Dr. Ravi Varma

Chemical Technology Div.

Argonne National Laboratory

Argonne, Ill

60439

Abstract

The Illinois State Geological Survey is currently developing a three step coal desulfurization process which depends upon the in-situ generation of catalytic troilite (FeS) by reduction of the pyrite (FeS_2) present in the mineral fraction of coal. After catalyst generation, ethanol is added to the system and is dehydrogenated to acetaldehyde and hydrogen which removes organic sulfur as hydrogen sulfide. The research reported in this thesis shows that the process can be improved by the use of dielectric heating in place of thermal heating for catalyst generation and perhaps organic sulfur removal. It is found that pyrite reduction takes place below 350°C at atmospheric pressure under a 10% carbon monoxide atmosphere. The same pyrite reduction can be produced thermally only by heating to 500°C. The lower operating temperatures possible with dielectric heating should improve the three-step desulfurization process by retaining important volatile compounds in the treated coal which are necessary for conventional combustion. XRD analysis of iron sulfides produced both thermally and by microwave heating in this project illustrate that the active catalyst is a form of pyrrhotite of general formula FeS designated pyrrhotite 2C or troilite.

Table of Contents

Introduction

Every day, coal is being burned as a source of energy and its use in the United States is increasing. With the United States possessing over half the total amount of coal in the non-communist world (1), refining coal as a power source is a worthwhile venture. Environmental problems, however, curtail the use of some coals which, upon combustion, produce such pollutants as sulfur dioxide (SO_2), nitrogen oxides (NO_x), particulates in excess, and organic compounds in low concentration (2). Particulates can be removed fairly easily by using baghouse filters or electrostatic precipitators (3). Sulfur dioxide and the nitrogen oxides, however, are more difficult to remove.

Sulfur dioxide and nitrogen oxides are major contributors to the formation of acid rain (4). Upon release to the atmosphere, the compounds become further oxidized, forming sulfates and nitrates which in turn precipitate as acid rain. Some researchers believe that the particulates given off by coal combustion act as a catalyst for this oxidation (5). In order to reduce these pollutants and conform to EPA regulations, many processes have been developed to remove sulfur before it is released into the atmosphere.

The most widely used process for removing sulfur is Flue Gas Desulfurization (FGD) or simply stack gas scrubbing, a post combustion process which involves removing the sulfur dioxide from the gases produced when coal is burned. A typical gas scrubber feeds the gases from combustion through a mist which contains calcium oxide in the form of calcined lime which is formed from calcium carbonate.

-1-

50%) (7,8,9,10) so many processes use thiophene as a test model. The inorganic sulfur is found in the mineral fraction of the coal as pyrite (FeS_2) and sulfates which can be removed physically. The sulfates, however, generally make up a small enough percent of the total sulfur amount that they are of no concern. One of the simplest methods for removing the pyritic sulfur is by exploiting its density. Pyritic sulfur has a specific gravity of 4.8 to 5.0 while the organic fraction of coal has a specific gravity of about 1.2 so most density separations take place around 1.8 in order to remove not only the pyritic sulfur but other minerals and clays of the mineral fraction as well. By mixing finely ground coal into a liquid of specific gravity 1.8 to 2.0, the mineral fraction of the coal will sink to the bottom while the organic fraction will float to the top. The organic fraction is collected off the top of the liquid and can be as much as 40% lower in sulfur than the untreated coal.
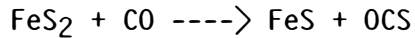
Other processes, such as tabling (11) and froth flotation (12), are similar to the float/sink technique. Tabling separates the coal fractions by using an oscillating rippled board to stimulate settling. Froth flotation, on the other hand, depends upon the hydrophobic nature of the organic fraction. By sending a fine stream of bubbles through the liquid, the hydrophobic organic fraction will adhere to the bubbles and be taken to the top while the hydrophilic mineral fraction will settle to the bottom. Other chemicals are generally added in order to help with the separation. Surfactants are introduced to help sustain the surface foam and make it easier to remove the organic fraction while other chemicals are added which will adhere to the mineral fraction and effectively weight it down to

-3-

promote the separation. On a newer frontier, scientists are investigating the use of microbiological organisms (13,14). These organisms, Thiobacillus ferrooxidans for example, catalyze the formation of elemental sulfur from pyritic sulfur in order to derive energy. Some work has been done to find organisms to reduce the amount of organic sulfur (15), however, contaminants already present in the coal may complicate the process. Magnetic properties are also used to separate coal fractions since the mineral fraction of coal has a slightly larger magnetic moment than does the organic fraction. By passing the coal through a magnetic gradient, the coal can be separated as the mineral fraction is retained in the magnetic field and the organic fraction passes straight through. Much research has gone into developing High Gradient Magnetic Separation (HGMS) for use in removing impurities from materials like coal (16,17), but the magnetic difference between the organic and the mineral fraction is small and magnetic separation can be difficult.
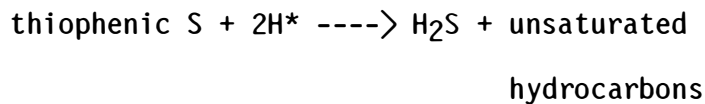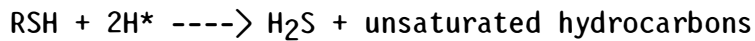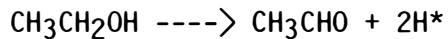
This research project is related to a proposed process which uses thermal energy and entails reaction with alcohol to remove both the pyritic and the organic sulfur from coal (18,19,20,21,22). The process proceeds in three steps. Step one: iron pyrite, found in the mineral fraction of coal, is converted to a form of pyrrhotite called troilite (FeS). This step not only reduces some of the pyritic sulfur but may generate a catalyst for the next step of the process. Step two: ethyl alcohol is added to the system and is dehydrogenated over the troilite to form acetaldehyde and hydrogen. In this second step, the hydrogen reacts with the thiophenic sulfur found in coal to form hydrogen sulfide. Step three: a small amount of oxygen converts some

of the troilite to iron oxides and magnetic Fe_7S_8 which are highly magnetic and can be easily removed using high gradient magnetic separation.
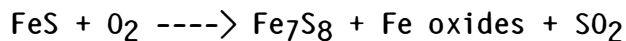
Step 1:

$$FeS_2 + CO ----> FeS + OCS$$

Step 2:

$$CH_3CH_2OH ----> CH_3CHO + 2H*$$

$$RSH + 2H* ----> H_2S + \text{unsaturated hydrocarbons}$$

$$\text{thiophenic S} + 2H* ----> H_2S + \text{unsaturated hydrocarbons}$$
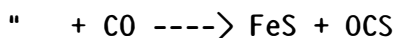
Step 3:

$$FeS + O_2 ----> Fe_7S_8 + \text{Fe oxides} + SO_2$$

The main portion of this research deals with step one, the conversion of pyrite, FeS_2, to troilite, FeS. Extensive research has gone into investigating the decomposition of pyrite (7,23,24,25,26) and the basic reduction occurs in two steps.

$$FeS_2 + CO ----> Fe_{(1-x)}S + OCS$$

$$Fe_{(1-x)}S + CO ----> FeS + OCS$$
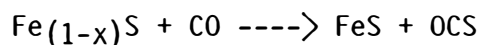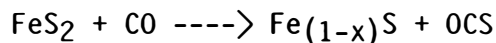
There are two parts to this process, the chemical reaction and the phase transformation. The chemical reaction is removal of sulfur from pyrite which can take place with either hydrogen (H_2), carbon monoxide (CO), carbon (C) or all by itself:

$FeS_2 + H_2 ----> FeS + H_2S$		Ref.
" $+ CO ----> FeS + OCS$		
" $+ C ----> Fe + CS_2$	Temp. $>1000°C$	(7)
$FeS_2 ----> Fe + S_2$	Temp. $550°$ to $600°C$	(7)

The hydrogen reaction is important above 500°C but takes place at lower temperatures, 250° to 300°C, when organics are present (7). The last two reactions play a very small role in the reduction of the pyrite. In order to better understand the reaction one should know the nature of pyritic sulfur.

Pyritic sulfur occurs in two forms. The least abundant form is marcasite (FeS_2), a hexagonal or rhombahedral form which is thermally unstable and usually found in meteorites. When heated to 400°C, marcasite will irreversibly convert to the most common form called pyrite (27). Pyrite has a face-centered cubic structure similar to a NaCl crystal with the iron atoms occupying the corners and faces of the crystals and the sulfur atoms forming a dumbbell shape between the irons (Fig. 1). Pyrite has a more compact form with a specific gravity of 5.0 as compared to that of marcasite at 4.8. Since the face centered form is so much more abundant, all FeS_2 forms in coal are called pyrite.
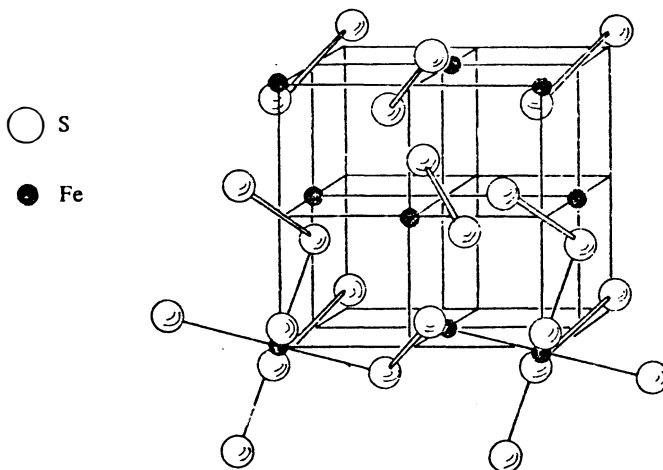

Figure 1: The crystal structure of Pyrite FeS_2 (ref. 36)

Pyrrhotite covers a far larger range of iron sulfides than does pyrite and has a general chemical formula of $Fe_{(1-x)}S$. Although some pyrrhotites are stable, this group is considered to be a solid solution of sulfur with a random placing of iron and vacancies. Research at the Illinois State Geological Survey (ISGS) has found that at 380°-420°C, under a hydrogen atmosphere (300 to 350 psig.), pyrite goes through three intermediates, Fe_7S_8, Fe_8S_9 and $Fe_{11}S_{12}$, before reaching a troilite state (FeS) (18,28) while if carbon monoxide is used, only one intermediate, $Fe_{11}S_{12}$, is formed. Since pyrrhotite is a non-stoichiometric solid solution, no definitive mechanism can be written. Decomposition of pyrite starts at about 325°C and finishes around 700°C. All pyrrhotites are catalogued by their iron-to-sulfur ratio and their crystalline structure since it is possible for one iron-to-sulfur ratio pyrrhotite to have more than one crystalline structure due to phase transitions. Some of the structures may be metastable and only exist at certain temperatures while others are stable below a characteristic temperature and are easily obtainable. The pyrrhotite notation shows major axis of the crystal plus iron-to-sulfur ratio. Since most pyrrhotites have a hexagonal shape similar to nickel arsenide (NiAs), the nomenclature used is based upon its cell dimensions. Using A,B and C for the cell dimensions of NiAs, troilite (FeS) has cell dimensions of a=1.73A, c=2C while the monoclinic pyrrhotite, Fe_7S_8, has cell dimensions a=2B, b=2A and c=4C. As one can see, the c axis not only describes a cell dimension but relates the general structure of the pyrrhotite as well. For pyrrhotites, $Fe_{(n-1)}S_n$ with $n \geq 8$, the number is n/2 for even n's and n for odd n's. Morimoto et al., concluded that, "The correspondence

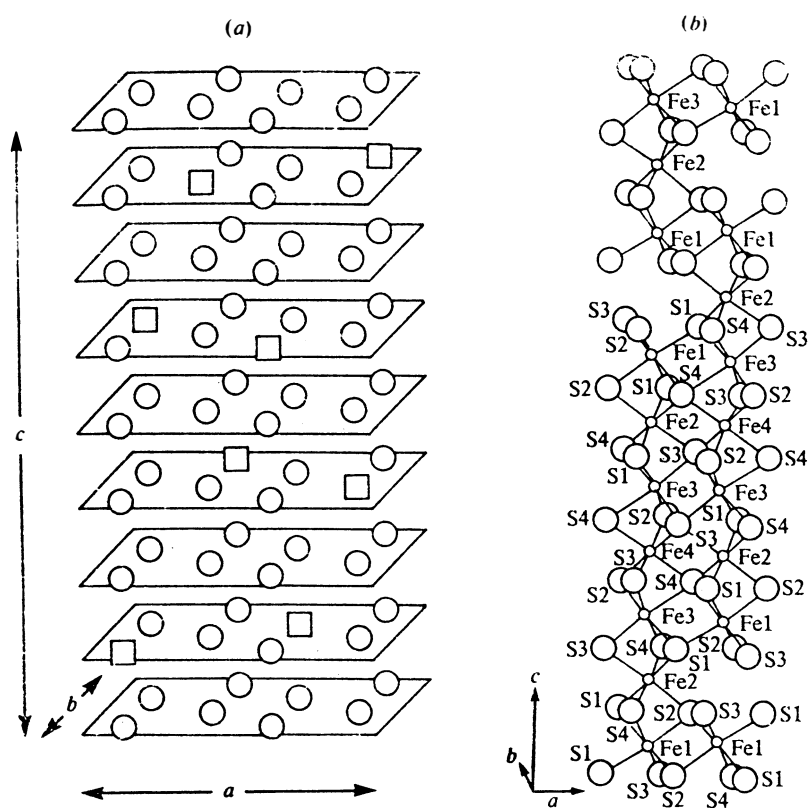| Name	Formula	Structure	Fe%	Ref.
Pyrite	FeS_2	cubic	33.33	
Pyrrhotite 4C	Fe_7S_8	monoclinic	46.67	29
Pyrrhotite 5C	Fe_9S_{10}	hexagonal	47.37	29
Pyrrhotite 11C	$Fe_{10}S_{11}$	orthorhombic	47.62	29
Pyrrhotite 6C	$Fe_{11}S_{12}$	hexagonal	47.83	29
Pyrrhotite 2C	FeS	hexagonal	50.00	29

Figure 2: The crystal structure of monoclinic pyrrhotite, Fe_7S_8. (a) ideal structure of iron atom layers proposed by Bertaut with squares showing vacancies. (b) refined structure by Tokonami (31). (ref. 36)

During the reaction, the iron sulfide undergoes crystalline changes which involve lattice rearrangement and phase transition. Phase transitions fall into two general categories, rapid and sluggish (32). Rapid transformations occur too fast to be controlled while sluggish transformations can be delayed and sometimes prevented by reducing such parameters as rate of heating or cooling. A more specific category would list transformations as first or second order. For a simple thermometric system, a first order transformation is characterized by a sudden jump in internal energy when the system reaches a certain temperature. A second order transformation shows a gradual change in internal energy as the temperature rises with a discontinuity in the slope of the energy curve (Fig. 3). Since some transformations for pyrrhotites are sluggish or second order, most intermediates are difficult to detect and synthesize. A basic synthetic procedure uses annealing for forming these intermediate pyrrhotites and involve long term heating and cooling. The general method is to mix iron and sulfur in an evacuated glass tube, heat it to a high temperature for a long period of time then slowly cool it to room temperature, sometimes holding it at some intermediate temperature. One research group (29) created their pyrrhotites by maintaining the mixture at 600°C for two months, cooling it to room temperature at 10°C/day, then storing it in a dessicator for one year at room temperature. Since the initial phase created may be metastable and composition depends upon regional iron to sulfur ratio, the room temperature pyrrhotite is sometimes a complex mixture of different stable forms.
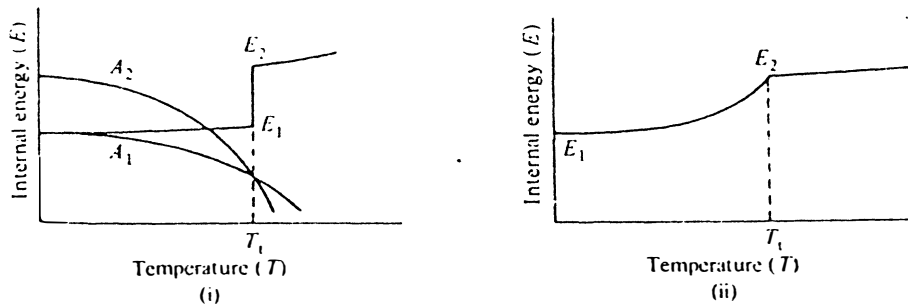
Figure 3: Change in internal energy for a (i) first order
phase transition and a (ii) second order phase
transition. (ref. 36)

Most transitions can take place by a twinning or cross-twinning
of the lattice. A popular theory for transitions has the structure go
from an ordered through a disordered to a reordered lattice. The
original structure becomes a mixture of unorganized atoms and as the
lattice starts to reorganize, the atoms will align themselves in a
planar fashion (Fig. 4). One experiment (33) in which marcasite was
heated in order to examine the sample for twinning found that
increased heating time increased the amount of twinning and where
twinning planes crossed, pyrite had formed. In this case, it is
surmised that the cross-twinning causes enough stress to bend the FeS_2
molecule and form the cubic structure. As one twinning plane orients
the sulfur in one direction the other plane orients the sulfur in the
other direction thus cancelling each other out. On a broader scale,
the molecules themselves may align in planes and cause mineral
intergrowths. Magnetite (Fe_3O_4) and Hematite (Fe_2O_3), for example,
exhibit oriented intergrowths which are due in part to similarities in
both composition and lattice structure (34) and this type of

intergrowth may explain the broad non-stochiometry of pyrrhotites. Upon cooling, a metastable form may start this twinning and intergrowth in order to reach a more stable structure thus forming a complex mixture of pyrrhotites in which some are iron-rich and others are iron-poor compared to the original form.
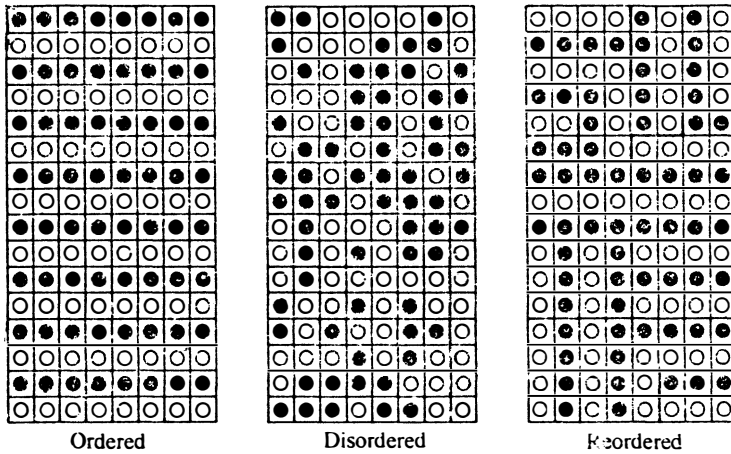

Figure 4: Transition due to twinning. (ref. 36)

The major difference between this research and the research done earlier on the process is the use of dielectric heating in place of thermal heating. There are three main reasons for using microwave energy in this process: cost, efficiency, and quality. Thermal heating depends upon conductivity of energy through the sample with the heat being absorbed on the surface of the sample and dissipated into the center. Owing to coal's insulating properties, heating in this fashion takes time and may not give uniform temperatures throughout the sample. On the other hand, dielectric heating heats the whole coal at once and should selectively heat the pyrite more than the coal. By selectively heating pyrite, it will take less time and energy to obtain the same results as with thermal heating plus, with

the organic fraction remaining at a lower temperature, more volatiles will remain in the product which will increase its heating capacity. The lower temperatures experienced by the organic fraction will also prevent caking and agglomeration of the coal which would hamper the process.

Dielectric heating in the microwave region involves rotational energy with molecules having dipole or induced dipole moments interacting with the electromagnetic radiation. As a gas, the molecules will rotate, trying to align themselves with the electrical field of the radiation. When the molecules are closer together as in a liquid, interference from other molecules makes it difficult to rotate and the interference starts to produce heat. If the molecules are locked into a solid matrix, rotation cannot take place but deformation can. The electrons of the molecules are bound to certain regions making the bonds between atoms and when exposed to the electromagnetic radiation, the electrons try to align themselves but can only go so far, deforming the bonds and molecular structure. Since each molecule interacts on its own, heating takes place uniformly throughout the matrix.

The main parameter for microwave or dielectric heating is the complex permitivity ϵ^*, which can be defined by the dielectric constant and the dielectric loss.

$$\epsilon^* = \epsilon' - i\epsilon''$$

where ϵ^* - complex permitivity

ϵ' - dielectric constant

ϵ'' - dielectric loss

When a condenser is placed in a static electric field, the condenser will become polarized and if the electric field starts to alternate,

the polarization of the condenser will also alternate. Ideally, the
polarization would follow the field but as the alternating frequency
increases, the condenser experiences a dampening effect which inhibits
total polarization. This dampening effect is due to absorption of
energy which is dissipated as heat. Vectorally, the charging current
due to polarization experienced by the material is ninety degrees out
of phase with the electric field while the loss current from the
dampening effect is in phase with the electric field. The total
induced current in the condenser can be represented as a combination
of the charging current and the loss current (Fig. 5). Both the
charging current and the loss current are characterized by the
dielectric constant (ϵ') and the dielectric loss (ϵ'') parameters. The
dielectric constant is a measure of the amount of energy stored by the
sample and the dielectric loss is a measure of the amount of energy
lost through heat. So, when looking at the different characteristics
of materials, it is the dielectric loss which will determine which
material will heat more than others.

It is the large value for the dielectric loss parameter, ϵ'', for
the pyrite which causes the pyrite to be heated more than the organic
coal fraction. In measuring the dielectric loss of pyrite, coal, and
coal fractions at different frequencies, Bluhm (35) found that pyrite
has a higher loss factor overall (Fig. 6). In selectively heating
coal, a lower frequency should be used for low sulfur content coals
and a higher frequency for high sulfur content coals. With the
separate coal fractions, the heavier (mineral) fraction has a higher
dielectric loss factor at higher frequencies than does the lighter
(organic) fraction (Fig. 7).

-14-
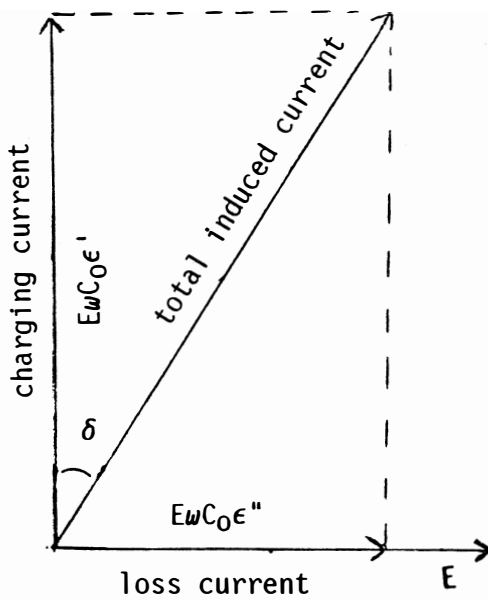
where

E = Electric field

ω = frequency

C_0 = capacitance for an ideal geometric condenser

ϵ' = static dielectric constant

ϵ'' = dielectric loss

δ = loss angle

(The charging or capacitive current, $E\omega C_0\epsilon'$, is 90° out of phase with the alternating electric field in a condenser. If absorptive polarization occurs (i.e. in cases of large molecules, polymers or solids), the current will aquire a new component, $E\omega C_0\epsilon''$, which is in phase with electric field. This latter ohmic or loss current results in energy loss as heat. The dielectric constant and dielectric are commonly show as a ratio characterized by the loss angle δ.)

$$\tan\delta = \epsilon''/\epsilon'$$

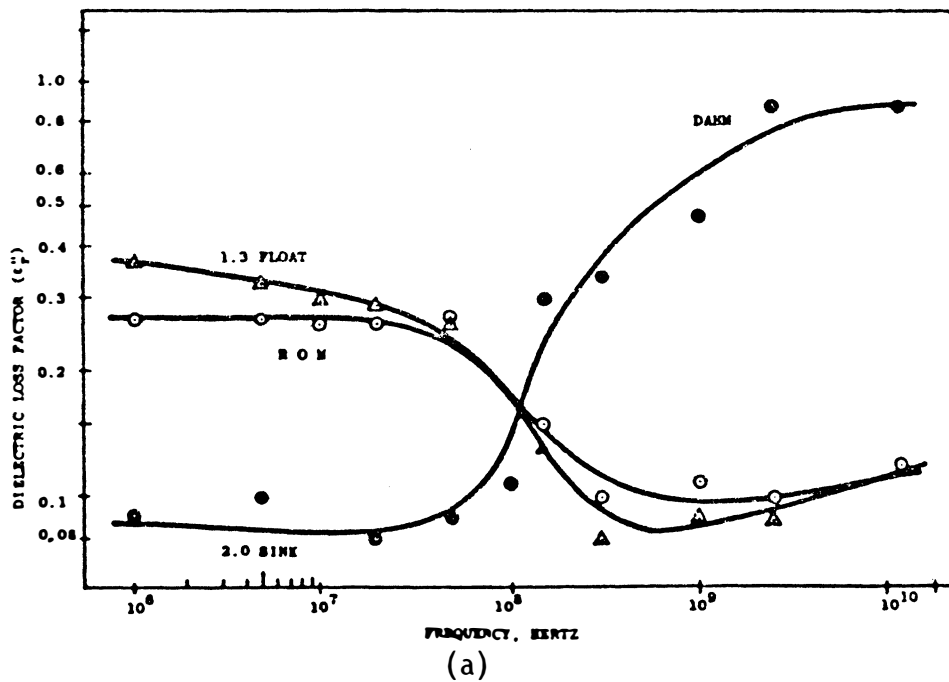Figure 5: Vector representation of dielectric heating
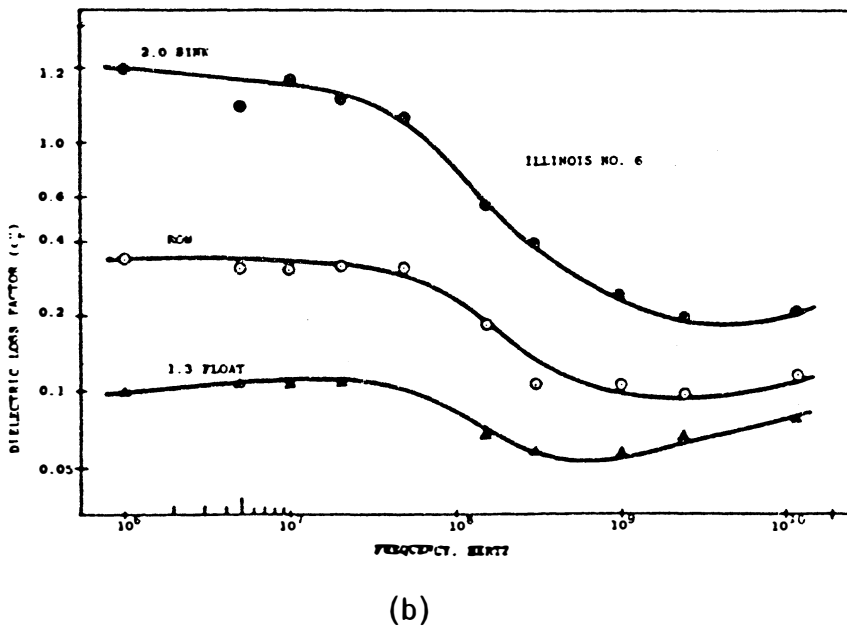
Figure 7: Dielectric loss v.s. frequency for

   (a) Dahm coal (Iowa)

   (b) Illinois #6 coal   (ref. 35)

being promoted to the e_g energy level thermally due to bond deformation and then further heating occurring due to conduction. Although the electrons still are not in the conduction band, they are closer and the possibility of creating a leak current due to polarization is higher. One can picture the Fermi level being at or near the top of each atom's potential well so that electrons located above the Fermi level have a small energy barrier to overcome in order to reach a neighboring atom. Jean-Charles Giuntini et al., in characterizing coals by their complex permitivity, found that coal was polarized in an alternating electric field which shows the existence of charge carrier hops between microdomains (37). In this case, the electrons would not be going from one neighboring iron to the next but from one region to the next (ie. between microcrystallites or grains). A perfect crystal would have difficulty in conducting since the lattice is stable and the electrons would not experience any force to promote movement, for example, being attracted to a positively charged region. Since the pyrite is part of a heterogeneous mixture, imperfections are easily formed. Some of the pyrite may be in the form of marcasite or there could be inclusions within the lattice. Also, if two solids are in intimate contact with each other and the Fermi levels do not match, electrons will flow from the higher level lattice to the other lattice until the levels are equal (38). Once pyrite starts to convert to pyrrhotite, the lattice forms vacancies and contains both Fe^{2+} and Fe^{3+} atoms which help to induce charge movement.

Other research projects have also used microwave radiation for desulfurizing coal. The main purpose in these projects, however, was

to reduce the pyrite to a more magnetic form of pyrrhotite in order to improve separation via HGMS. Both Bluhm (35) and Zavitanos (40) were able to reduce a part of the pyrite to some form of pyrrhotite and improve magnetic separation. Zavitanos then investigated including sodium hydroxide solution in conjunction with the process to further reduce pyritic and organic sulfur and ash. Later, Bluhm also incorporated sodium hydroxide into the process with some success.

Dielectric heating has also been tried with oil shale (41) with the goal of developing a process for underground oil recovery. The samples used were based upon earlier dielectric property research which showed consistent trends for other western U.S. oil shale (42). The latter research shows that while microwave radiation is applicable for above ground heating, radio frequencies are best for underground heating. Using this microwave heating process, the group was able to extract an average oil yield of 90.6% based on the Fischer assay of the New Brunswick oil shale used (41).

The purpose of this research was to investigate and identify the phase transitions of the iron pyrite and to duplicate the transitions using dielectric heating. The research would involve characterizing pyrite and 1.8 sp gr coal fractions using differential thermal/thermogravimetric analysis (DTA/TGA) and x-ray diffraction analysis (XRD). The DTA/TGA instrument was also used for heating at desired temperatures in order to prepare representative thermally heated samples. A microwave system operating at 2.45 GHz with the capability of producing 6 Kw of power was used to heat the coal fractions to different temperatures under different atmospheres with gas samples taken during the runs and XRD analysis of the bed after

the runs in order to see what reactions may be occurring and what
phases were formed. Attempts were made to produce troilite with the
microwave system followed by preliminary tests involving ethanol
dehydrogenation. Three main differences between the research
performed at the Illinois State Geological Survey and this research
were the use of dielectric heating in place of thermal heating, a
flowing atmosphere instead of a static flow or simulated flow system
and all runs being performed at atmospheric pressure instead of 300 to
500 psig. This research will show whether dielectric heating is an
improved method for this process of coal desulfurization.

Experimental

Coal Preparation

Eagle #2, an Illinois #5 coal provided by the Illinois State Geological Survey (ISGS), was used through most of the experiment. The coal was crushed and sieved to 45x60 mesh then stored under argon. At Argonne, the coal was turned and split into two portions and each portion was turned and split into two portions. All four portions were then stored under nitrogen and labeled.

A fractioned sample of a table concentrate of Ill #5 coals, +1.8 sp gr and -1.8 sp gr, was also provided by the Illinois Geological Survey. The coal was separated by mixing it in a solution of bromoform and petroleum ether of density 1.8. The fractions were then washed with petroleum ether, bottled and mailed to the laboratory. While Eagle #2 is a specific coal, the table concentrate is a mixture of Ill #5 coals and will be refered to as Ill #5.

Fraction Separation

1.6 float/sink fraction

Approximately 125 g of Eagle #2 coal was mixed into 600 mL of carbon tetrachloride (sp gr 1.59) and allowed to settle. The floating fraction of coal was removed with a homemade sieve and stirred into a beaker of acetone. As the floating fraction is removed, fresh coal is added for separation and the floating fraction is added to the previously collected fraction in the acetone. After standing for 1/2 hour, the acetone was decanted and replaced with fresh acetone. Acetone washings were repeated a total of three times. The process

was repeated using a solution of acetone:water (1:1 ratio) for a total of three times and again with water for three times. The float fraction was then filtered through a Whatman #41 filter using vacuum. The sink fraction was filtered through a Whatman #41 filter and the used carbon tetrachloride collected for later separations. The sink fraction was washed in the same manner as the float fraction using acetone, 1:1 acetone:water, then water. The sink fraction was then vacuum filtered through a Whatman #41 filter. If either fraction still smelled of acetone the washing process was repeated with 1:1 acetone:water then water until the solvent odor was absent. The fractions were spread out in separate drying dishes and placed in a nitrogen purged oven set at about 70°C for two hours. The dried fractions were placed in labeled bottles and stored under nitrogen.

1.8 float/sink fraction

The 1.6 sink fraction from the previous separation was mixed with 600 mL of a bromoform/hexane solution (adjusted sp gr 1.8) and allowed to settle. The float fraction was removed with a homemade sieve and thoroughly washed with consecutive washings of acetone, acetone:water (1:1 ratio), and water. The sink fraction was filtered and the bromoform/hexane solution collected for later separations. The sink fraction was washed with acetone, acetone:water, and water. Both fractions were spread out in separate drying dishes and dried in a nitrogen purged oven set at about 70°C. All acetone and acetone:water washings were collected for disposal. All solutions used in separation were checked with hydrometers for specific gravity and adjusted to the desired density.

DTA/TGA runs

A Rigaku DTA/TGA instrument with dual cup probe was used for all
runs (Fig. 9). After the instrument and water cooling system had
equilibrated for 1/2 hr, 50 mg of the sample is placed in the platinum
sample cup with 50 mg of aluminum oxide in the reference cup and the
system is closed. The system is then evacuated to about 15 mm Hg
(abs.) and argon is bled back into the system until the pressure in
the system is slightly geater than atmospheric. This purging process
is repeated a total of three times. After purging, the flowing
atmosphere in the system is adjusted for a 90% argon/10% carbon
monoxide mixture at 170 mm/min. The TGA sensitivity, DTA range,
heating rate and temperature range are selected with trip switches set
to limit the temperatures for the run. The run is then started and
allowed to go to completion. When the run ends (the trip switch
turning off the furnace), the atmosphere is changed to argon, the
recording components are turned back on to follow cooling of the
system and a fan is used to increase the furnace cooling rate. Once
the furnace is back to room temperature, the instrument is turned off
and the sample is placed in a vial and stored under nitrogen.
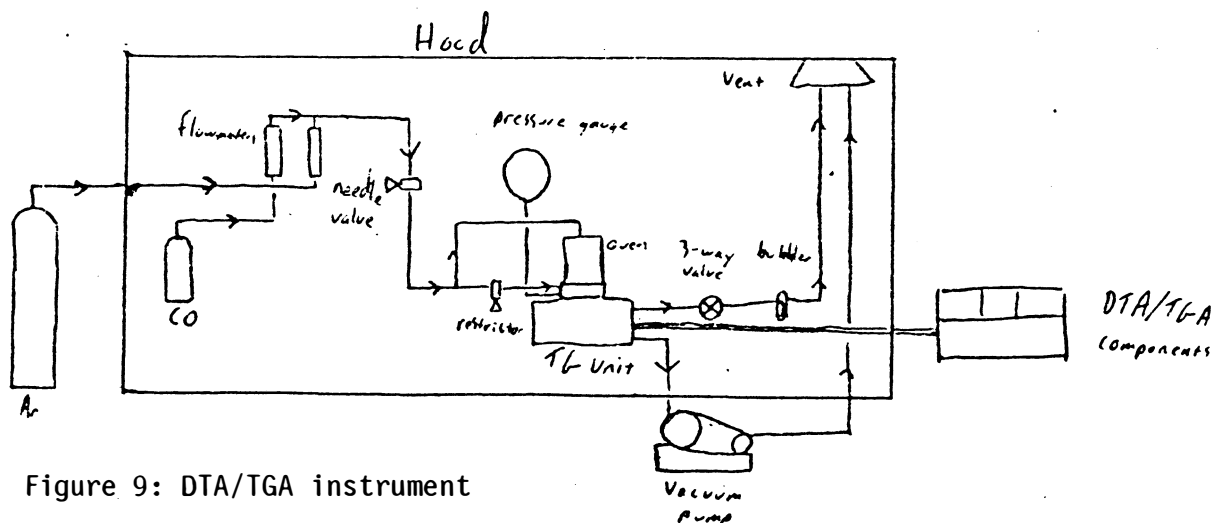
Figure 9: DTA/TGA instrument

Prepared samples from the DTA/TGA instrument

After the sample has been placed in the instrument and the
purging process has been completed, the sample is heated to the
desired temperature at 10K/min. Once the furnace is close to
temperature, the instrument is set to a steady state mode and the
temperature is manually adjusted to the desired temperature. The
temperature is maintained for one half to one hour or until the DTA
reading is constant. The instrument is then cooled down, shut off and
the sample is placed in a vial under nitrogen.

Microwave Heating

The microwave system used consists of a Colber Electronics S6F
microwave generator capable of producing adjustable power up to 6 kW
at 2.45 GHz. The cavity is equipped with two sets of entry sleeves,
two side ports and a hinged door with a choke screen/glass window
(Fig.10). A reactor tube (23mm inside diameter) of fused quartz was
designed in three parts for easy installation in the cavity, the
center part having a glass frit pinched in the tube for supporting the
sample which is located in the tube such that when the reactor tube is
in position, the side port used for temperature readings (via ir
sensor) would be looking at the center of a six inch bed of reaction
material. The bed itself consisted of a layer of activated alumina
followed by a glass wool plug then the reaction material (Fig. 11).
Once the bed is prepared in the central portion, the reaction tube is
assembled in the microwave cavity with the ends coming through one set
of entry sleeves. Using Tygon tubing inside the hood, the gas flow
system goes from the gas cylinder, through a flowmeter to the bottom

-25-

of the reactor tube. From the top of the reactor tube, the gas flows through a small cold finger trap being used as a deentrainer, to a single arm Erlenmeyer flask for catching tars and oils, then through a gas sampling tube, a water bubbler and to the vent (Fig. 12). With the flow system intact, the flowrate is measured by connecting a wet test meter to the last bubbler and using a nitrogen flow. The bubbler is then reconnected to the vent and the atmosphere changed if necessary. The switching of atmospheres is done by closing a valve to the nitrogen cylinder and opening a valve to the carbon monoxide cylinder without adjusting the flowmeter. The pressure in the regulators of both cylinders is adjusted to 20 psig. The valve system is designed to send the gas to either the small or the large microwave setups, with the ability to purge the lines with nitrogen after carbon monoxide runs. If ethanol is to be used in the runs, a gas cleaning bottle with barrel frit is filled with ethanol and placed in the flow system after the flowmeter. A single arm Erlenmeyer flask partially filled with glass wool is placed between the ethanol bubbler and the bottom of the reaction tube in order to catch any ethanol mist. Once the flow is established, the microwave radiation is started at some preset power level. As the temperature of the bed becomes apparent, the power level is adjusted for the desired temperature. After the bed has equilibrated for five minutes at the desired temperature, the temperature is maintained for one half hour after which the power is turned off and five minutes later, the system purged with nitrogen while the bed cools to room temperature. The bed is then removed and bottled under nitrogen. Gas samples are taken throughout the run.

Sample Analysis

Solid samples were sent to the Illinois Geological Survey for X-ray diffraction analysis. Gas samples were sent to the chemistry division of Argonne National Laboratory for mass spectroscopic analysis.
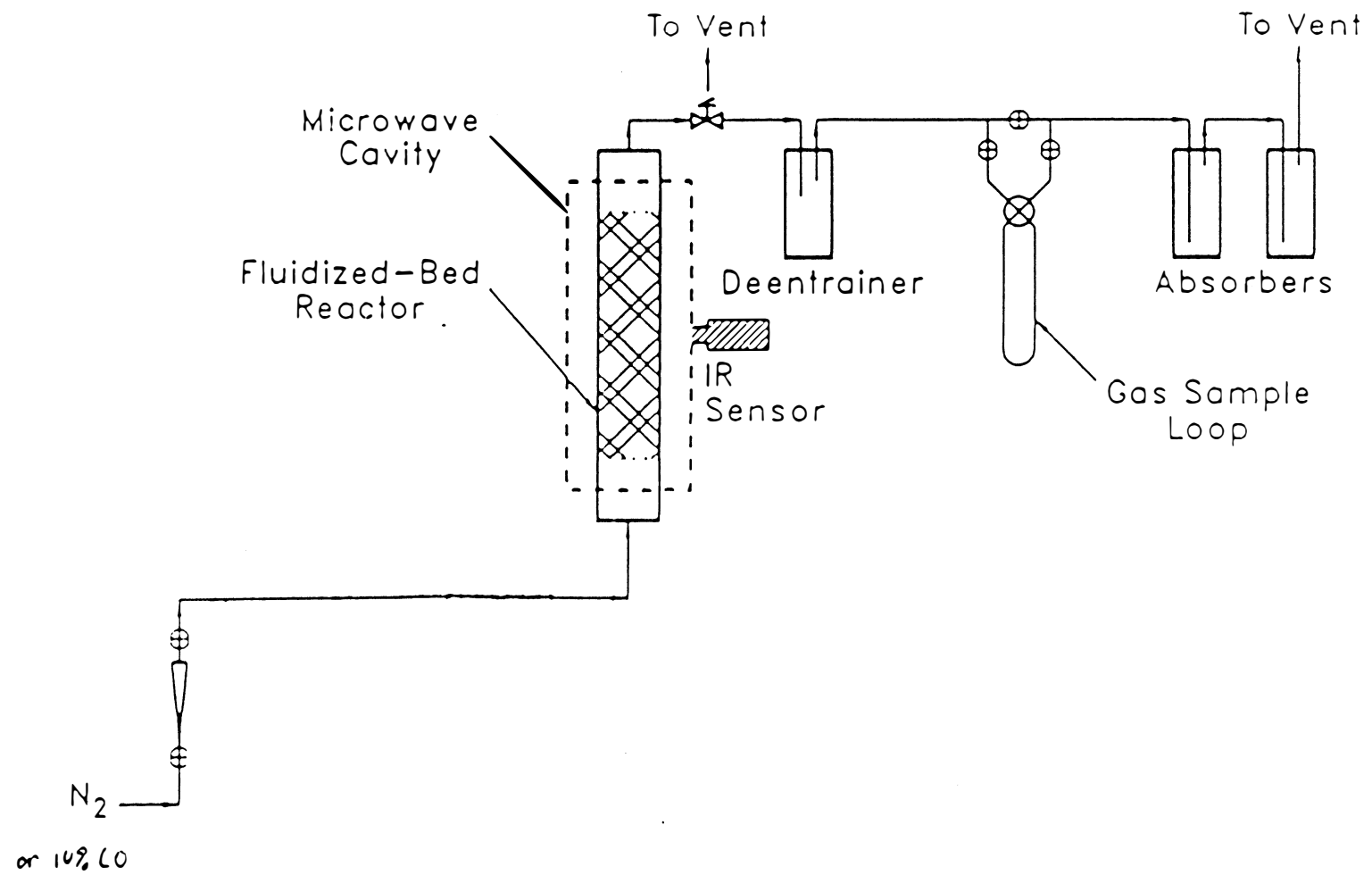
MICROWAVE HEATING ASSEMBLY
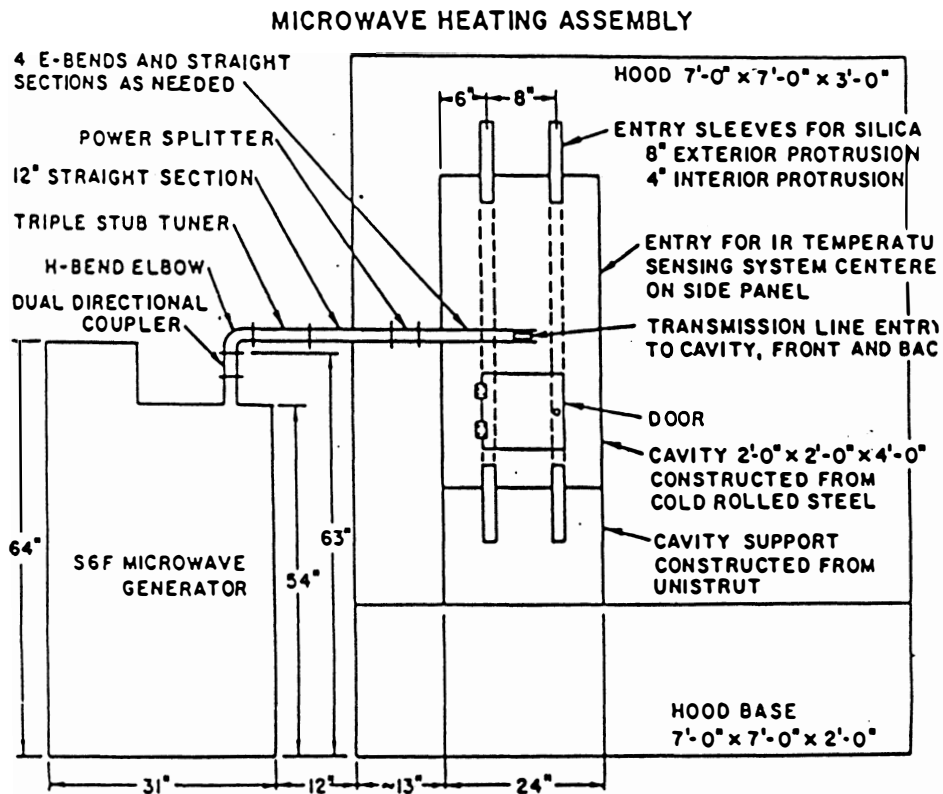
Figure 10: Microwave system

top

standard fitting

coal fraction

flow

glass wool

activated alumina

glass frit

standard fitting

bottom
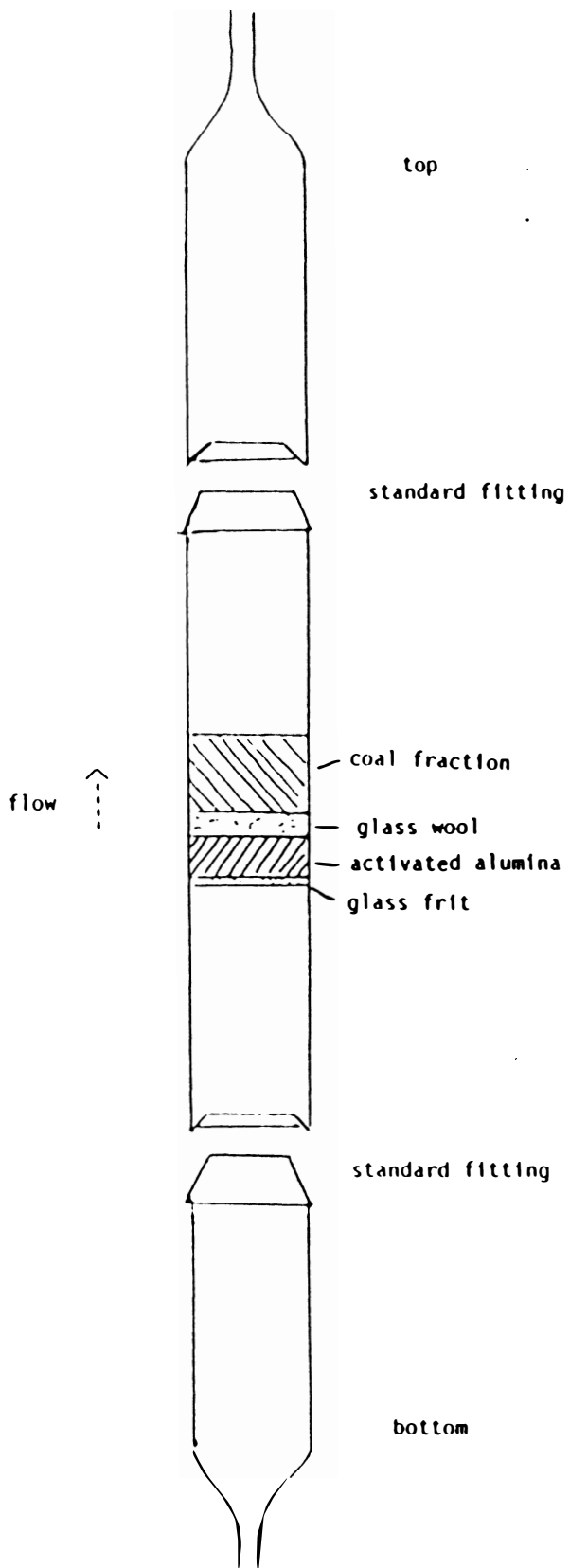
Figure 11: Reactor tube with sample bed

Microwave
Cavity

Fluidized-Bed
Reactor

IR
Sensor

To Vent

Deentrainer

Gas Sample
Loop

To Vent

Absorbers

N_2

or 10% CO

SCHEMATIC DIAGRAM OF THE MICROWAVE REACTOR SETUP

Results and Discussion

X-ray Diffraction Analysis

A list of characteristic peak locations for some common minerals found in coal is given in Table 1 with a list of the different experimental runs and pyrrhotites formed in Table 2. References made throughout this section to the different pyrrhotites formed are based upon this XRD data. Peak areas are calculated by multiplying the peak height by the width at one half the peak height then, if applicable, dividing by the peak area of a quartz peak being used as an internal standard. Tentative conclusions can be made towards pyrite conversions and concentrations of minerals. The use of an internal standard helps to reduce problems arising from crystal orientation. Calcium carbonate, for example, may align itself in layers because it cleaves very cleanly making sheets which will lie on the stage used for XRD analysis giving a preferred orientation thus a stronger peak intensity.

Differential Thermal (DTA) and Thermogravimetric (TGA)
Analysis (Table 4)

From the research done by O'Gorman et al. (23), the derivative thermogravimetric analysis (DTGA) of pyrite under nitrogen atmosphere at 10K/min shows decomposition occurring in two steps, reduction to pyrrhotite $Fe_{1-x}S$ followed by further reduction to troilite FeS. The DTG curve shows two peaks at 525°C and 650°C not readily seen in the weight loss (fig.13). A review by Attar (7) reports for pyrite under vacuum three small endothermic peaks at 320°-350°C, 500°-540°C and

560°-600°C with a deep endothermic peak at 700°C. The pyrite was
converted to FeS_{2-x} (0.1 < x < 0.3) at 350°C with troilite being
formed at 640°-670°C. In comparison, run DP-9 shows two distinct
peaks at 528°C and 672°C which correspond to the 525°C, 650°C peaks of
O'Gorman and the small 500°-540°C and deep 700°C peak from Attar's
review. The deep endothermic peak is present in all pyrite DTA runs
which reach that high a temperature. Runs DP-5 and DP-8, in which
pyrite samples were heated to 606°C for 400 min and 594°C for 317.5
min, respectively, both produced Fe_9S_{10} (5C) with the same weight loss
of 23.6%. Runs DP-9 and DP-10 in which pyrite samples were heated to
1000°C at 10K/min, show the same DTA peaks and approximately the same
weight loss, 25.2% and 25.8%. With the reproducability of the runs
and the agreement between published DTA findings and runs of
comparable heating rates, it is shown that the DTA/TGA instrument will
produce adequate examples of thermally treated samples.
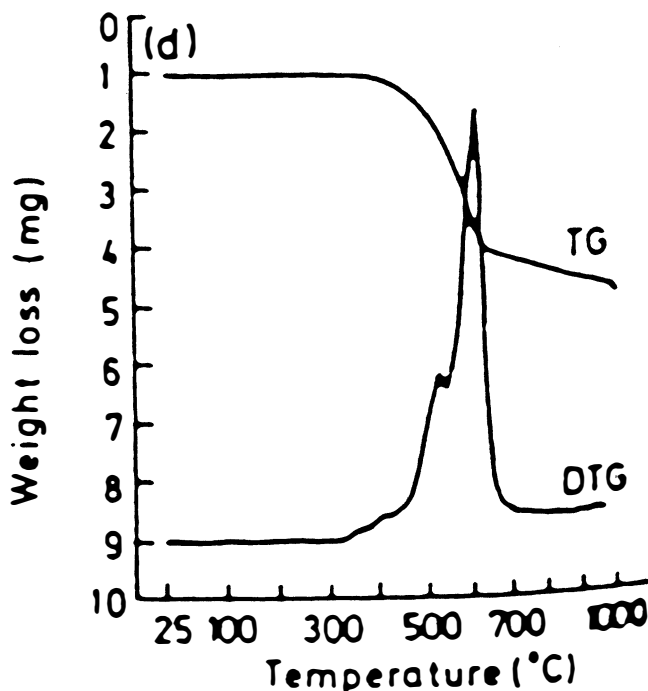
Figure 13: DTA/TGA of Pyrite (ref. 23)

The 1.8 sp gr fractions from Eagle #2 and Ill #5 coals do not show such well defined peaks as the pyrite runs but are quite similar in appearance to each other. Both show a very broad endothermic peak at 230°-560°C, followed by a broad exothermic peak (700°C for Ill #5 and 744°C for Eagle #2) and ending with a small exothermic peak (915°C for Ill #5 and 950°C for Eagle #2). The only distinctive peak between the two samples is an endothermic peak showing up in the Eagle #2 run at 150°C (fig. 14). This peak is the dehydration of gypsum ($CaSO_4*2H_2O$) to bassinite ($CaSO_4*1/2H_2O$). XRD analysis of the Eagle #2 fraction shows little or no bassinite in an untreated sample but definite bassinite formation with a slight increase in anhydrite ($CaSO_4$) after heating to 246°C.
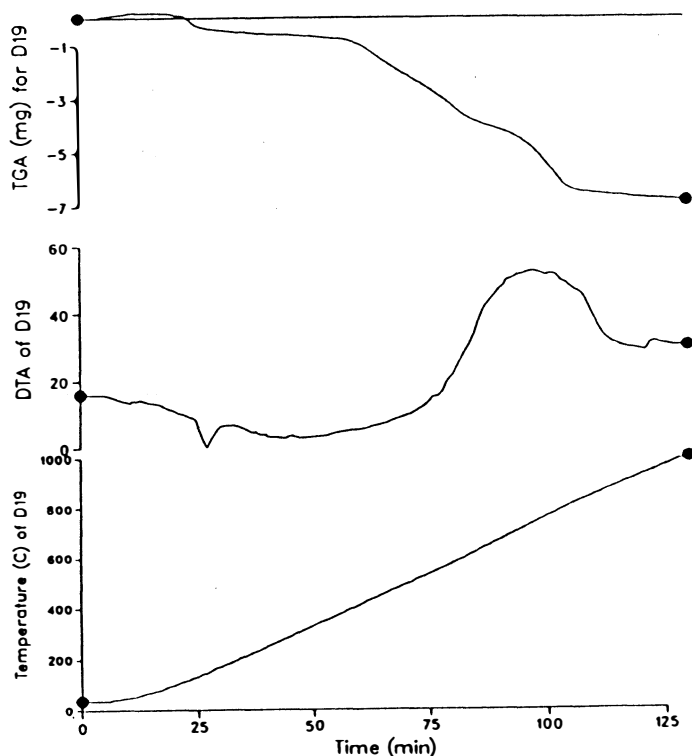
Figure 14: DTA/TGA of 1.8 sp gr Eagle #2

A series of runs using the DTA/TGA instrument were performed in order to examine the effects of different heating rates to 1000°C on the reduction of pyrite under a flowing atmosphere of 10% CO/90% Ar, DTA/TGA and XRD results are as follows:

Run	Rate (K/min)	Pyrrhotite formed	wt. loss %
DP-2	5	6C w/ little 2C	22.8
DP-9	10	6C w/ trace 5C	25.8
DP-4	20	6C under magnification	24.3

The dominate phase throughout the runs is $Fe_{11}S_{12}$ (6C) which correlates with the findings of the ISGS that 6C is the major intermediate pyrrhotite formed when pyrite is reduced to troilite under a carbon monoxide atmosphere (22,28). The trace amounts suggest that the samples need to be left above decomposition temperatures for reduction and equilibration to reach completion. When iron sulfide enters a new phase region, it needs time to equilibrate to the different conditions. In run DP-2, the sample remains above decomposition temperatures longer than DP-9 or DP-4 and shows more reduction in the form of 2C. The XRD analysis of run DP-4 was run on a small amount of sample and scale expansion was necessary to bring out the peaks. Any trace components would not be visible under these conditions, but the characteristic pyrrhotite peak seen is sharp and definite with no signs of a shoulder. Also, the percent weight loss equals that for total 6C conversion suggesting that 6C is the only phase present. Further XRD analysis determined the lattice constants for the pyrrhotite from run DP-4 to be a = 6.904 (3.452 x 2), and

c = 34.74 (5.79 x 6) which corresponds to the 6C type pyrrhotite based upon table 3 from Morimoto et al. (29).

The percent weight loss in the pyrite runs show an increasing trend with 10K/min being an optimum heating rate for this system and supporting possible inhibited phase transition. A run at 2.5K/min (to be discussed later) has a weight loss of 22.6%, with the 5K/min run showing 22.8%, 10K/min showing 25.8%, and 20K/min showing 24.3%. The slower heating rates may deter a phase transition, causing less of the sample to be reduced. Except for DP-4, the weight loss increases with increase in heating rate with the largest jump coming between 5K/min and 10K/min. In run DP-4, the sample was heated quickly enough to overcome the second order phase transition but leaves the sample above decomposition temperature for less time than DP-9 so the sample has less time for reduction. XRD analysis supports the observed weight loss of the samples with an increase in peak area for the characteristic peak in the 43° (2θ) range. The peak areas increase from 23.4 to 46.4 to 52.2 for DP-3, DP-2, and DP-9 respectively. To combine ideas of phase transition and equilibrium, the slower heating rates inhibit phase transition so less pyrite is reduced but they keep the pyrrhotite formed above the decomposition temperature longer, enabling further reduction of the pyrrhotite. When the samples are analyzed, the slower heating rates show less pyrite conversion but what has been converted is of a more highly reduced form. At higher heating rates, the phase transition occurs but the sample still needs

time to equilibrate. A 1.8 sp gr fraction from Eagle #2 coal was
heated to 1000°C at different rates to give the results shown below:

Run	Rate (K/min)	Pyrrhotite formed	wt. loss %
D-17	5	6C/2C	16.7
D-19	10	6C/2C	14.1

Pyrrhotite 6C is the only intermediate pyrrhotite seen between FeS_2
and FeS for these runs. Since the pyrite used in these runs is part
of a coal fraction, some of the organic fraction will still be present
and may aid in the reduction (7). The weight loss difference between
D-17 and D-18 may be due to the organics helping the reduction and the
run which leaves the sample above the decomposition temperatures
longer shows the greater weight loss. Adjusted peak areas from XRD
characteristic peaks (43°, 2θ) correlate to the weight loss with 5.4
for D-17 and 3.3 for D-19.

Runs with both pyrite and 1.8 sp gr Eagle #2 were done at
2.5K/min with the following results:

Run	Pyrrhotite formed	wt. loss %
DP-3	4C w/ some Fe_3O_4, Fe_2O_3, and py	22.6
D-18	poss. 5C/4C	14.9

Run DP-3 shows a mixture of iron sulfides and oxides with the
presence of Fe_7S_8 (4C), hematite (Fe_2O_3) and magnetite (Fe_3O_4)
indicating extensive oxidation. The formation of the iron oxides with
4C correlate to ISGS research that 4C can only be formed if the iron
sulfide is reduced past the 4C stage and is then oxidized back (22).
The presence of such extensive oxidation in the form of hematite,
however, would indicate a 2 to 5% oxygen atmosphere. The DTA/TGA
system does have a small leak which is seen when the system is

evacuated and pressure readings are taken every few minutes. The flow system used splits the gas flow and has the gas enter at the top and bottom of the furnace. The first runs using just argon gave oxidized irons and when carbon monoxide was added to the gas flow, the oxides disappeared but there was no increase in pyrite reduction. Investigation revealed that the tube leading to the top of the furnace was too small for the gas to flow through freely. Adjustments in exit gas flow in order to force gas through the small tubing resulted in pressure buildup in the system. A needle valve was then installed in the bottom gas line in order to restrict gas flow and to force more of the gas to enter through the top of the furnace and onto the sample, producing the reduction expected. From these steps, the leak appears to be at the bottom of the furnace with the added carbon monoxide reacting with the oxygen to form carbon dioxide and eliminating enough of the oxygen to prevent oxidation of the sample. If oxidation took place during cooling, when the carbon monoxide is turned off and the system is purged with argon, then most runs would show some amount of oxidation since the cooling procedure is the same for all runs. Since the only difference in the runs is the heating rate, the oxidation may be from the sample being left at high temperatures for a longer period of time. The run with the 1.8 sink fraction of Eagle #2 seems to support the pyrite run with a 5C/4C mixture forming. A possible explanation for DP-3 is the pyrite being reduced to 5C or 6C when oxidation starts to take place. Since the reaction is a surface reaction any pyrite which has not been reduced will be in the center of an iron sulfide particle. At the end of the run, the particles would have an upper layer of the iron oxides with a lower layer of 5C

or 6C which has been oxidized to 4C all of which surround a pyrite center. The longer time allows more mass transport time and greater damage from oxidation. Thorpe et al. (43), while examining oxidation of pyrite in an oxygen deficient atmosphere, found that pyrite will form a layer of Fe_3O_4 which then turns to Fe_2O_3. The Fe_2O_3 impedes further oxidation unless the temperature is rapidly increased which helps explain why the whole sample was not oxidized. Difficulty arises in determining whether hematite has truly been formed. Since hematite has a similar lattice structure to magnetite, the d-spacing will also be similar which means some of the characteristic XRD peaks will be very close. If closer examination could show only Fe_3O_4, then less oxygen would have been needed, making oxidation during the run more plausable.

The ISGS, in studying reduction of pyrite, determined that under carbon monoxide, 6C is the major intermediate pyrrhotite formed between FeS_2 and FeS, suggesting that the appearance of any other pyrrhotite, such as 4C, 5C etc., would be due to oxidation pushing back some of the 6C. ISGS determined what intermediates would be found from reduction under hydrogen or carbon monoxide by performing isothermal thermogravimetric analysis and plotting $\log(w_t-w^*)$ versus time for different temperatures, where w_t is the weight of the sample at time t and w^* is the weight of the sample at the reduced form of FeS (28). From the plots, rate constants were determined and where there is a slope change there is a change in reaction rate and evidence for an intermediate pyrrhotite. For carbon monoxide, only one slope change took place at a corresponding pyrrhotite weight of $Fe_{11}S_{12}$ (6C) (fig. 15). The experiment does not show that other

intermediates are not formed but that their rate constants are equal
so just as fast as they are produced, they are further reduced with
the conversion from $Fe_{11}S_{12}$ to FeS being the rate determining step.
For the system's leak to be the main cause for oxidation, run DP-2,
which kept the sample at high temperatures longer than DP-9 should
show more oxidation in the form of other pyrrhotites but the opposite
is seen, DP-9 shows slight trace amounts of 5C while DP-2 shows
increased reduction with the presence of a small amount of 2C.
Oxidation of pyrites takes place at about 400°C in air, 350°C in 2%
oxygen and 450°C in nitrogen (26). Runs DP-5 and DP-8, in which the
samples were heated to about 600°C, both show 5C as a final product
with appropriate weight loss percentages of 23.6%. If the pyrite of
these runs were to be reduced to 6C then oxidized back to 5C, the iron
sulfide conversion would be this:

$$\text{wt. loss \%}$$

$$11\ FeS_2 \quad ---> Fe_{11}S_{12} \qquad 24.3$$
$$12\ Fe_{11}S_{12} ---> 14Fe_9S_{10} + 2\ Fe_3O_4 \quad 24.3$$
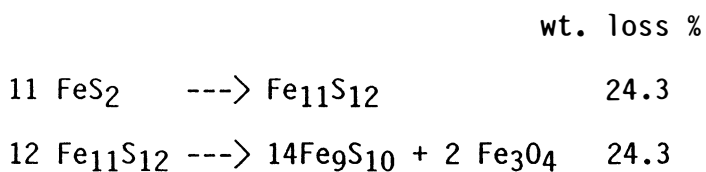
It is hard to imagine both runs reducing then oxidizing to the same
pyrrhotite form with the correct weight loss. Since 5C formation is
reproducable, the leak in the system would have to be constant, but in
that case, all long time runs would show some kind of oxidation. The
closest run in terms of time is run DP-6, in which the sample was
heated to 860°C in a recycling mode. Although the sample from run
DP-6 spent less time above 500°C (at least 90 min less), it was heated
to a higher temperature and only 6C was formed. If the longer time
causes oxidation, then some iron oxide should be seen but none appear
for any of these runs.
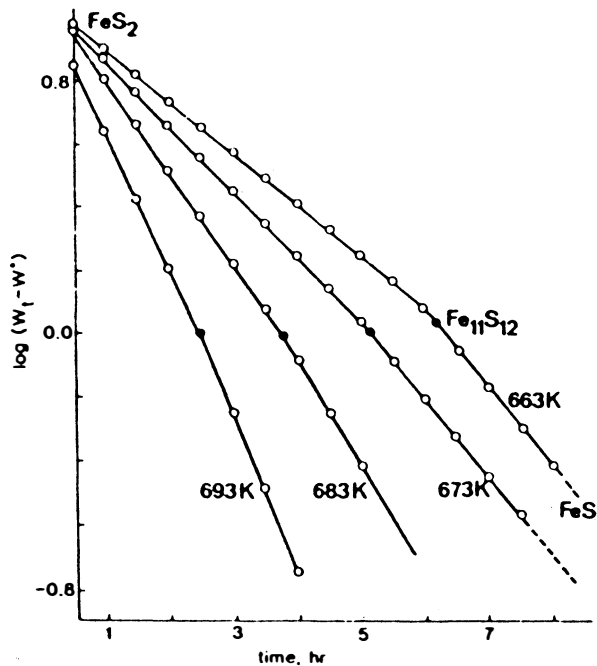
Figure 15: $\log(w_t - w^*)$ v.s. time for reduction under

carbon monoxide   (ref. 28)

The only other run to show any evidence of oxidation via the
presence of iron oxide is run D-18, in which the XRD analysis shows
possible oxide peaks. While the sample from run DP-3 formed 4C and
iron oxides, the sample from run D-18 formed a possible 5C/4C mixture.
If oxidation took place due to time spent at high temperatures other
runs should show oxidation as well. Runs DP-5, DP-7, and DP-8 all
spent over eighty minutes more above 500°C than either DP-3 or D-18
and runs DP-6 and D-22 spent 20 minutes more above 700°C but none of
these runs show any oxide peaks in XRD analysis. The reason for oxide
formation in runs DP-3 and D-18 seems to be due to the heating rate
since both runs were heated at 2.5K/min. Oxidation due to rate of
heating suggests that the inhibited phase transition experienced by
the pyrite may indirectly aid in the oxidation. With the presence of

-39-

carbon monoxide, reduction is the favored reaction but if the heating rate inhibits the phase transition, oxidation has the opportunity to take place.

Oxidation due to the leak in the system appears to be a problem only for runs with a heating rate of 2.5K/min. While the presence of pyrrhotite 5C is seen in some runs, it is possible to produce 5C on a regular basis (runs DP-5, DP-7, DP-8) showing that for this system the presence of pyrrhotites other than 6C or 4C is not evidence of oxidation. Rate of heating appears to promote oxidation by inhibiting phase transition in reduction but more experimentation is needed. There is no clear reason for the extensive oxidation of run DP-3. If all of the oxidation seen took place during the run, then it is due to the inhibited phase transition and long term heating at high temperatures. Presently, the ISGS is conducting experiments in pyrite oxidation in low level oxygen atmospheres which may help explain run DP-3 but no results have been released (44).

The second order phase transitions of iron sulfide are quite apparent when studying the pyrite runs of different heating rates. The deep endothermic peak becomes broader and more shallow as the heating rate decreases from 20K/min to 2.5K/min with the corresponding weight loss becoming slower and more drawn out. Run DP-3 (2.5K/min heating rate) shows only one clear peak about 590°C with only one definite weight loss occurring while run DP-4 (20K/min) shows a myriad of peaks with the deep peak appearing at 714°C and another small peak at 558°C with a possible broad peak around 320°C. Interpretation of run DP-4 is hampered by a sloping baseline caused by a difference in heat capacity between the reference and sample used. Changes in the

amount of reference material used did not significantly change the slope so partial decrease in the sloping was done through instrument adjustment. At higher heating rates the sloping becomes more prominent, making identification of some peaks more difficult.

The DTA runs show the ability of the instrument to produce adequate thermally treated samples. The heating rate series of pyrite runs suggest a balance is needed between heating rate and time for equilibration but further runs would need to be done for conclusive evidence. There is also evidence that pyrrhotite oxidation in an oxygen deficient atmosphere may be aided by a slow heating rate but again, more experimentation is needed. The second order phase transition of pyrite reduction is also clearly seen by the broadening of DTA peaks and the decrease in rate of weight loss.

Microwave Runs (Table 5)

Two series of runs were done using the 1.8 sp gr fraction of Il. #5 coal with different atmospheres. Under nitrogen, the first series of runs show a slow formation of pyrrhotite.

Run #	Temp (°C)	pyrrhotite formed
E-6	275	---
E-7	300	possible 5C/2C mixture
E-8	350	5C/2C

The second series, using a 10% CO/90% Ar atmosphere shows more definite pyrite reduction.

Run #	Temp (°C)	pyrrhotite formed
E-9	296	---
E-10	325	6C w/ possible 2C
E-11	350	6C/5C

The two series show that some reduction will occur just from heating but addition of carbon monoxide causes greater reduction as is expected. Peak areas from the XRD analysis correlates well for the carbon monoxide series. The adjusted peak area of pyrite for run E-9 is 1.64. After being heated to 325°C, the pyrite peak area drops to 1.28 with a pyrrhotite peak area of 0.35 (1.28 + 0.35 = 1.63) and, after being heated to 350°C, the pyrite peak drops further to 1.13 and the pyrrhotite peak increases to 0.85 (1.13 + 0.85 = 1.98). Two more runs were performed using 10% CO/90% Ar with the sample being heated to 275°C (E-13) and later to 350°C (E-14). While no pyrrhotite is detected in run E-13, a 6C/2C mixture is seen in run E-14.

Examination of runs of similar temperature shows pyrrhotite formation to take place between 325°C and 350°C. Even with carbon monoxide, no pyrrhotite is formed at 275°C. At 300°C, there is little to no pyrrhotite formed, but, definite pyrrhotite formation takes place at 325°C and pyrrhotite is seen in all 350°C runs. Although in run E-11 (10% CO at 350°C) a 6C/5C mixture with a peak location of 43.6° (2θ) is produced, run E-1 (the only microwave run to use 1.8 sp gr from Eagle #2 coal) and run E-14 both show a 6C/2C mixture under the same conditions and correlate with run E-10 (10% CO at 325°C), in which 6C with possible 2C is formed. From these runs, conditions for optimum pyrrhotite conversion will be a 10% carbon monoxide atmosphere

with a temperature between 325°-350°C, depending upon length of heating time.

Using the bed from run E-11, a test run using nitrogen bubbled through ethanol was done at 350°C (E-12). The pyrrhotite is expected to dehydrogenate the ethanol to form acetaldehyde and hydrogen. Analysis of gas samples taken during the run and of the bed after the run show definite hydrogen and acetaldehyde formation in the gas stream plus iron sulfide reduction with the 6C/5C mixture being reduced to 6C and 2C. Since the bed had been pretreated under a reducing atmosphere (10% CO) at 350°C for one half hour, no further reduction is expected from the heating. The pyrite reduction, therefore, is due to the hydrogen being formed and reacting with the iron sulfide and is seen by the detection of hydrogen sulfide in the gas samples. A second run (E-15) performed for reproducability was designed to see at what temperature dehydrogenation takes place. A pretreated bed (the bed used in run E-14) was heated to 275°C for one half hour, then heated to 325°C for another one half hour, then heated to 350°C for one hour. XRD analysis shows almost pure troilite (FeS) formation with a trace of troilite "B", a pyrrhotite named by the ISGS as a form close to but not quite FeS. Gas samples taken during the run shows hydrogen formation at 325°C but no definite acetaldehyde formation. A portion of the gas sample appears to be mostly ethylene and may include some acetaldehyde which are both products of ethanol reactions over iron sulfide, acetaldehyde being the product of dehydrogenation and ethylene being the product of dehydration. The run does still show the formation of hydrogen for the process to work but better conditions need to be determined.

The most important comparison is between the microwave runs and the DTA/TGA runs of set temperature. Samples were prepared in the DTA/TGA at a set temperature for one half hour under 10% carbon monoxide with the CO left on for five minutes after turning off the furnace in order to duplicate conditions of the microwave runs.

Run #	Type	Temp (°C)	Coal Type	Atm.	Pyrrhotite formed
DI-9	DTA/TGA	355	Ill #5	10% CO	---
DI-10	DTA/TGA	307	"	"	---
D-24	"	305	Eagle #2	"	---
D-25	"	350	"	"	---
E-1	MW	350	"	"	6C,2C
E-7	"	300	Ill #5	N_2	poss. 5C/2C type
E-8	"	350	"	"	5C,2C
E-9	"	296	"	10% CO	---
E-11	"	350	"	"	poss. 6C/5C mixture
E-14	"	350	"	"	6C/2C

At 300°C and 350°C, no pyrrhotite was formed in either Eagle #2 or Ill #5 mineral fractions thermally, while pyrrhotite formation is seen in the 300°C of a nitrogen atmosphere microwave run (E-7) and definite pyrrhotite formation is seen in all 350°C microwave runs (E-1, E-8, E-11, E-14). These runs show that under the same conditions, dielectric heating will reduce pyrite at a lower temperature than thermal heating.

In terms of the process developed by the ISGS, dielectric heating produced the pyrrhotite needed at atmospheric pressure. From the ethanol runs, the pyrrhotite helped produce the hydrogen necessary for the removal of organic sulfur. Experimentation still needs to be performed in order to optimize the conditions but judging from the results of this research, the process will work with dielectric heating.

There are many factors which need to be considered in order to incorporate dielectric heating into the process. Preliminary runs using whole coal, for example, show a problem with agglomeration and tar formation. Run E-2, in which whole Eagle #2 coal was heated, experienced a sudden temperature rise to 350°C accompanied with oil and tar formation. While XRD analysis of the sample shows that the pyrrhotite formed in the short time of heating was all FeS, pyrolysis took place with the loss of some volatiles and agglomeration. Either the coal will have to be separated and the mineral fraction treated separately or preliminary runs using the mineral fraction will need to be performed in order to set the power levels. With the correct power settings, the mineral fraction will obtain the proper temperature while the organic fraction will be at a lower temperature. Since the system uses an ir sensor, the temperature registered is an average temperature of the sample. With selective heating, the registered temperature will be less than the actual temperature of the mineral fraction and an overall temperature of 350°C will not be needed for desulfurization.

Conclusion

The coal desulfurization process being developed by the ISGS, which reduces pyrite (FeS_2) to troilite (FeS) at pressures of 300 to 500 psig and temperatures of 350°C to 550°C, can be done through dielectric heating at atmospheric pressure and temperatures between 325°C and 350°C. Pyrite reduction, which is not seen in thermal runs, is quite apparent in dielectric runs. Preliminary runs with ethanol show formation of hydrogen necessary for the second step of the process. Pyrite reduction is also hindered by slow heating rates which may be due to second order phase transition, evident from broadening DTA peaks and decreasing weight loss rate.

APPENDIX

Table 1

Peak Locations for Some Minerals

Name	Formula	Angle (2θ)	
Illite		8.8	
Kaolinite		12.4	
Bassinite	$CaSO_4*1/2H_2O$	14.7	
Quartz	SiO_2	20.8	
Anhydrite	$CaSO_4$	25.4	
Orthidose		27.4	
Plogidose		27.9	
Calcite	$CaCO_3$	29.4	
Oldhamite	CaS	31.3	
Pyrite	FeS_2	33.1	
Pyrrhotite 2C	FeS	43.2	56.2
" 6C	$Fe_{11}S_{12}$	43.5	56.95
" 5C	Fe_9S_{10}	43.7	57.3
" 4C	Fe_7S_8	44.0	57.7
Iron	Fe	44.7	

-48-

Table 2

XRD Results of DTA and Microwave Runs

Run #	Temp (°C)	Run Figure		Pyrrhotite Found
Pyrite	DTA	DTA	XRD	
DP-2	5K to 1000	16	37	6C, trace 2C
DP-3	2.5K to 1000	17	38	4C
DP-4	20K to 1000	18	39	6C not enough sample for good run
DP-5	10K to 606	19	40	5C
DP-6	10K 160/860*	20	41	6C
DP-7	20K 660/548*	21	42	5C 43.6+ (2θ)
DP-8	10K to 594	22	43	5C
DP-9	10K to 1000	23	44	6C, trace 5C

1.8 sink Eagle #2 DTA

D-17	5K to 1000	24	45	6C, 2C
D-18	2.5K to 1000	25	46	possible 5C/4C mix. 43.76 (2θ)
D-19	10K to 1000	26	47	6C, 2C
D-20	10K to 246	27	48	---
D-21	10K to 500	28	49	possible 5C/4C mix. 43.9 (2θ)
D-22	10K to 754	29	50	2C, 5C
D-24	10K to 305	30	51	---
D-25	10K to 350	31	52	---

Run #	Temp (°C)	Run Figure		Pyrrhotite Found	
1.8 sink Ill #5 DTA		DTA	XRD		
DI-3	10K to 1000	32	53	5C/4C mix 43.9 (2θ)	
DI-7	10K to 732	33	54	5C/4C mix plus 44.15 peak	
DI-8	10K to 768	34	55	6C/5C mix 43.6 (2θ)	
DI-9	10K to 355	35	56	---	
DI-10	10K to 307	36	57	---	
1.8 sink MW					
E-1	10%CO 350	--	58	2C, 6C	Eagle #2
E-6	N$_2$ 275	--	59	---	Il. #5
E-7	N$_2$ 300	--	60	no definite Po 5C/2C?	"
E-8	N$_2$ 350	--	61	2C, 5C	"
E-9	10%CO 296	--	62	no Po	"
E-10	10%CO 325	--	63	6C, possible 2C (troi. B) Ill #5	
E-11	10%CO 350	--	64	possible 6C/5C mix 43.6 (2θ)	"
E-12	N$_2$ + EtOH 350	--	65	6C, 2C plus 6C/2C mix 43.4 (2θ)	"
E-13	10%CO 275	--	66	no Po	
E-14	10%CO 350	--	67	6C/2C	
E-15	N$_2$ + EtOH 350	--	68	2C	
Whole Coal Eagle #2					
E-2	N$_2$ 350	--	69	2C	
E-3 top	N$_2$ **	--	70	possible 6C/2C 43.3 (2θ)	
E-3 bottom	N$_2$ **	--	71	---	

* recyling run

** no temperature reading

all DTA runs are with 10% CO atmosphere

Table 3   (ref. 29)

Composition, symmetry, and cell dimensions of five structure types of pyrrhotite.

Type	Com-position	Atomic percent of iron	Symmetry (space group)	Cell dimensions			
				a (Å)	b (Å)	c (Å)	β (°)
2C	FeS	50.00	Hexagonal ($P\bar{6}2c$)	5.97 (3.45 × √3) 5.958 (3.440 × √3) 5.965 (3.444 × √3)	.	11.76 (5.88 × 2) 11.740 (5.870 × 2) 11.750 (5.875 × 2)	
6C	Fe₁₁S₁₂	47.83	Hexagonal*	6.90 (3.45 × 2) 6.904 (3.452 × 2)		34.56 (5.76 × 6) 34.51 (5.752 × 6)	
11C	Fe₁₀S₁₁	47.62	Orthorhombic (Cmca or C2ca)	6.892 (3.446 × 2)	11.952	63.184 (5.744 × 11)†	
5C	Fe₉S₁₀	47.37	Hexagonal*	6.88 (3.44 × 2) 6.892 (3.446 × 2) 6.884 (3.442 × 2)		28.70 (5.74 × 5)† 28.630 (5.726 × 5) 28.610 (5.722 × 5)	
4C	Fe₇S₈	46.67	Monoclinic (F2/d)‡	6.860 (3.430 × 2) 6.872 (3.436 × 2)	11.903 11.903	22.788 (5.697 × 4) 22.780 (5.695 × 4)	90.5 90.4

* Orthorhombic symmetry is possible as explained in the text.   † The c-length is not exactly 11C or 5C, as expl:
‡ to the second setting of this space group, the a and b axes must be interchanged.

-51-

Table 4

Instrument settings for DTA/TGA Runs

DTA/TGA

Run #	Temp (°C)	Heating Rate (K/min)	Program setting
Pyrite			
DP-2	1000	5	---
DP-3	"	2.5	---
DP-4	"	20	---
DP-5	606	10	450
DP-6	160/860*	10	---
DP-7	660/548*	20	420/480
DP-8	594	10	450
DP-9	1000	10	---
DP-10	"	10	---
Eagle #2			
D-17	1000	5	---
D-18	"	2.5	---
D-19	"	10	---
D-20	246	10	250.5
D-21	500	10	393
D-22	754	10	524.5
D-24	305	10	290
D-25	350	10	315

Run #	Temp (°C)	Heating rate (K/min)	Program setting
Illinois #2			
DI-3	1000	10	---
DI-7	732	10	519
DI-8	768	10	535
DI-9	355	10	315
DI-10	1000	10	---

* recycling run

Program setting used for steady state runs at set temperature.

Table 5

Instrument settings for Microwave Runs

Run #	Temp (°C)	Power setting (Kw)	sample wt. (gr)	sample
E-1	350	0.3	39.3259	Eagle #2
E-6	275	0.9	45.6315	Illinois #5
E-7	300	0.65	37.1290	"
E-8	350	0.7	31.2405	"
E-9	296	0.4	38.1688	"
E-10	325	0.6	31.3376	"
E-11	350	0.7	25.4151	"
E-12	350	0.38	---	"
E-13	275	0.59	40.2135	"
E-14	350	0.5	25.4372	"
E-15	275/325/350	0.3/0.38/0.5	21.8226	"

Power settings are initial settings subject to slight adjustments during run.

All runs with flow rate of 1.22 L/min.

Table 6
XRD Peaks for all Analyzed Runs

DTA runs

Run #	Temp (°C)	Pyrrhotite Found	XRD Peak (2θ)	
Pyrite				
DP-2	5K to 1000	6C, trace 2C	sharp peak	43.5
			small shoulder	43.2
DP-3	2.5K to 1000	4C, Fe oxides	sharp peak	44.0
			sharp peak	35.41
			peak	33.25
DP-4	20K to 1000	6C	sharp peak	43.5
DP-5	10K to 606	5C	sharp peak	43.7
DP-6	10K 160/860*	6C	sharp peak	43.5
DP-7	20K 660/548*	5C	sharp peak	43.7
DP-8	10K to 594	5C	sharp peak	43.7
DP-9	10K to 1000	6C, poss. trace 5C	sharp peak	43.5
			slight shoulder	43.7
1.8 sp gr Eagle #2				
D-17	5K to 1000	6C, 2C	slight broad peak	43.5
			shoulder	43.2
D-18	2.5K to 1000	poss. 5C/4C	broad peak	43.75
D-19	10K to 1000	6C, 2C	overlapping peaks	43.5
				43.2
D-20	10K to 246	---	-----	
D-21	10K to 500	poss. 5C/4C	slight broad peak	43.9
D-22	10K to 754	2C, 5C	peak	43.2
			shoulder	43.7

1.8 sp gr Eagle #2 con't

Run #	Temp (°C)	Pyrrhotite Found	XRD peak (2θ)
D-24	10K to 305	---	-----
D-25	10K to 350	---	-----

1.8 sp gr Ill #5

DI-3	10K to 1000	poss. 5C/4C	broad peak 43.3 to 43.9
DI-7	10K to 732	poss. 5C/4C	" " 43.9
DI-8	10K to 768	6C/5C	" " 43.5
			slight shoulder 43.7
DI-9	10K to 355	---	-----
DI-10	10K to 307	---	-----

Microwave runs

1.8 sp gr Eagle #2

E-1	10%CO 350	2C, 6C	peak 43.2
			shoulder 43.5

1.8 sp gr Ill #5

E-6	N_2 275	---	-----
E-7	N_2 300	poss. 5C/2C	short broad peak 43.3
			short broader peak 43.7
E-8	N_2 350	2C, 5C	overlapping peaks 43.2
			43.7
E-9	10%CO 296	---	-----
E-10	10%CO 325	6C, poss. 2C	broad peak 43.5
E-11	10%CO 350	poss. 6C/5C mix	broad peak 43.6
E-12	N_2 + EtOH 350	6C, 2C + mix	overlapping peaks 43.2
			43.4
			shoulder 43.6

1.8 sp gr Ill #5 con't

Run #	Temp (°C)	Pyrrhotite Found	XRD Peak (2θ)	
E-13	10%CO 275	---	-----	
E-14	10%CO 350	6C, 2C	broad peak	43.4
E-15	N_2 + EtOH 350	2C, poss. 6C	peak	43.2
			slight shoulder	43.6

Whole coal Eagle #2

E-2	N_2 350	2C	broad peak	43.2
E-3 top	N_2 **	poss. 6C/2C	broad peak	43.3
bottom	N_2 **	---	-----	

* recycling run

** no temperature reading

all DTA runs are with 10% CO atmosphere
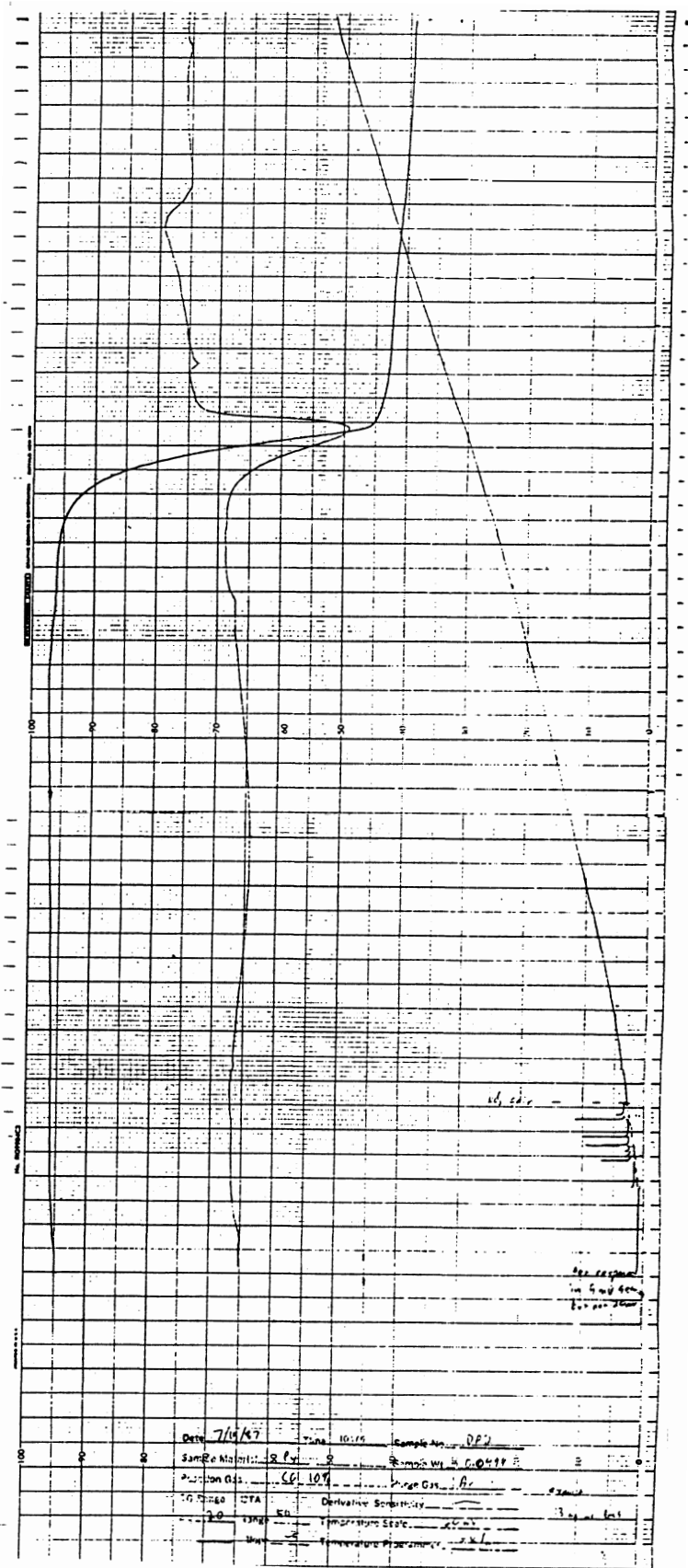
Figure 16: DTA/TGA recording for run DP-2

-58-
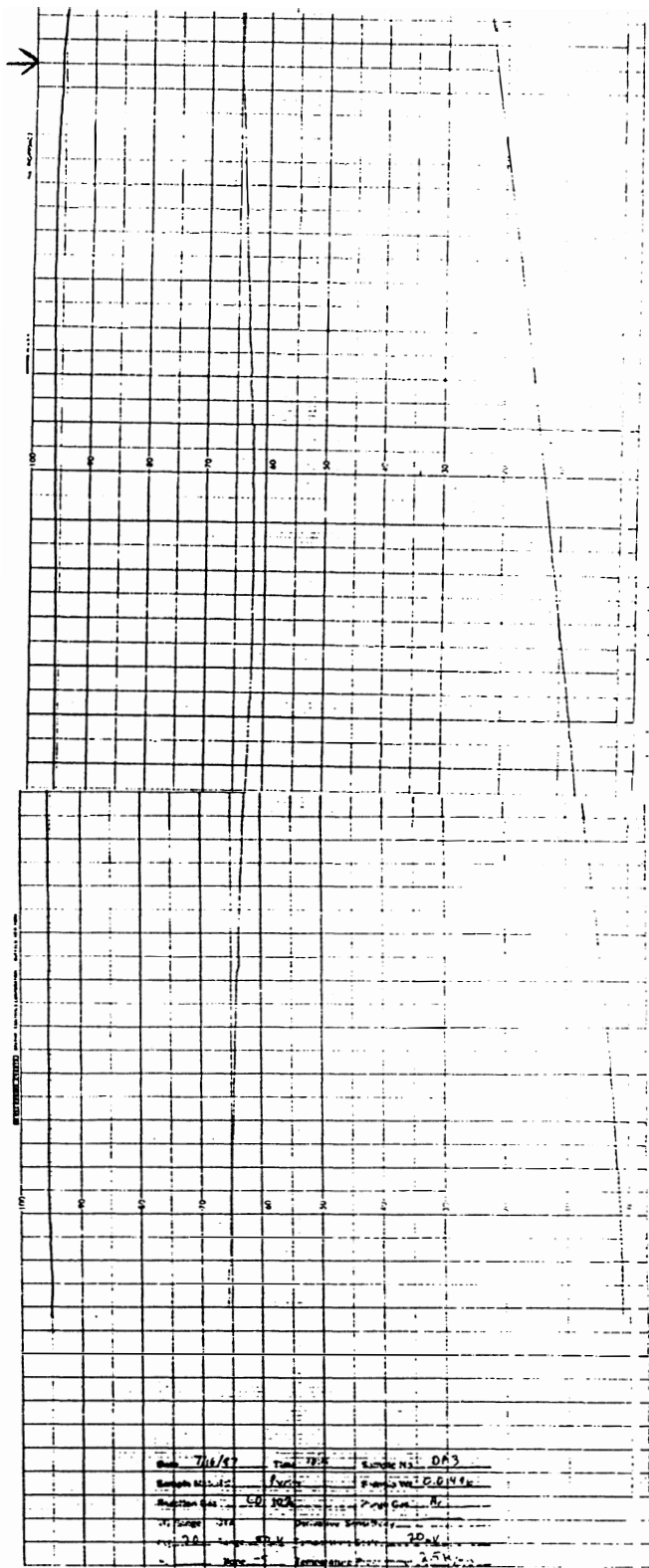
Figure 17: DTA/TGA recording for run DP-3
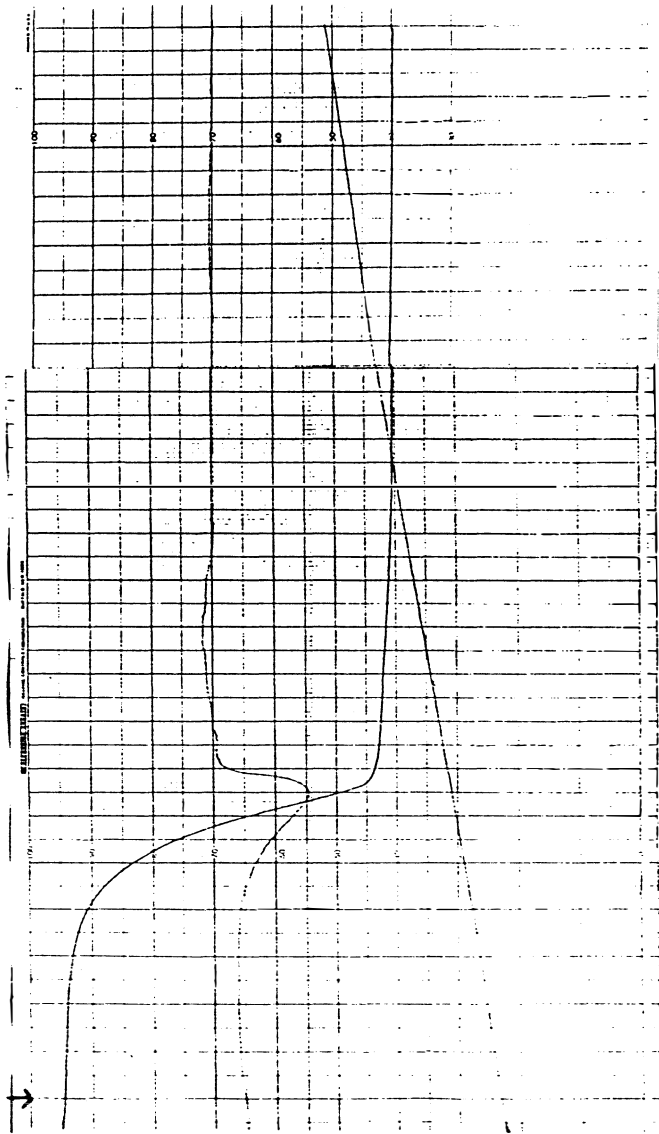
Figure 17 cont': DTA/TGA recording for run DP-3

Date 7/17/87   Time 9:30   Sample No. DP4
Sample Material: Pyrite   Sample Wt. 0.0493
Reaction Gas   CO 10%   Purge Gas Ar
2n Range   DTA   Derivative Sensitivity
rix 20   Range 50 μV   Temperature Scale 70 μV
Slope -5   Temperature Programm 20 K/min
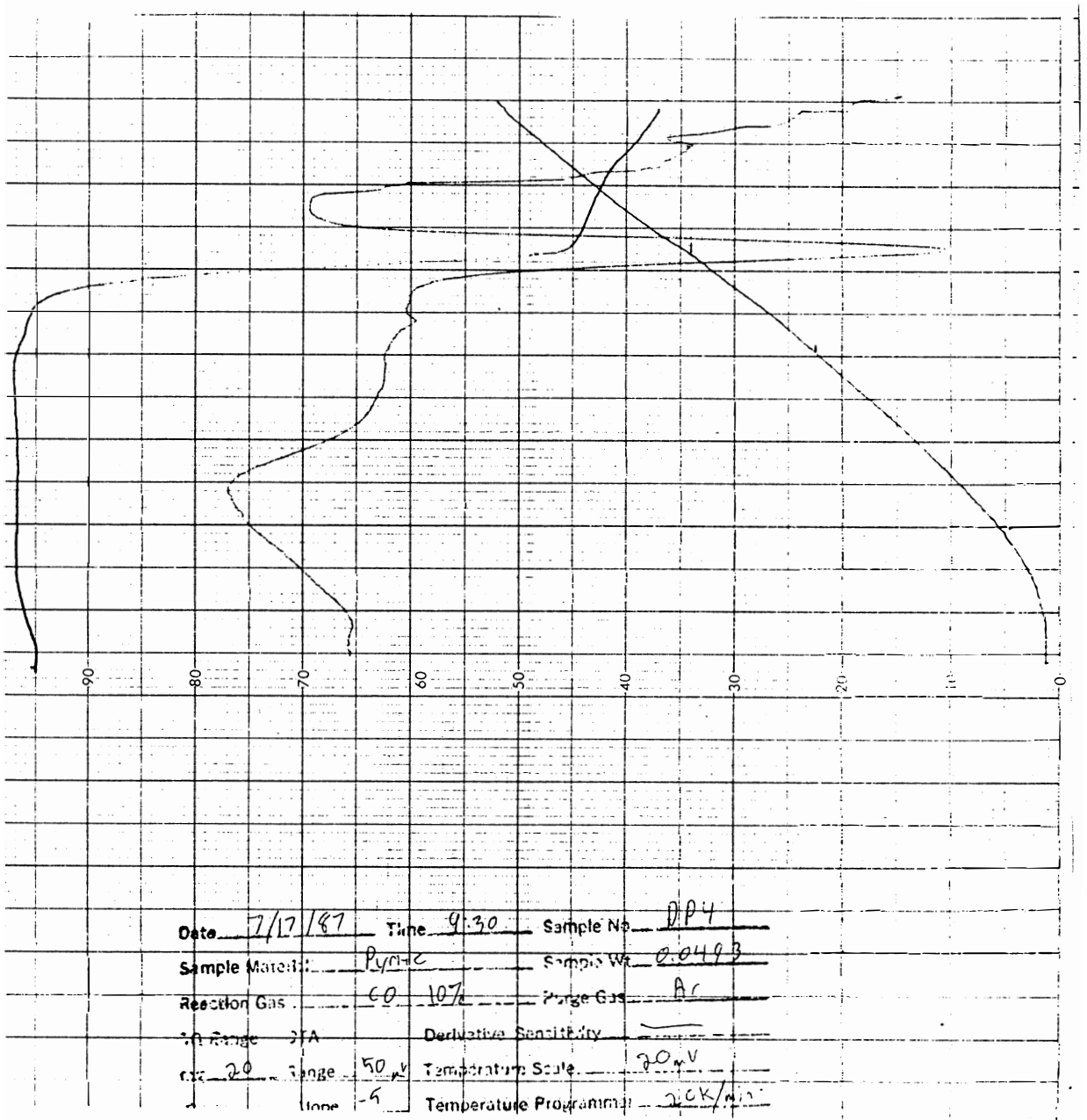
Figure 18: DTA/TGA recording for run DP-4
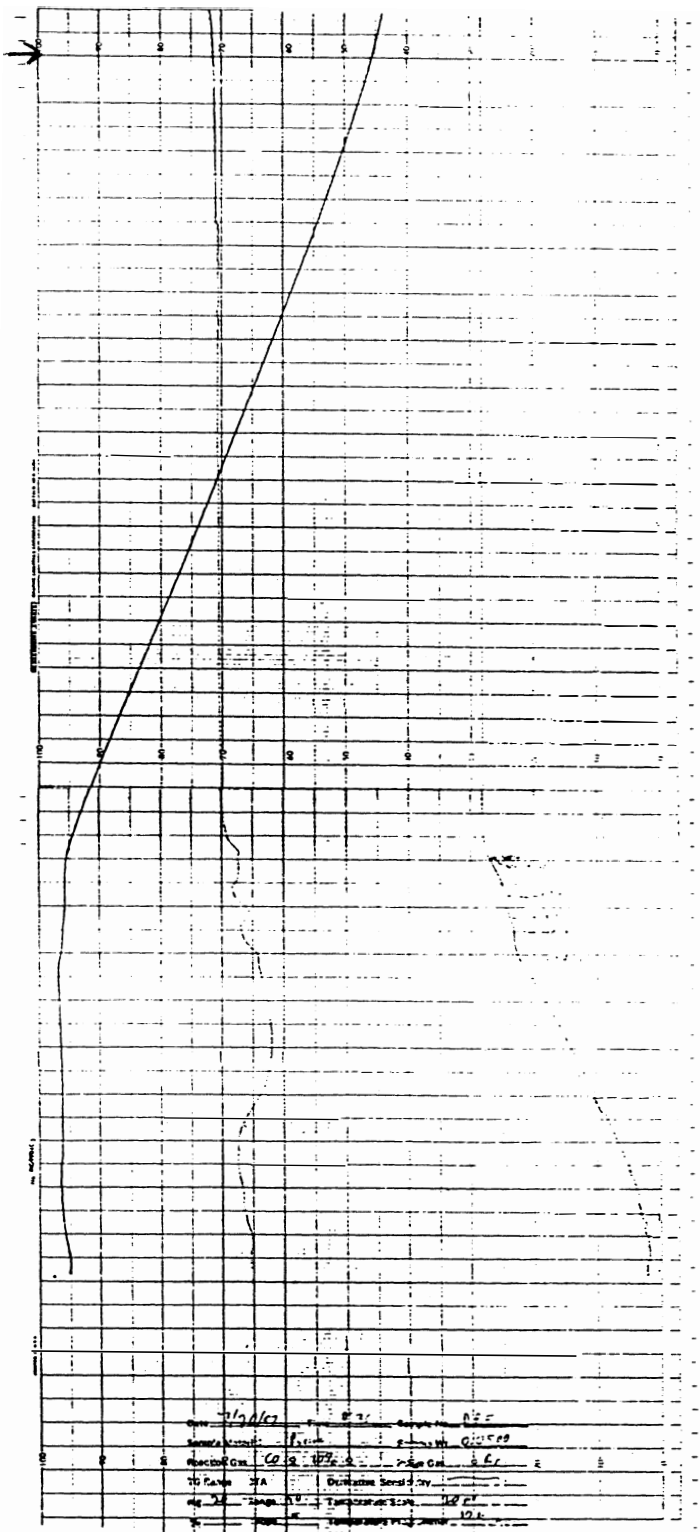
Figure 19: DTA/TGA recording for run DP-5
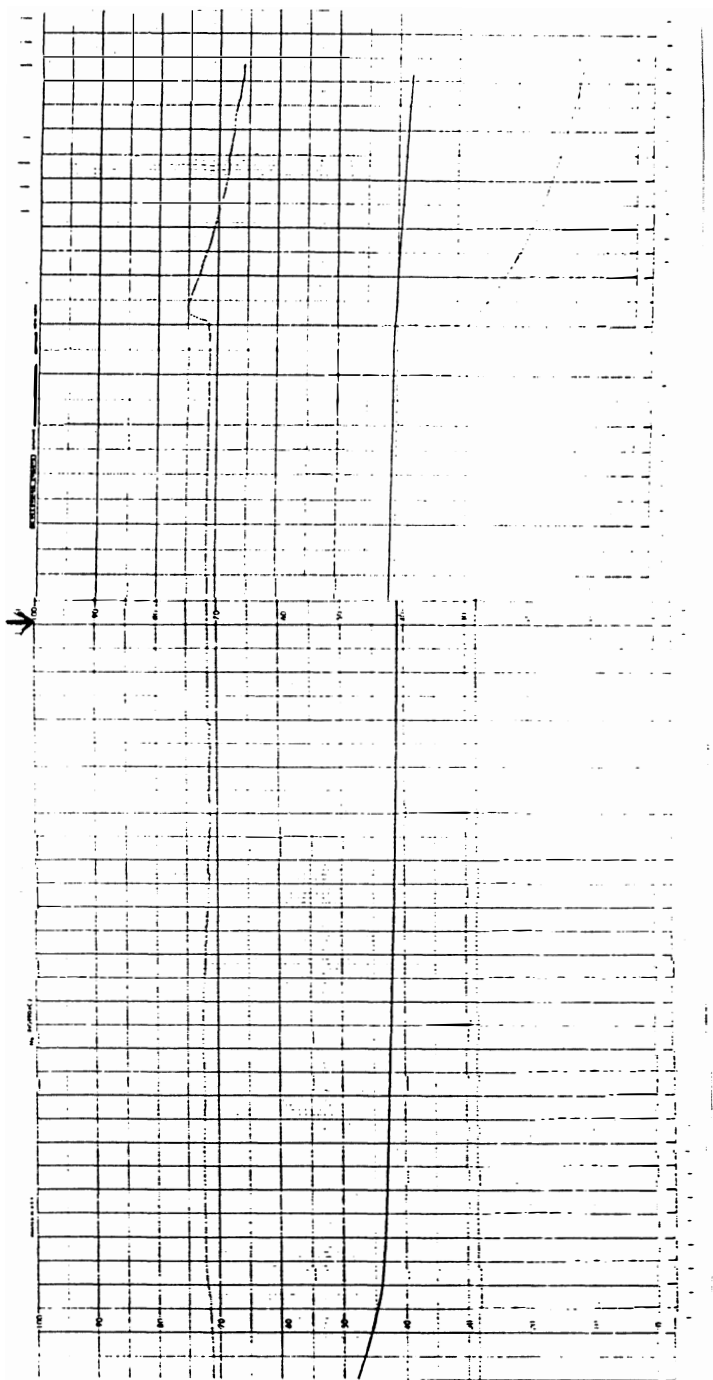
Figure 19 cont': DTA/TGA recording for run DP-5
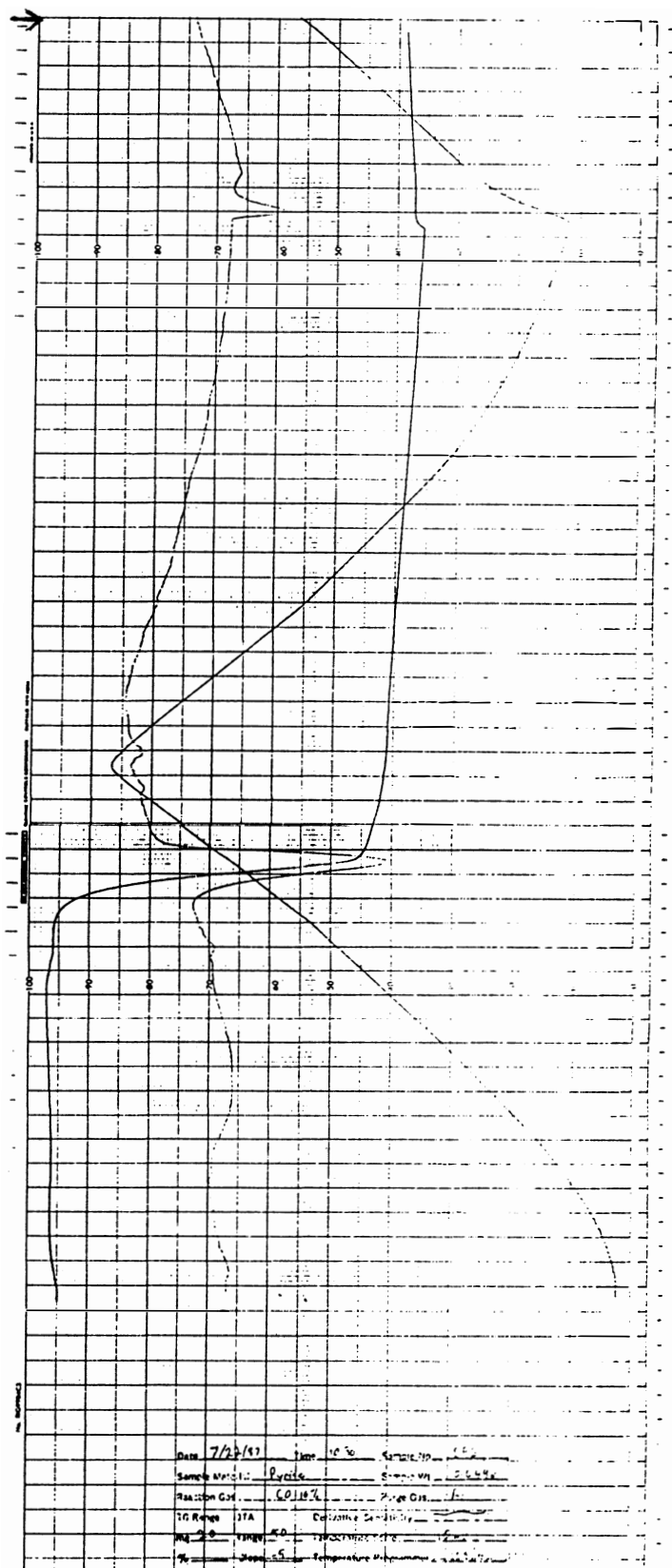
Figure 20: DTA/TGA recording for run DP-6
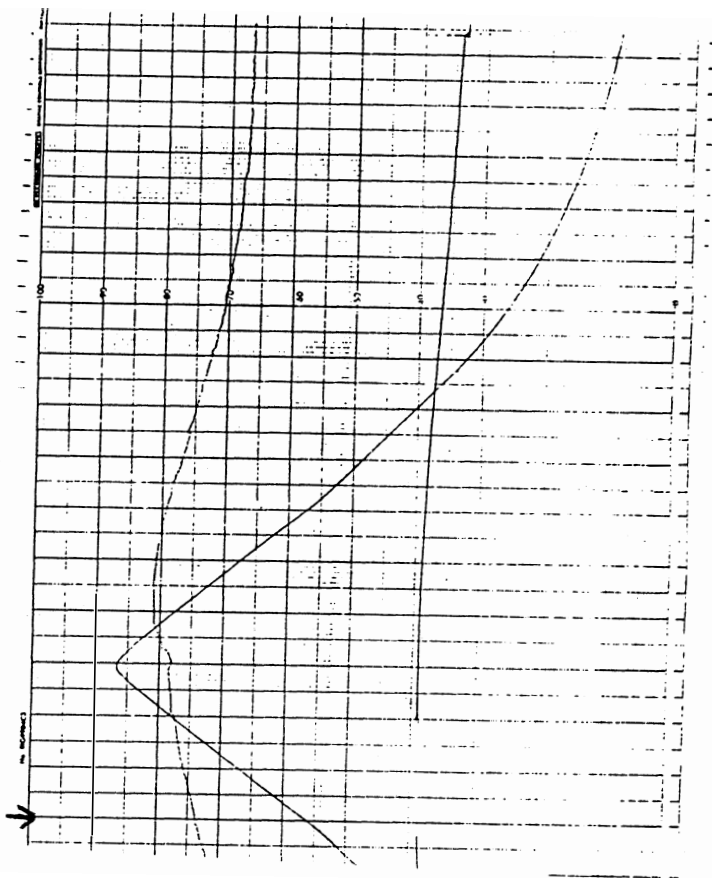
Figure 20 cont': DTA/TGA recording for run DP-6
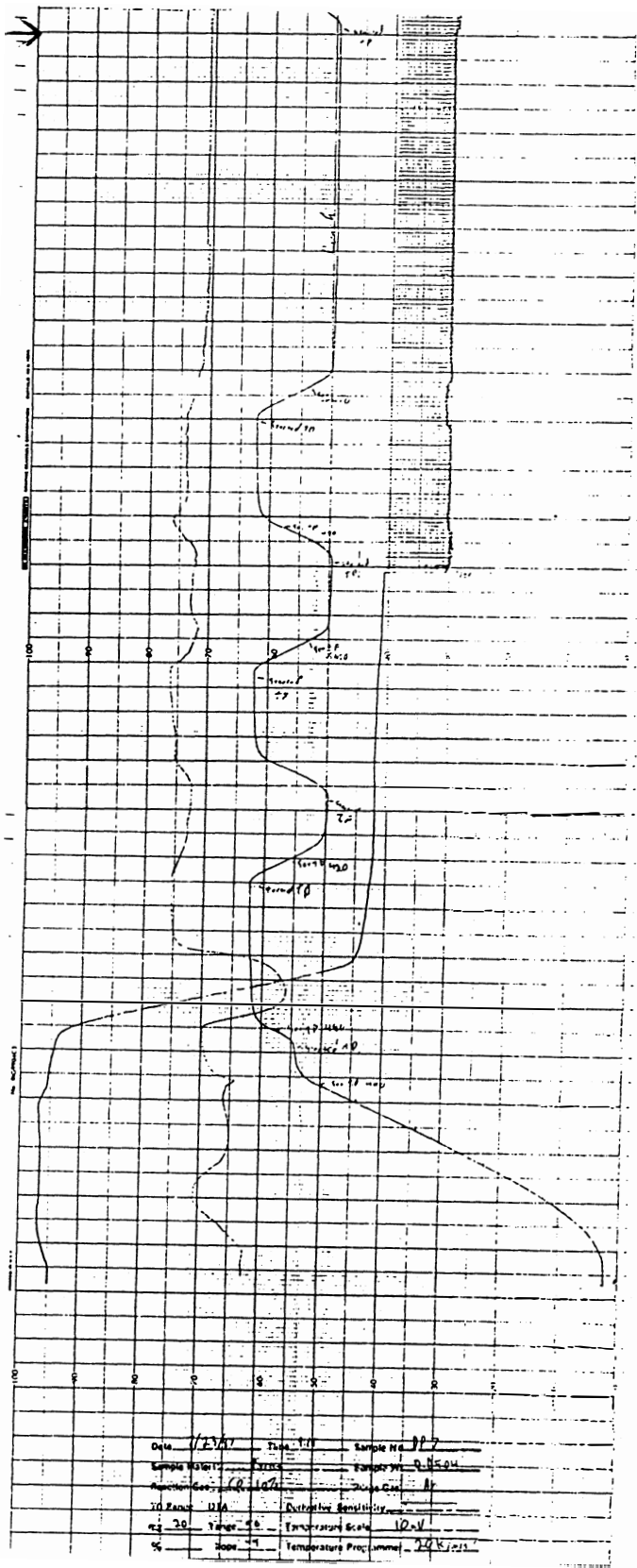
Figure 21: DTA/TGA recording for run DP-7
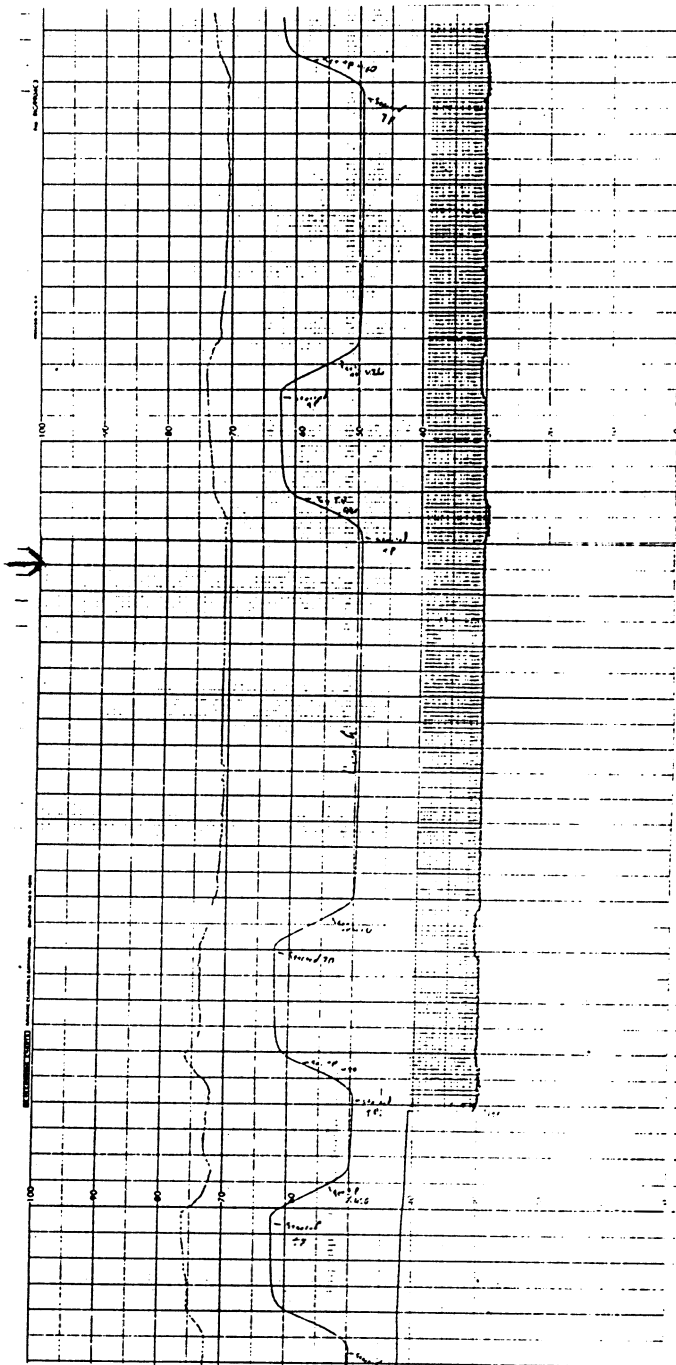
Figure 21 cont': DTA/TGA recording for run DP-7
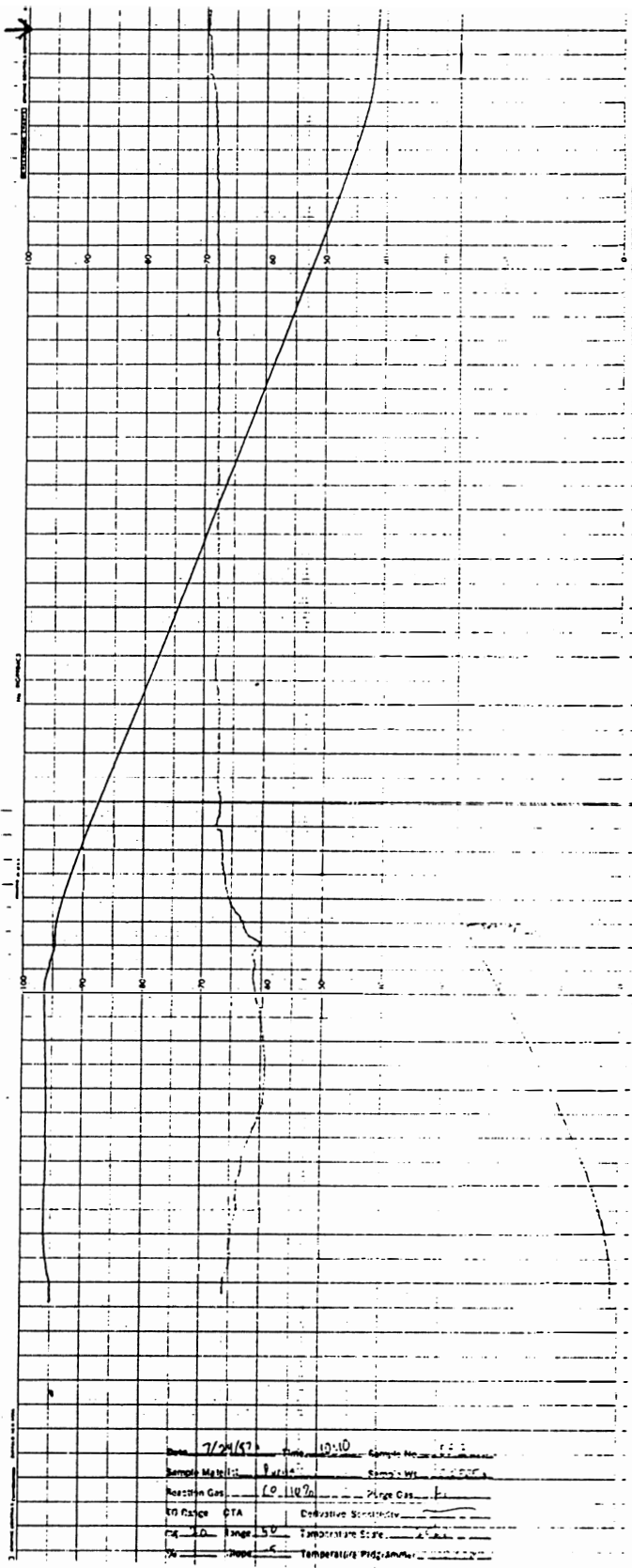
Figure 22: DTA/TGA recording for run DP-8
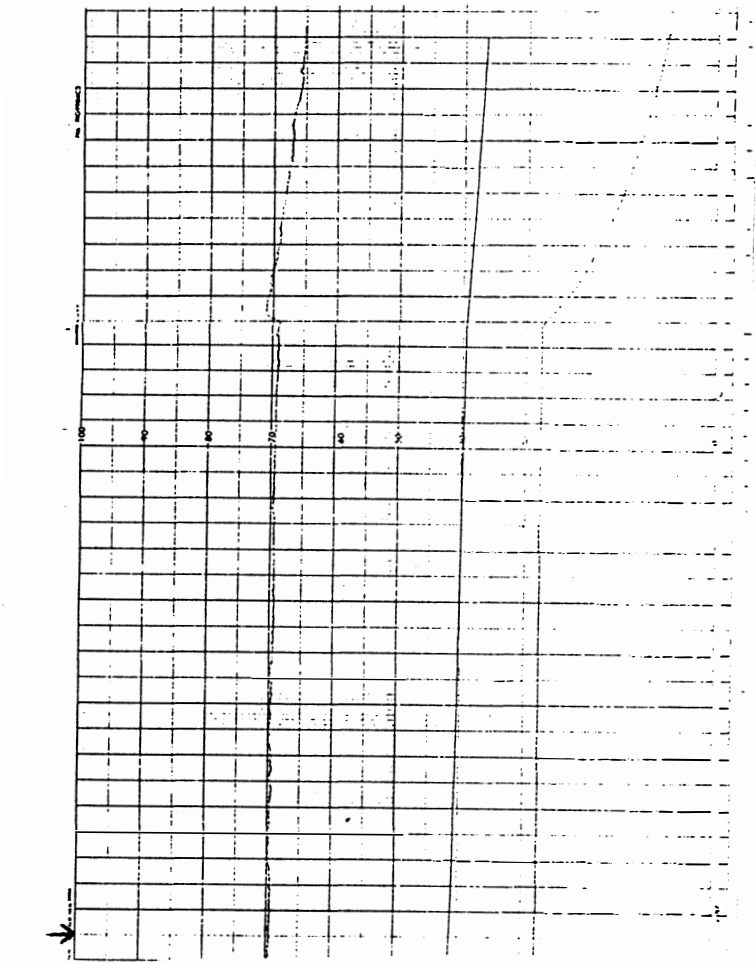
Figure 22 cont': DTA/TGA recording for run DP-8
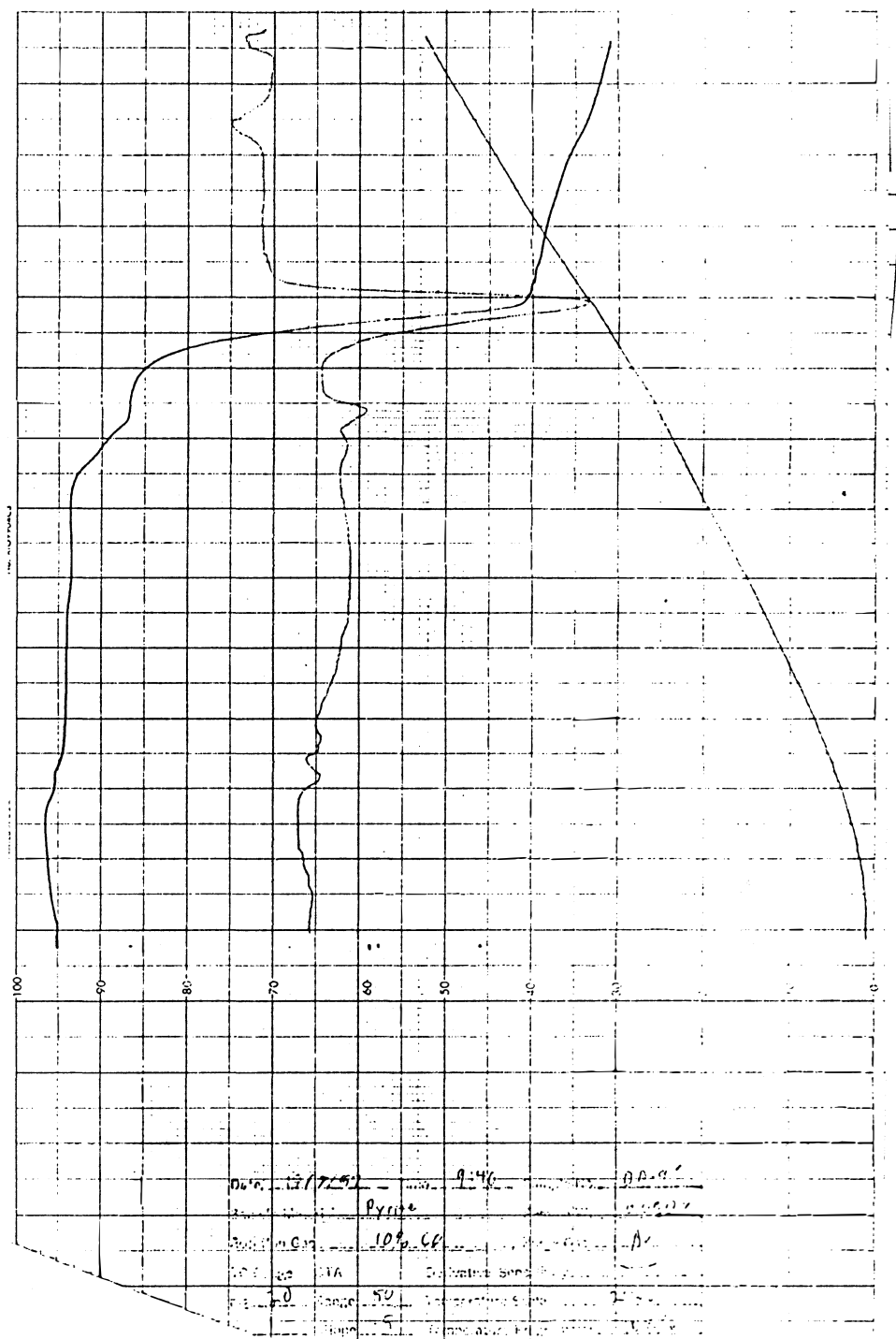
Figure 23: DTA/TGA recording for run DP-9
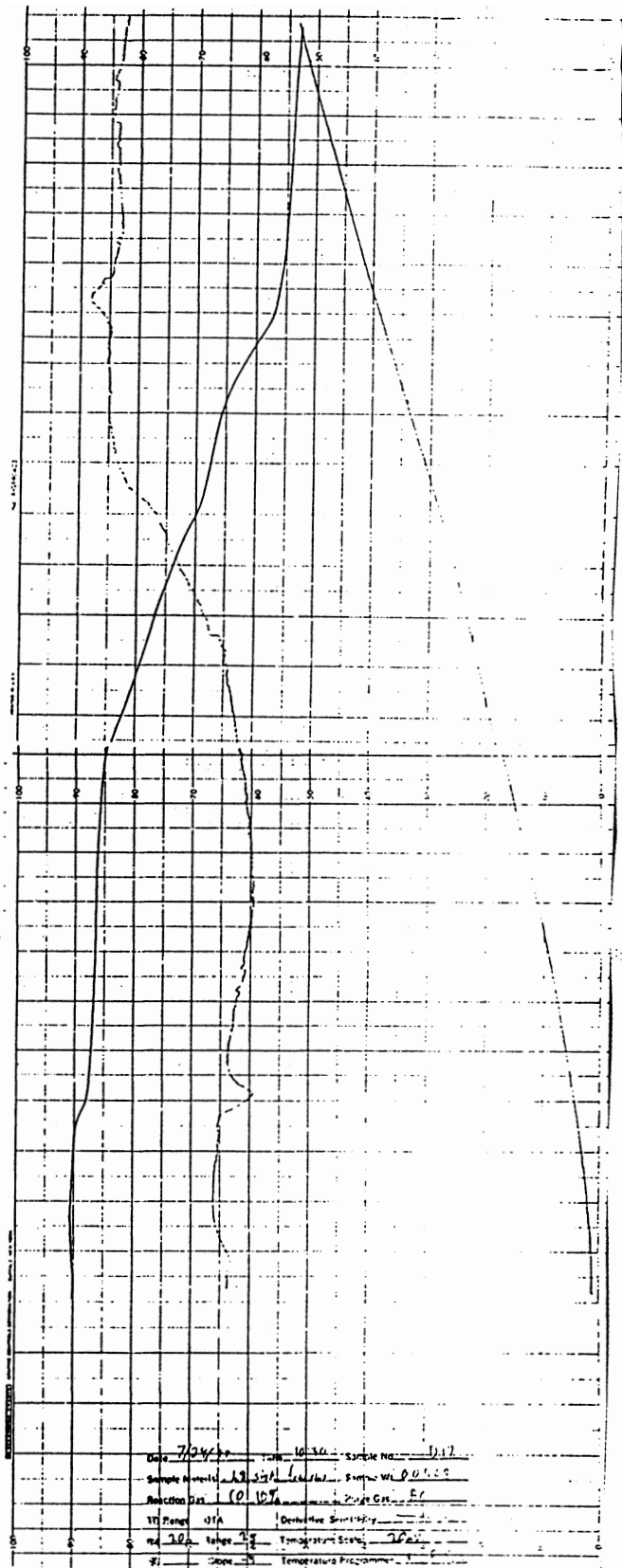
Figure 24: DTA/TGA recording for run D-17
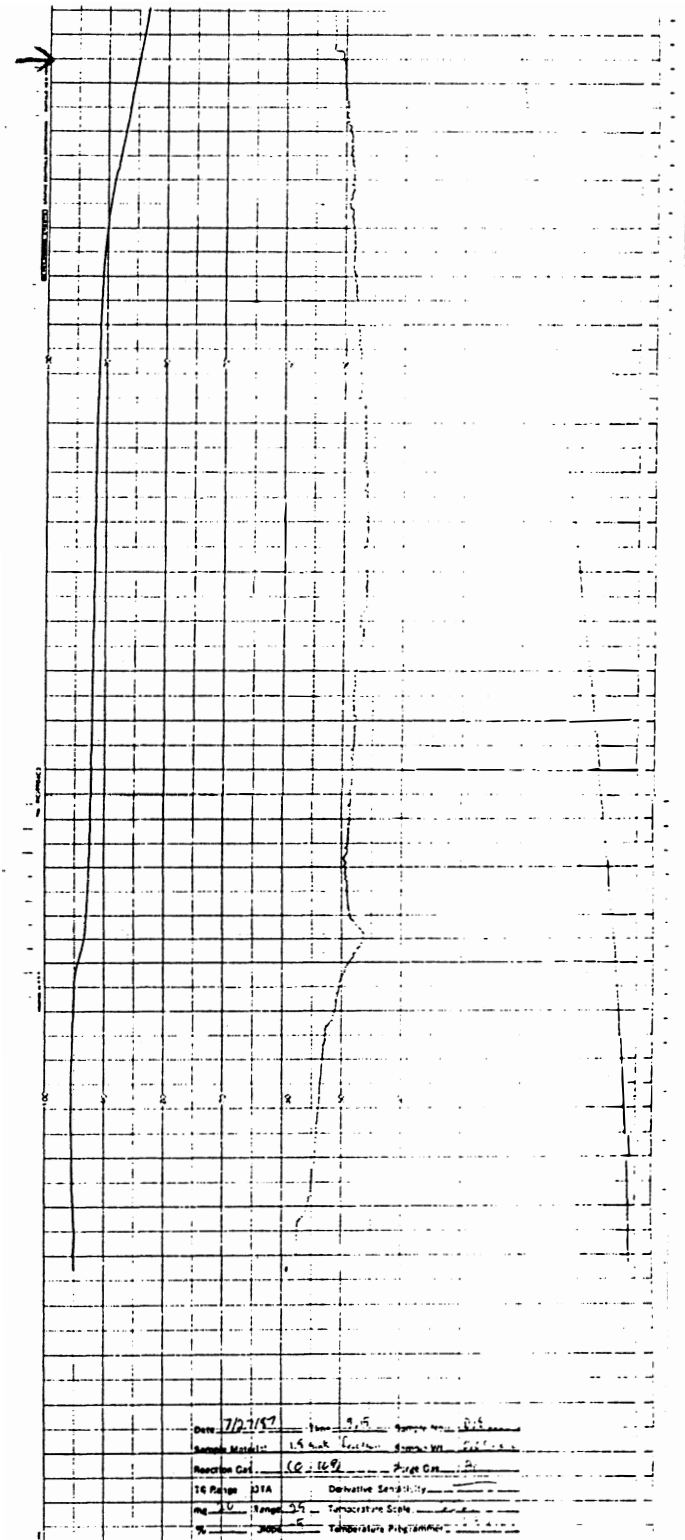
Figure 25: DTA/TGA recording for run D-18
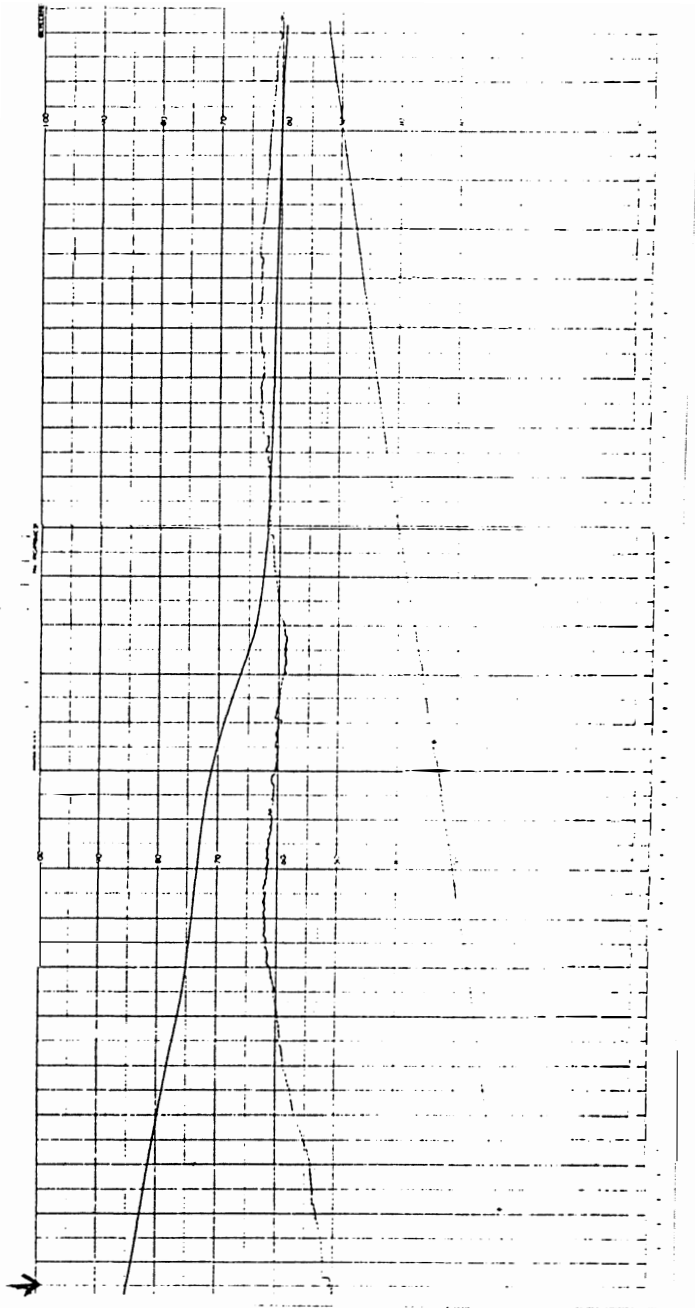
Figure 25 cont': DTA/TGA recording for run D-18
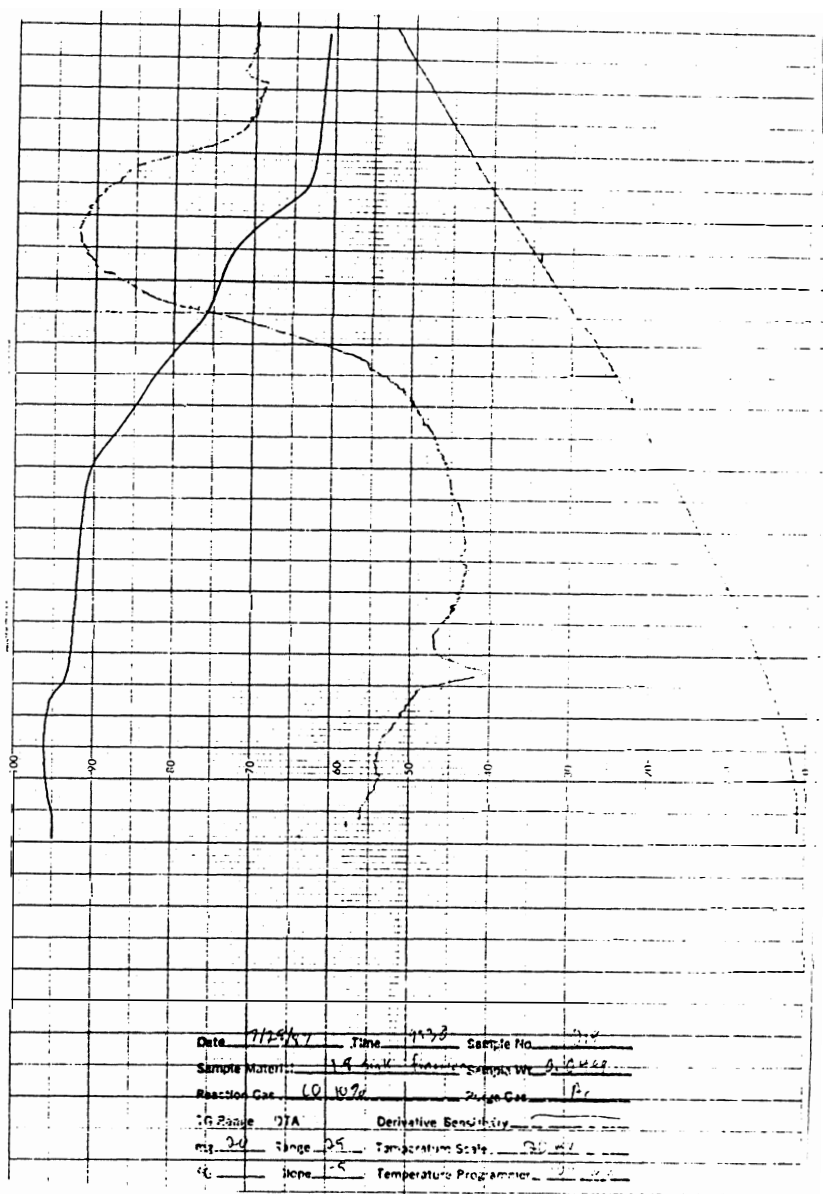
Figure 26: DTA/TGA recording for run D-19

-74-
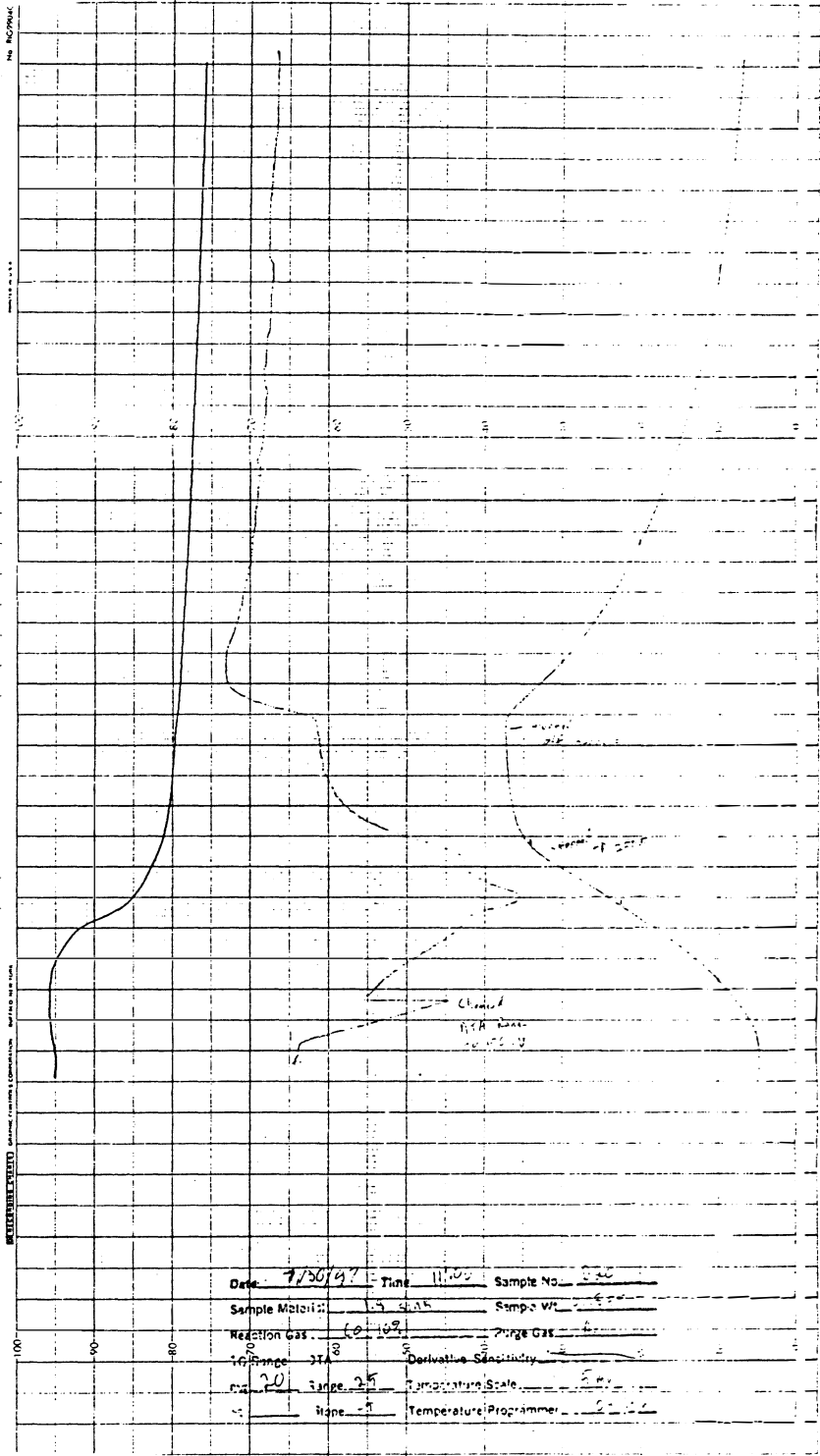
Figure 27: DTA/TGA recording for run D-20
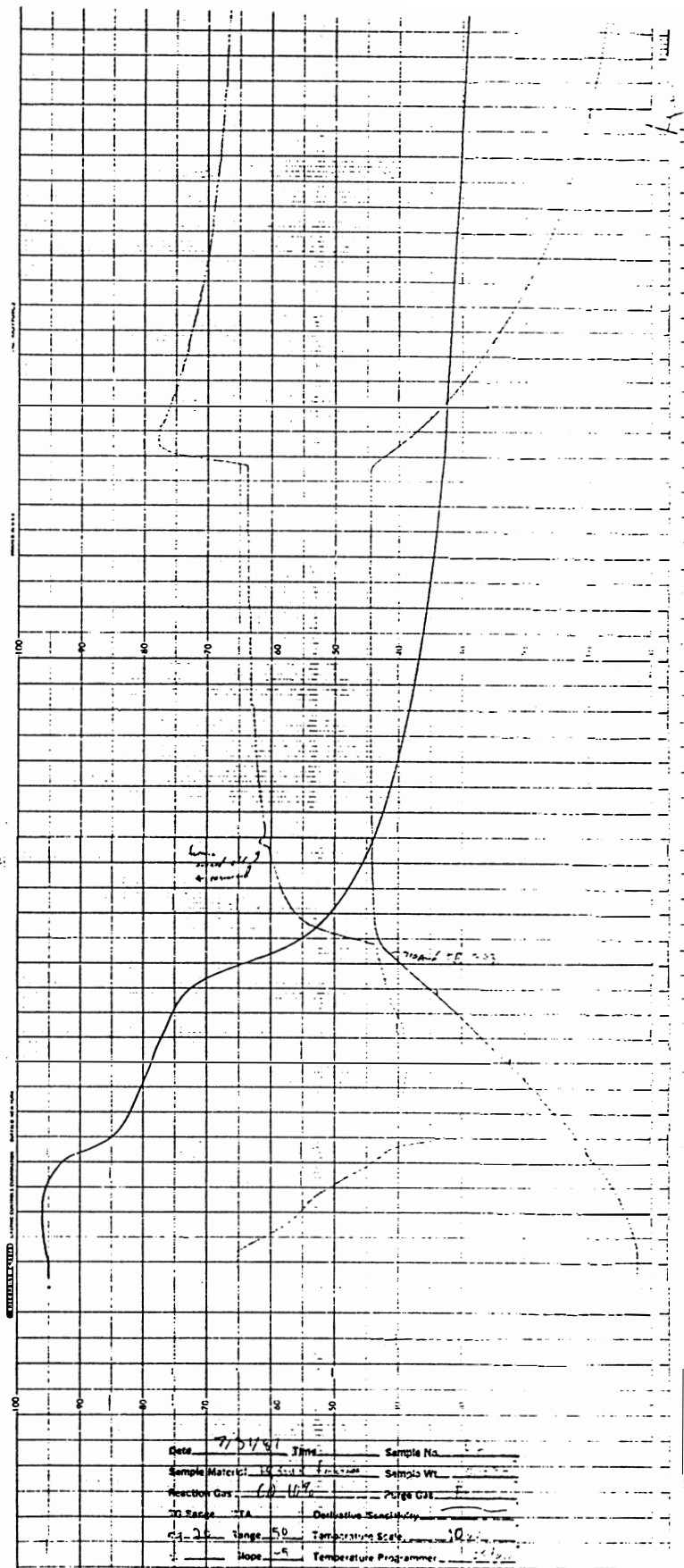
Figure 28: DTA/TGA recording for run D-21
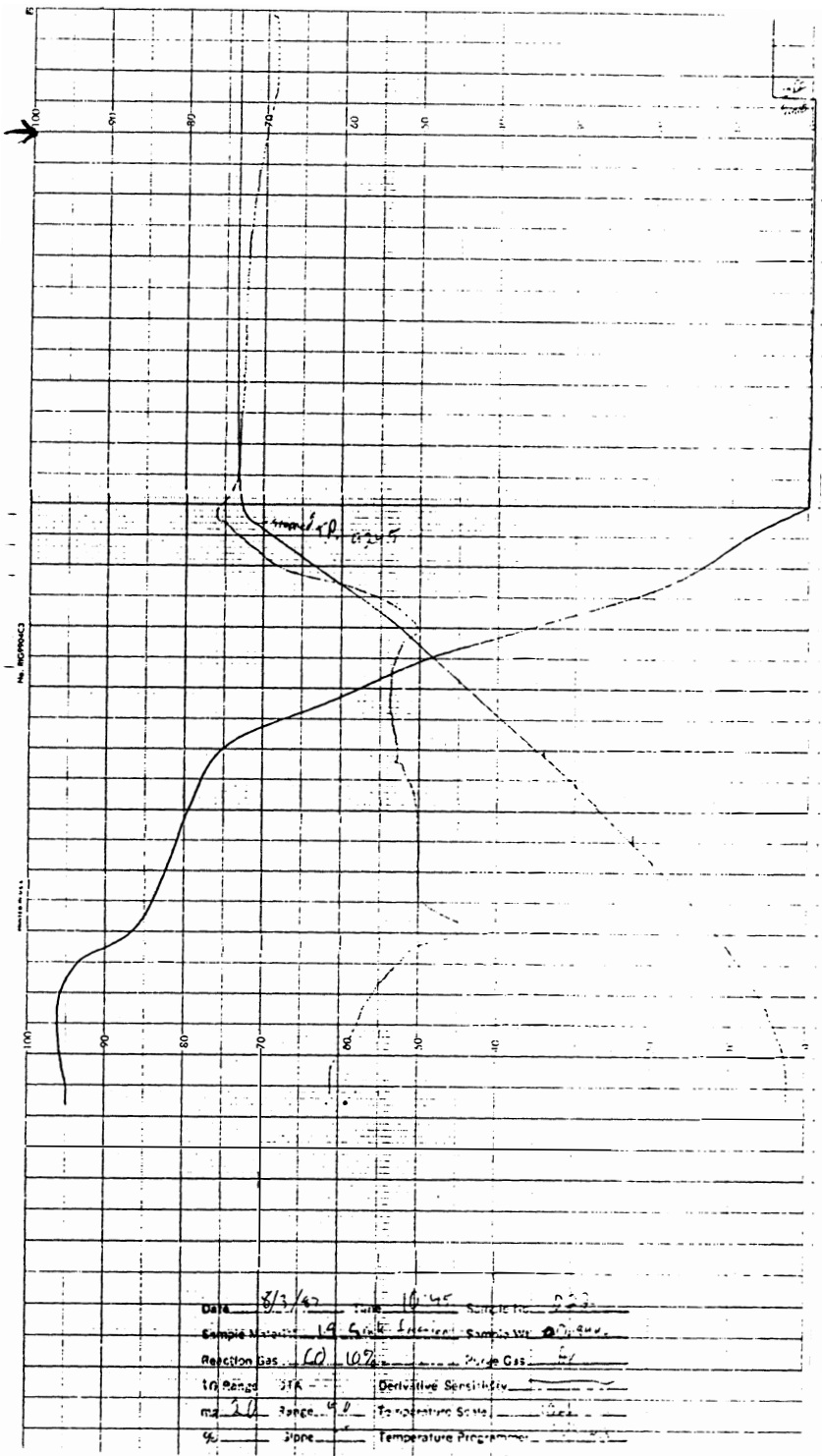
Figure 29: DTA/TGA recording for run D-22
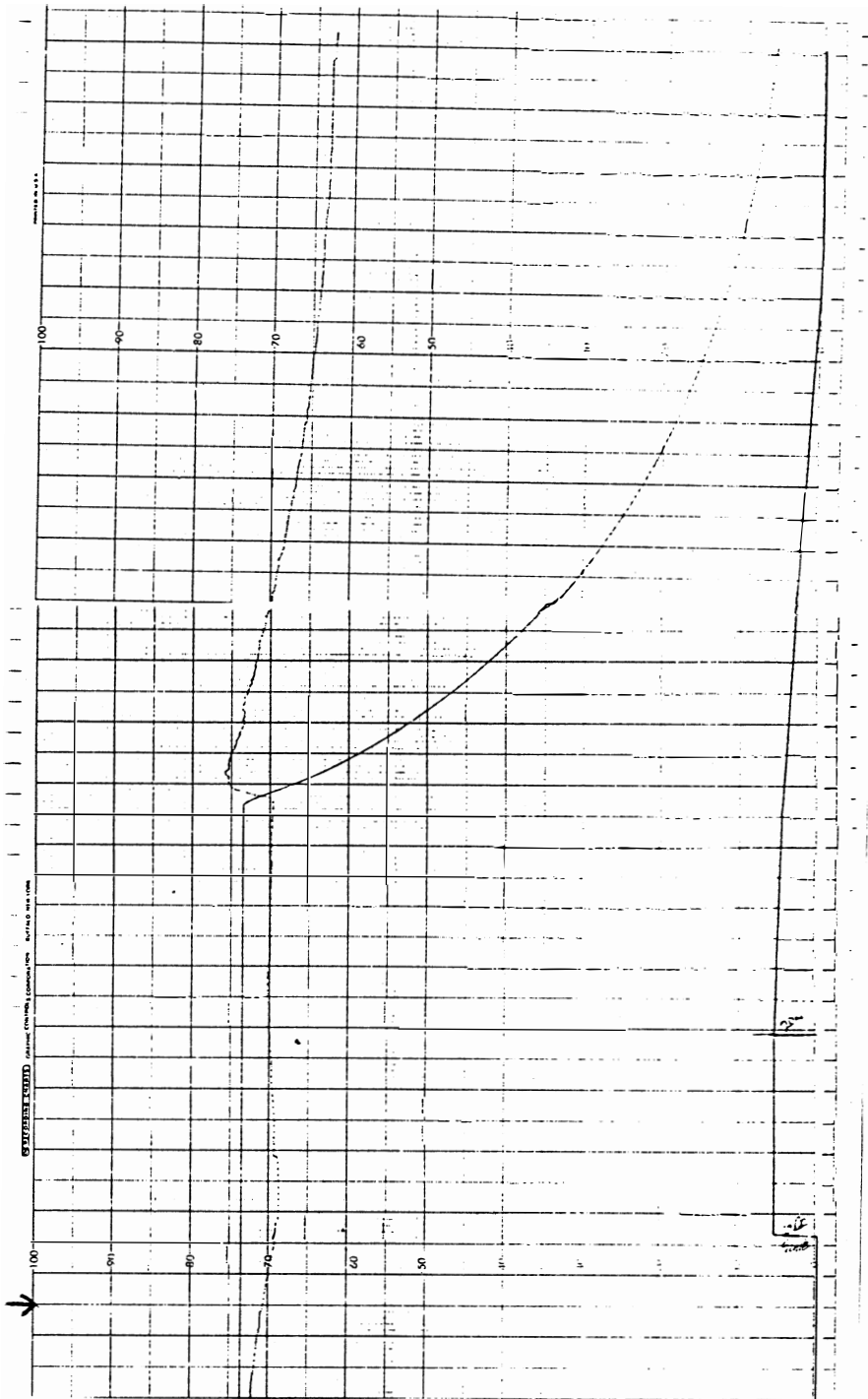
Figure 29 cont': DTA/TGA recording for run D-22

Figure 30: DTA/TGA recording for run D-24

Figure 31: DTA/TGA recording for run D-25
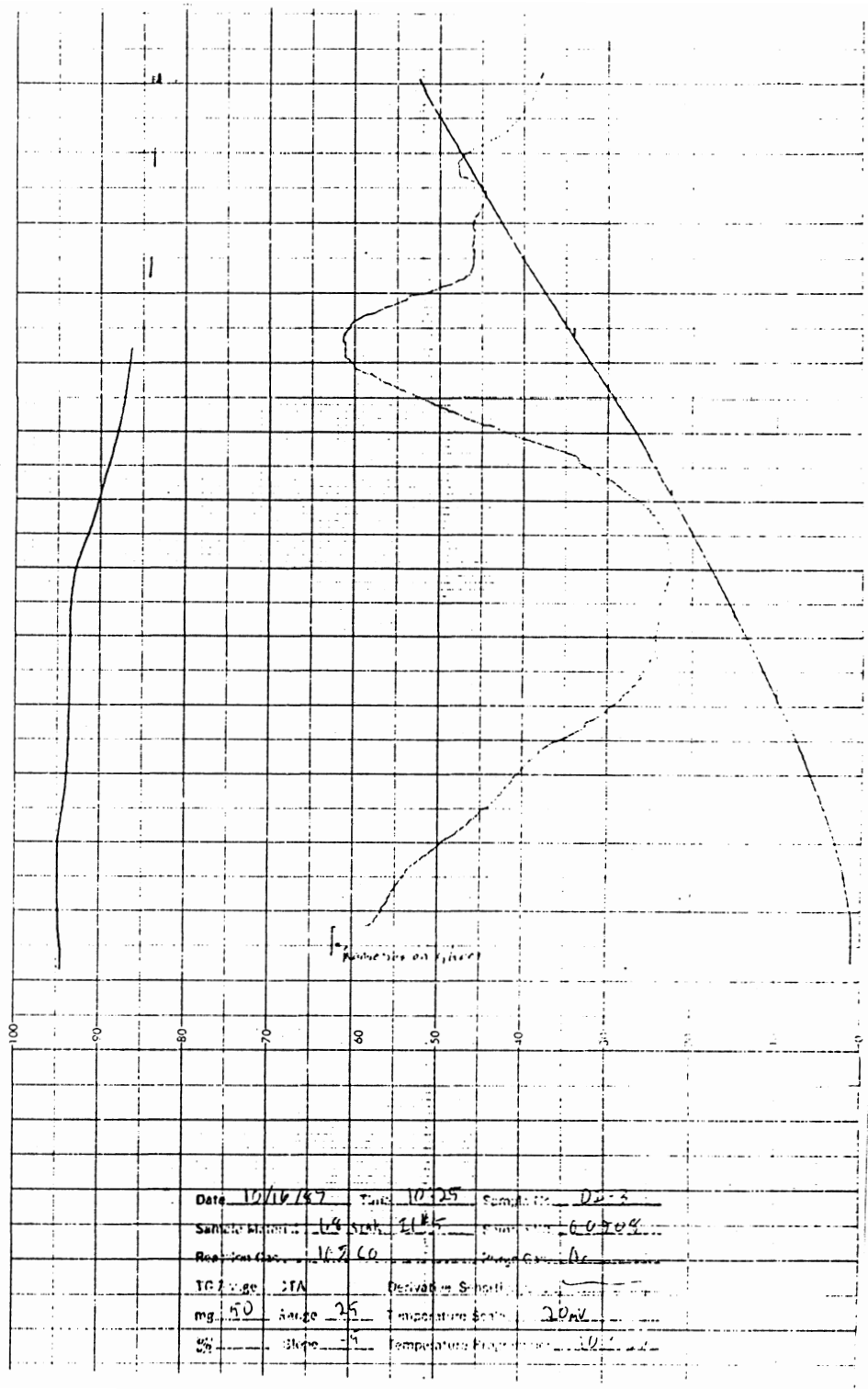
Figure 32: DTA/TGA recording for run DI-3
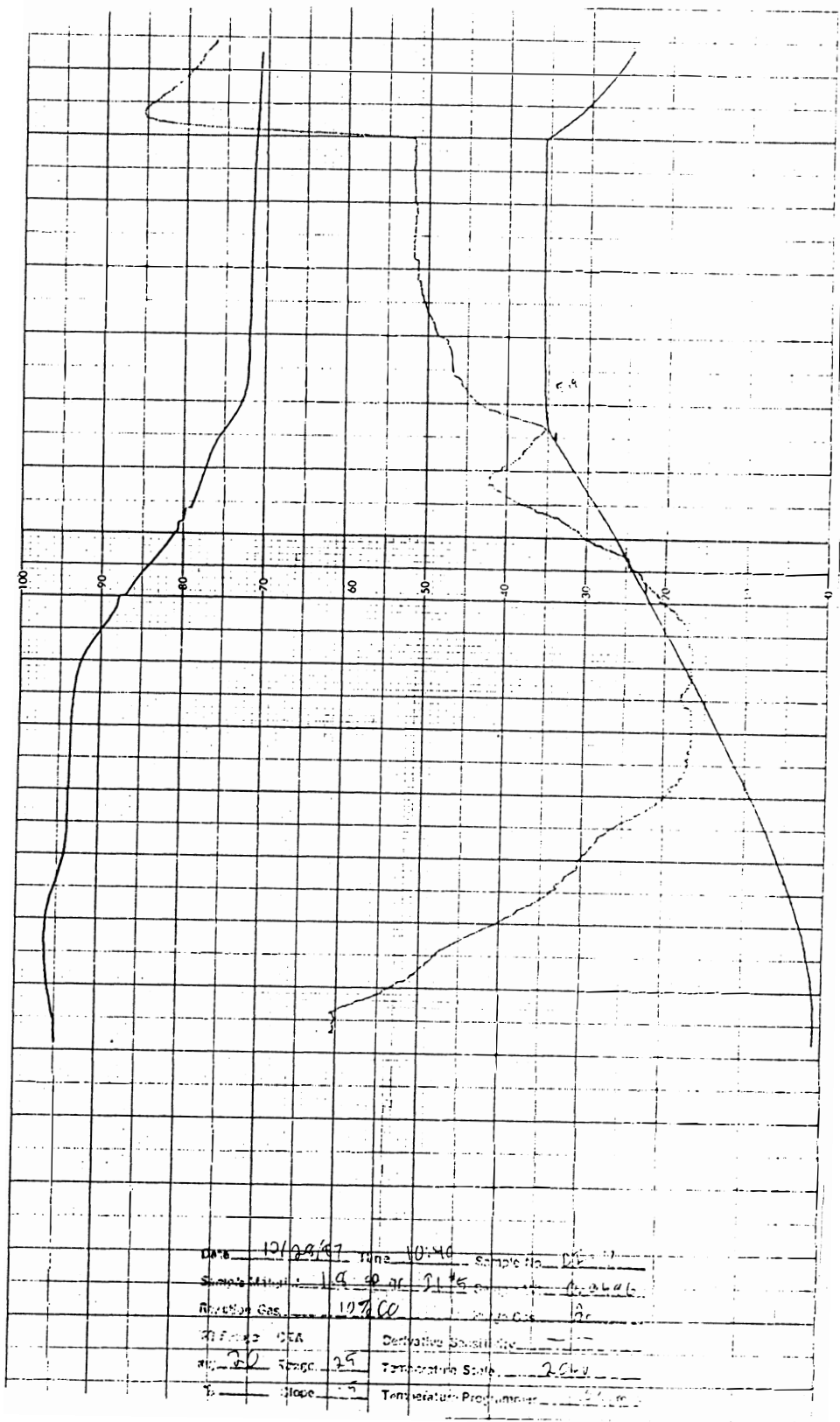
Figure 33: DTA/TGA recording for run DI-7
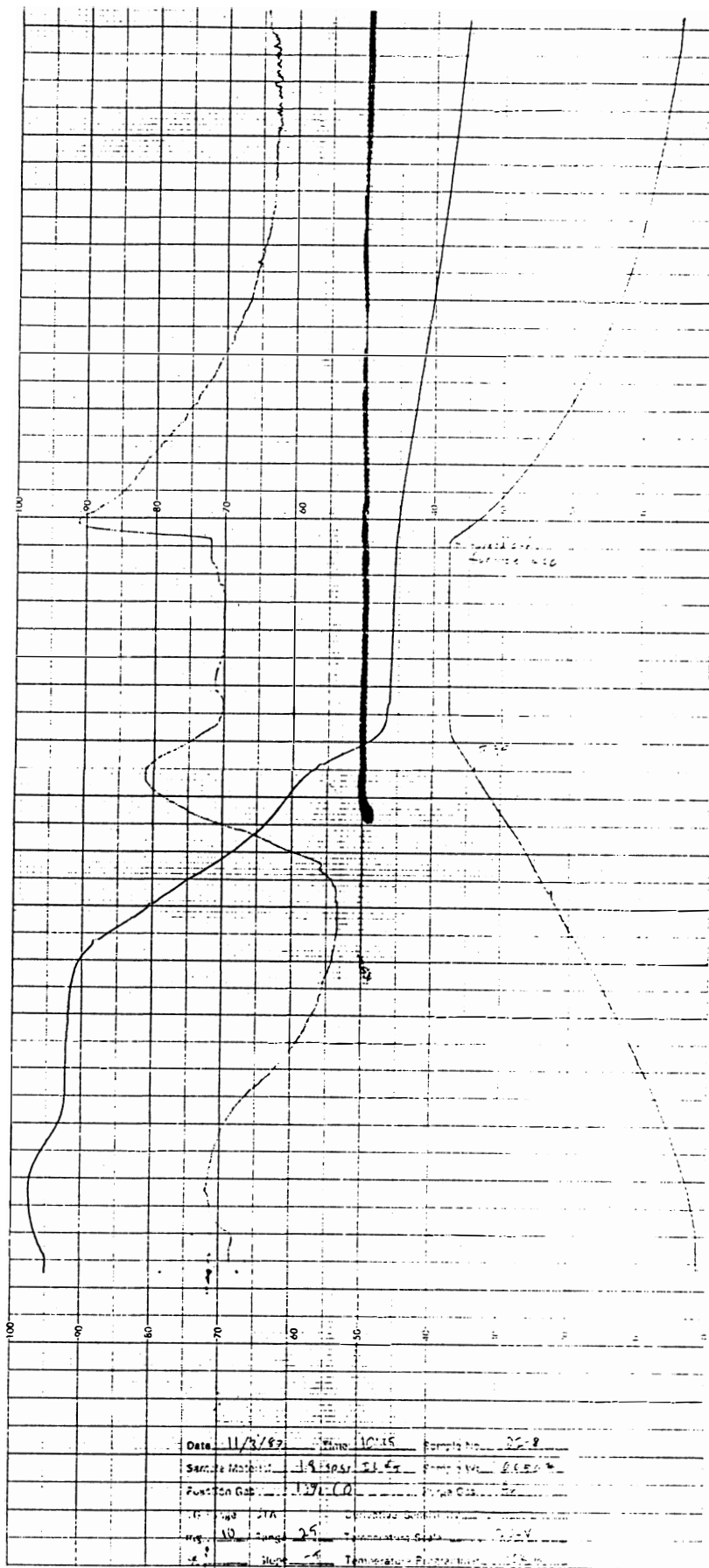
Figure 34: DTA/TGA recording for run DI-8
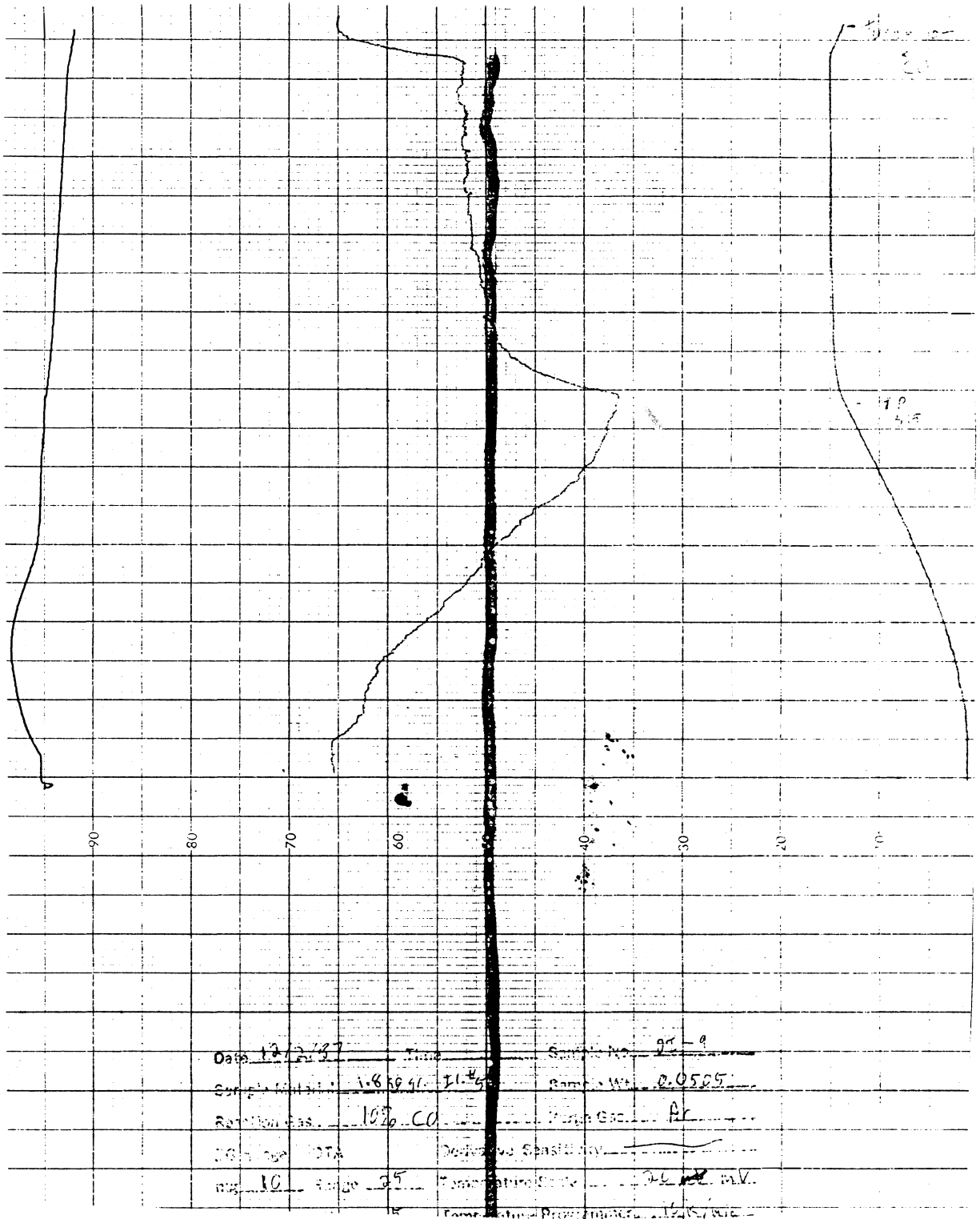
Figure 35: DTA/TGA recording for run DI-9

-84-

90 80 70 60 50 40 30 20 10

Date: 17/3/82

19 sp.m I dg   0.0 503.5

10% CO   Ar

10   15   20 mV

None   19 K/min
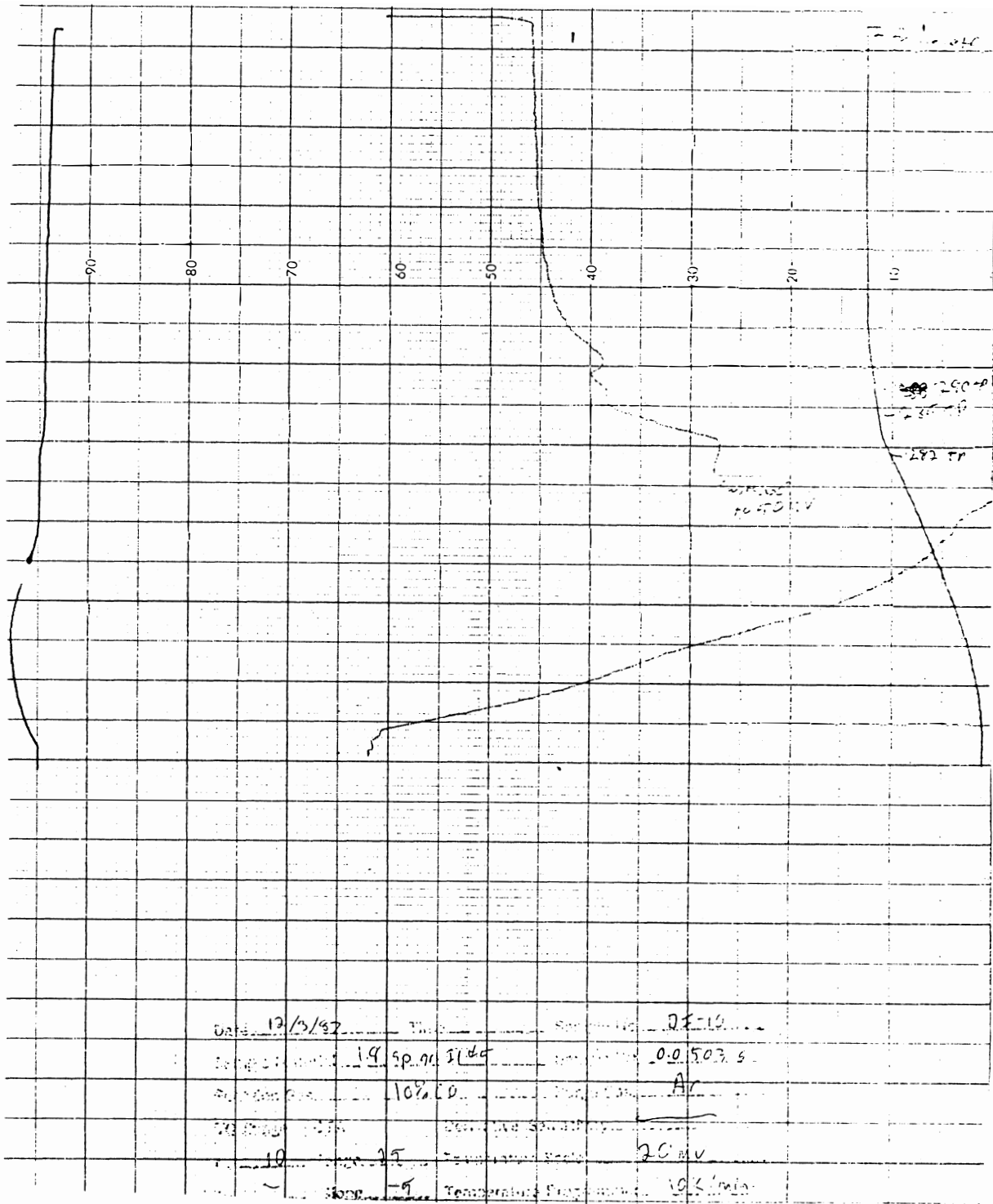
Figure 36: DTA/TGA recording for run DI-10
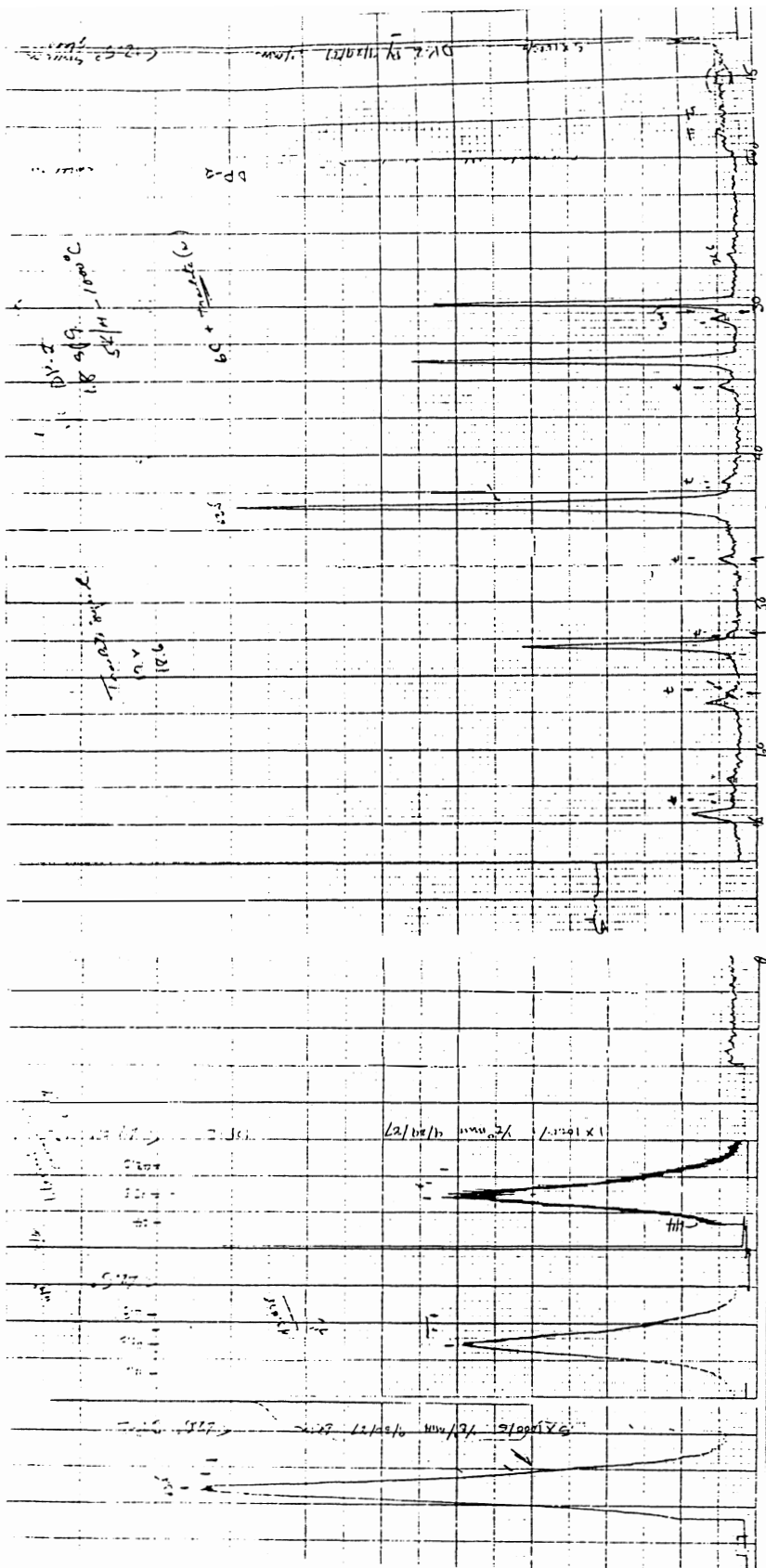
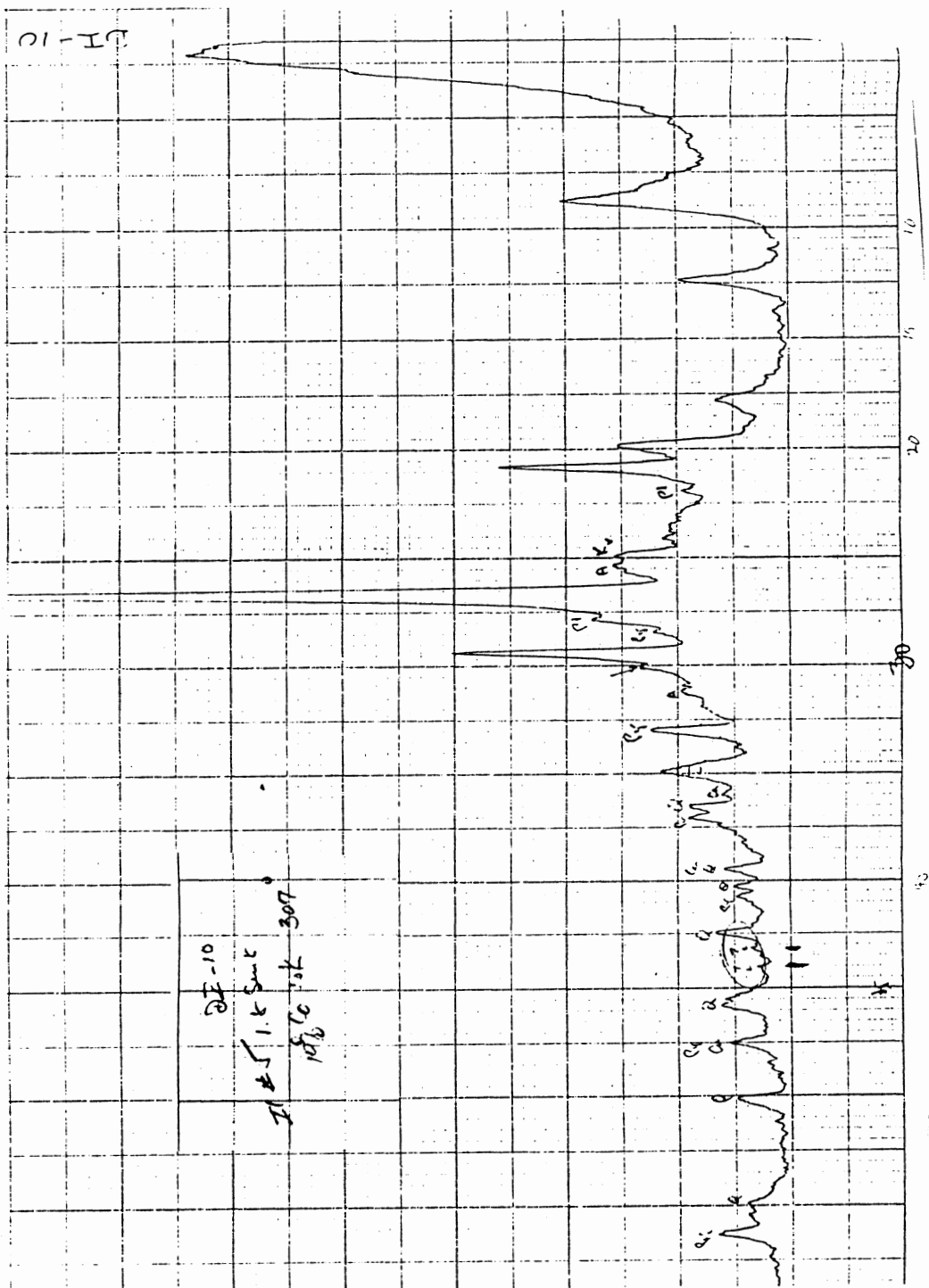Figure 37: XRD recording for run DP-2
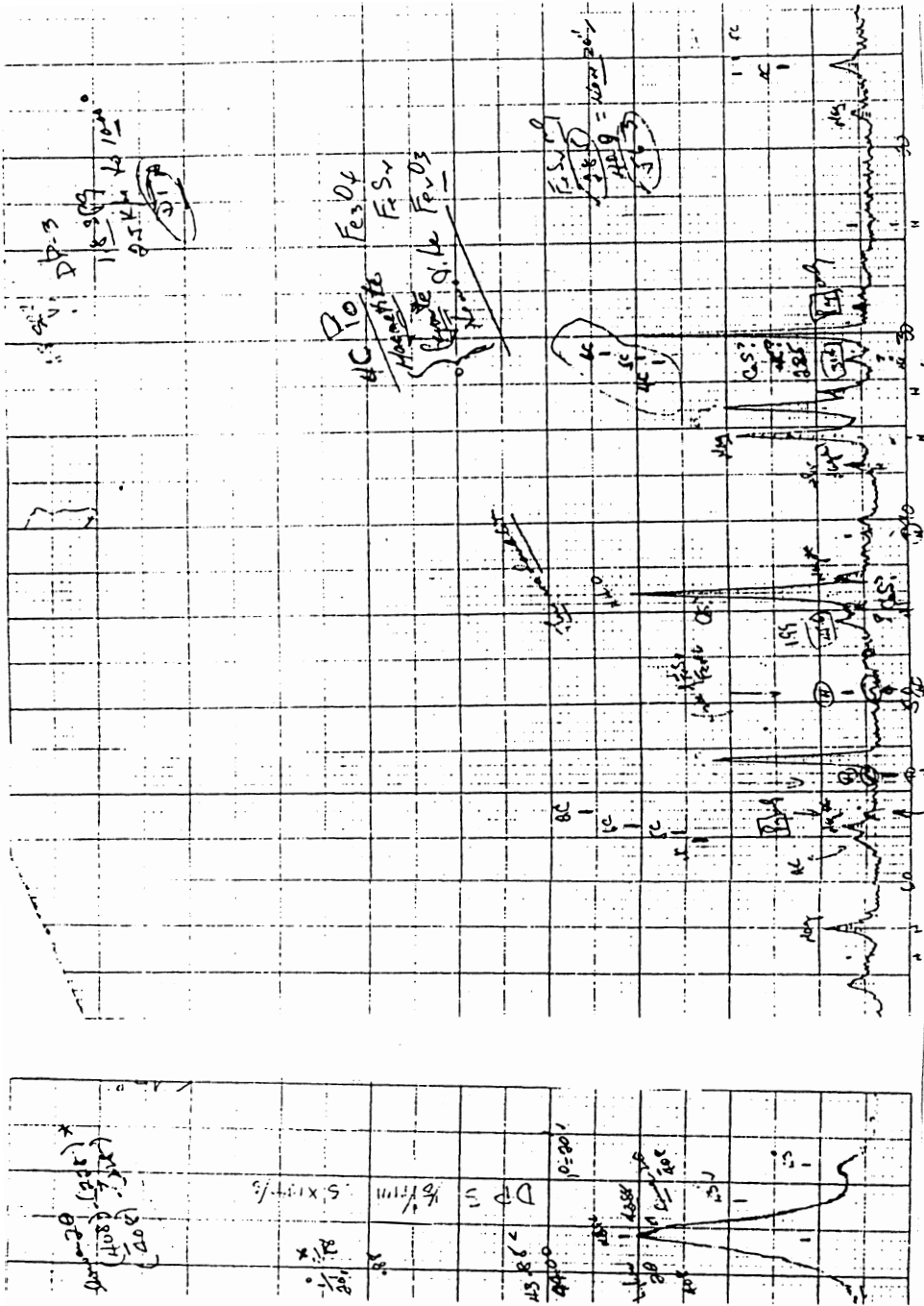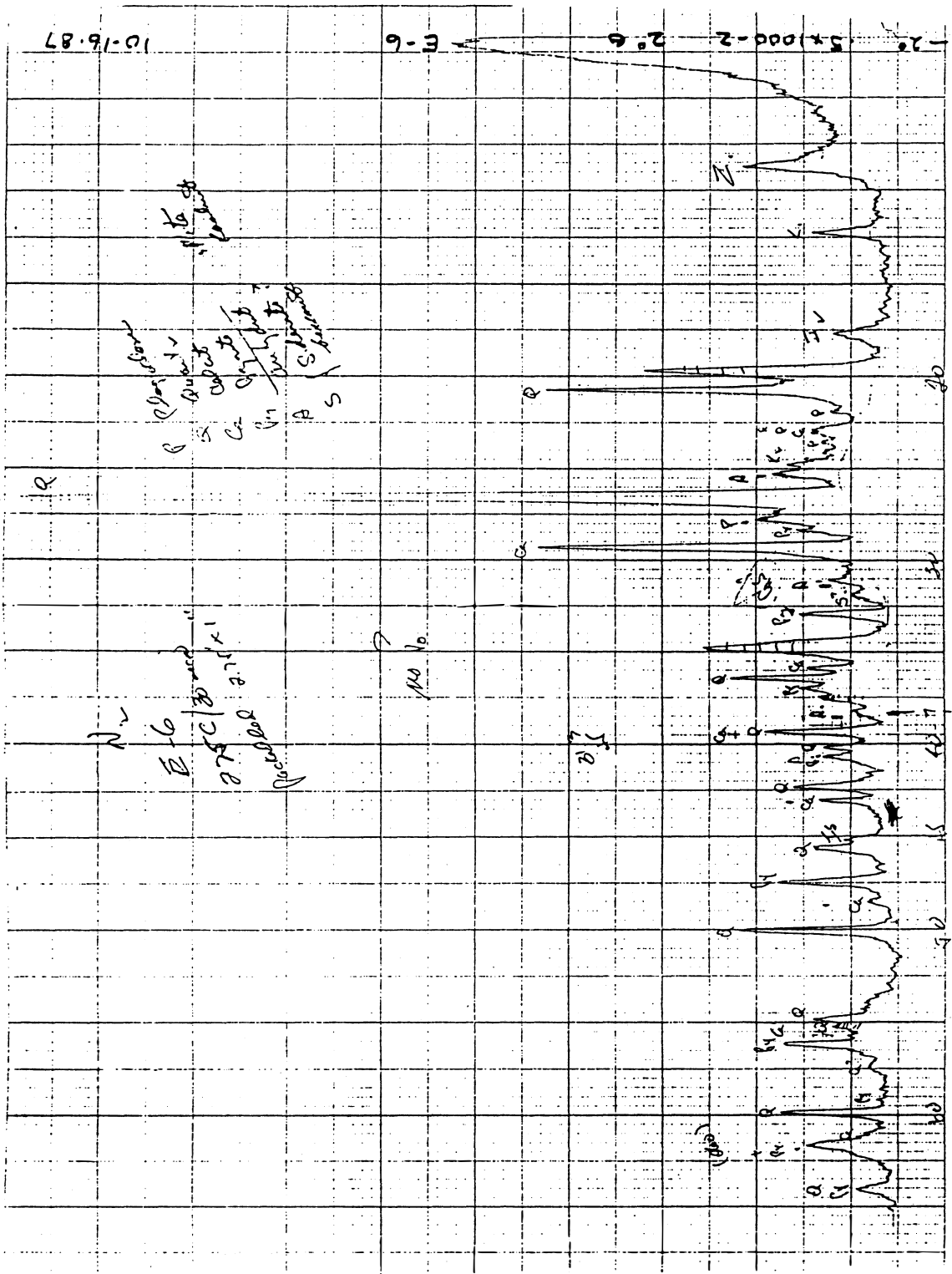
Figure 38: XRD recording for run DP-3
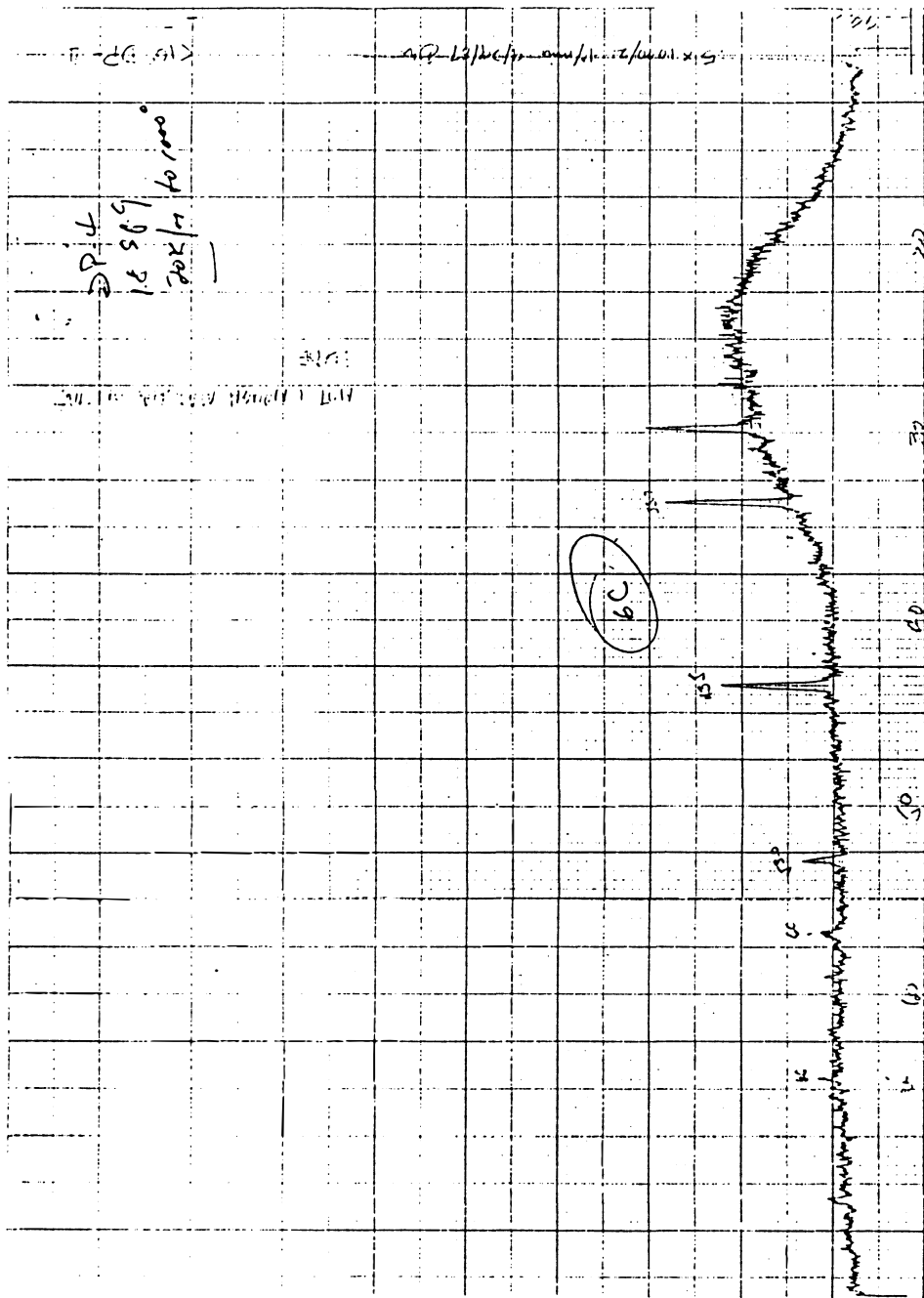
Figure 39: XRD recording for run DP-4
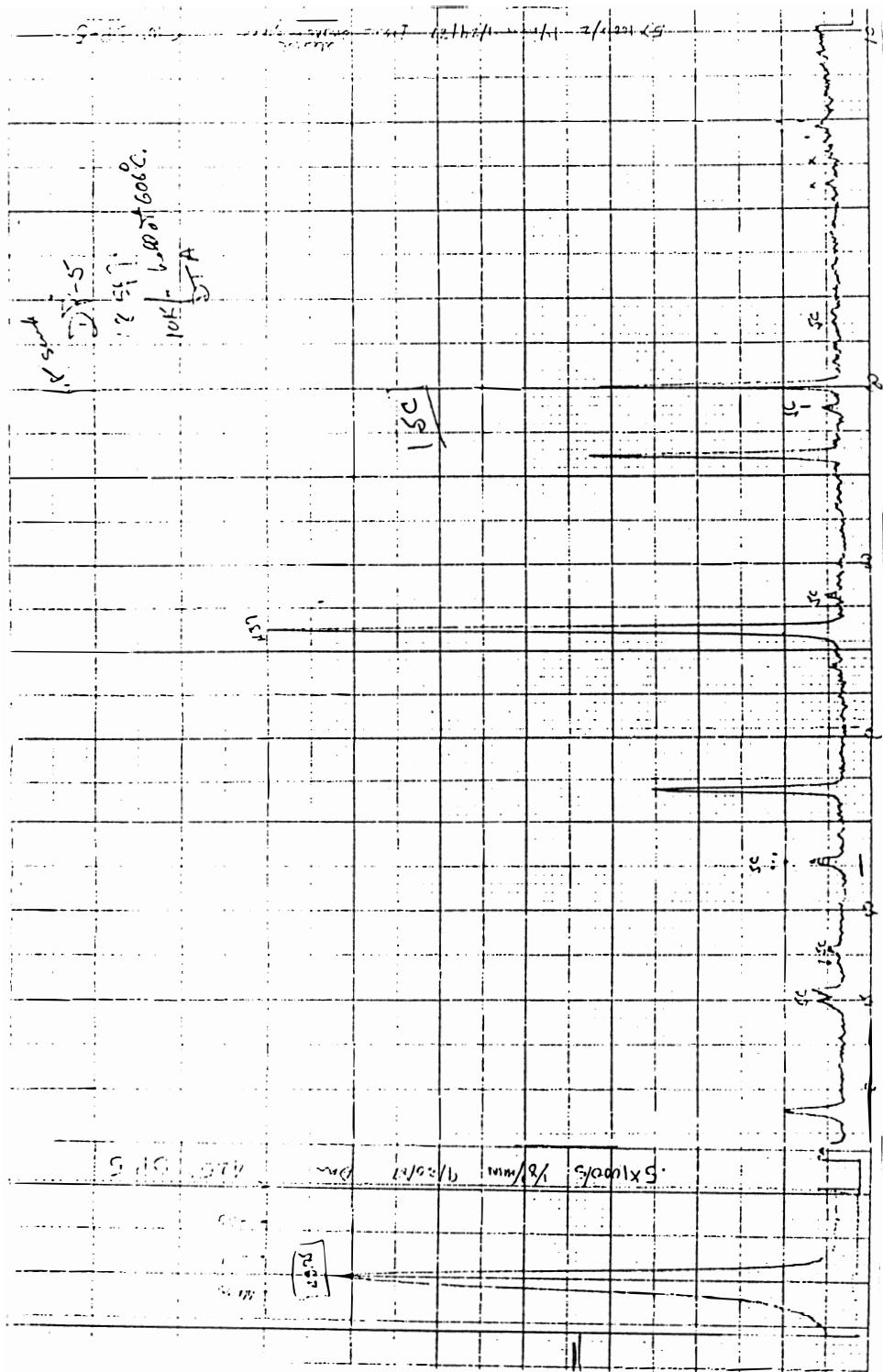
Figure 40: XRD recording for run DP-5
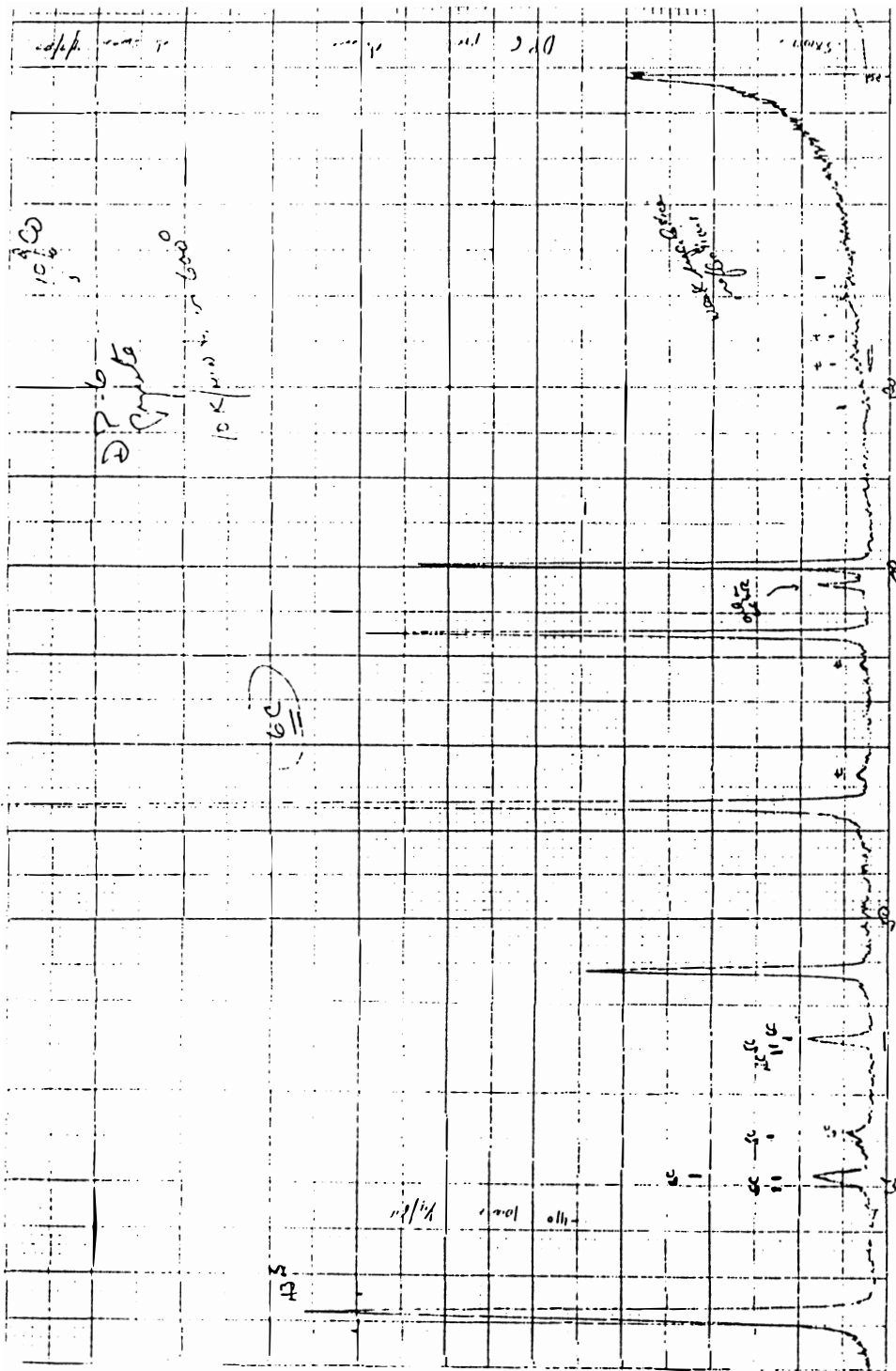
Figure 41: XRD recording for run DP-6

-90-
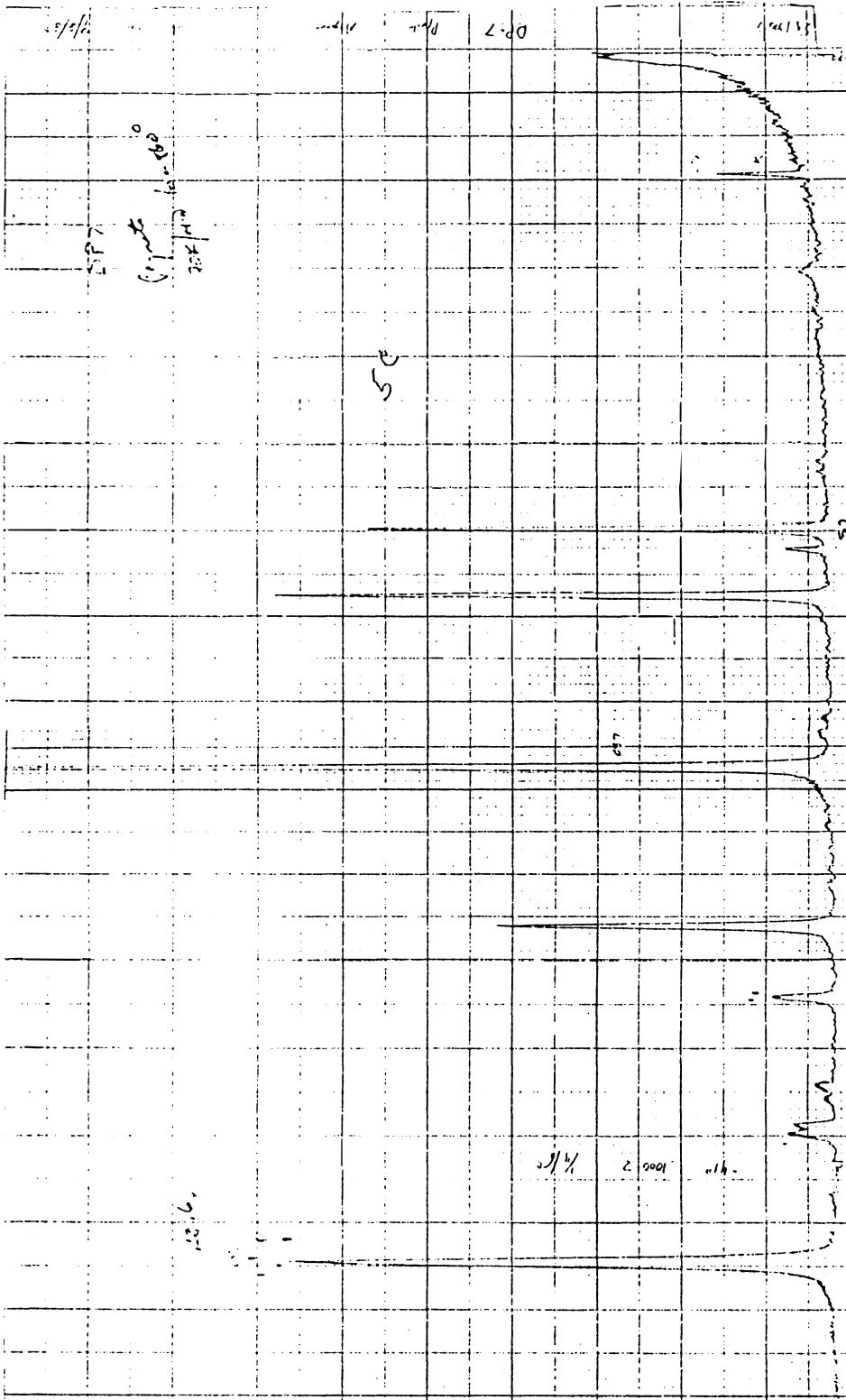
Figure 42: XRD recording for run DP-7
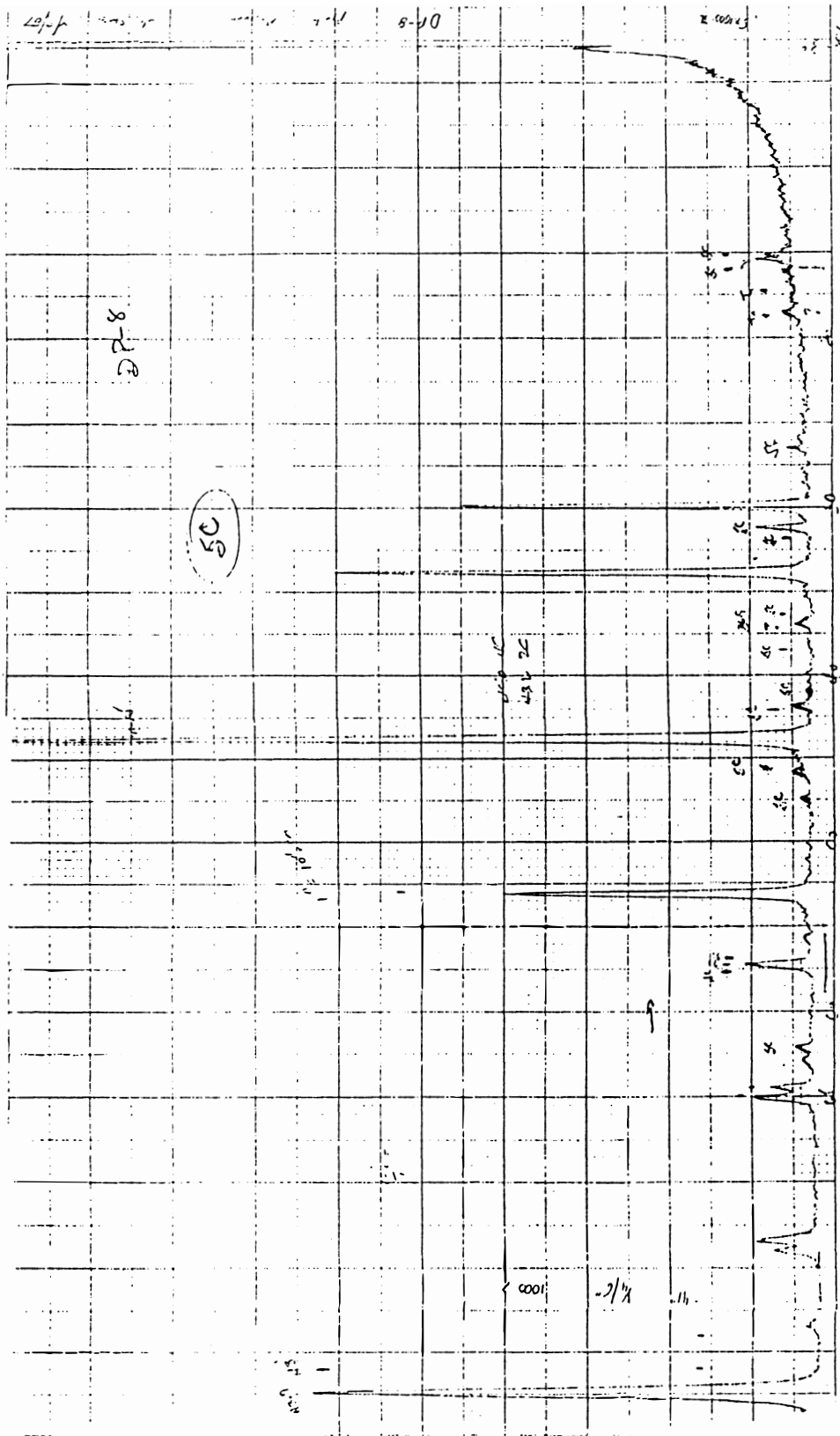
Figure 43: XRD recording for run DP-8
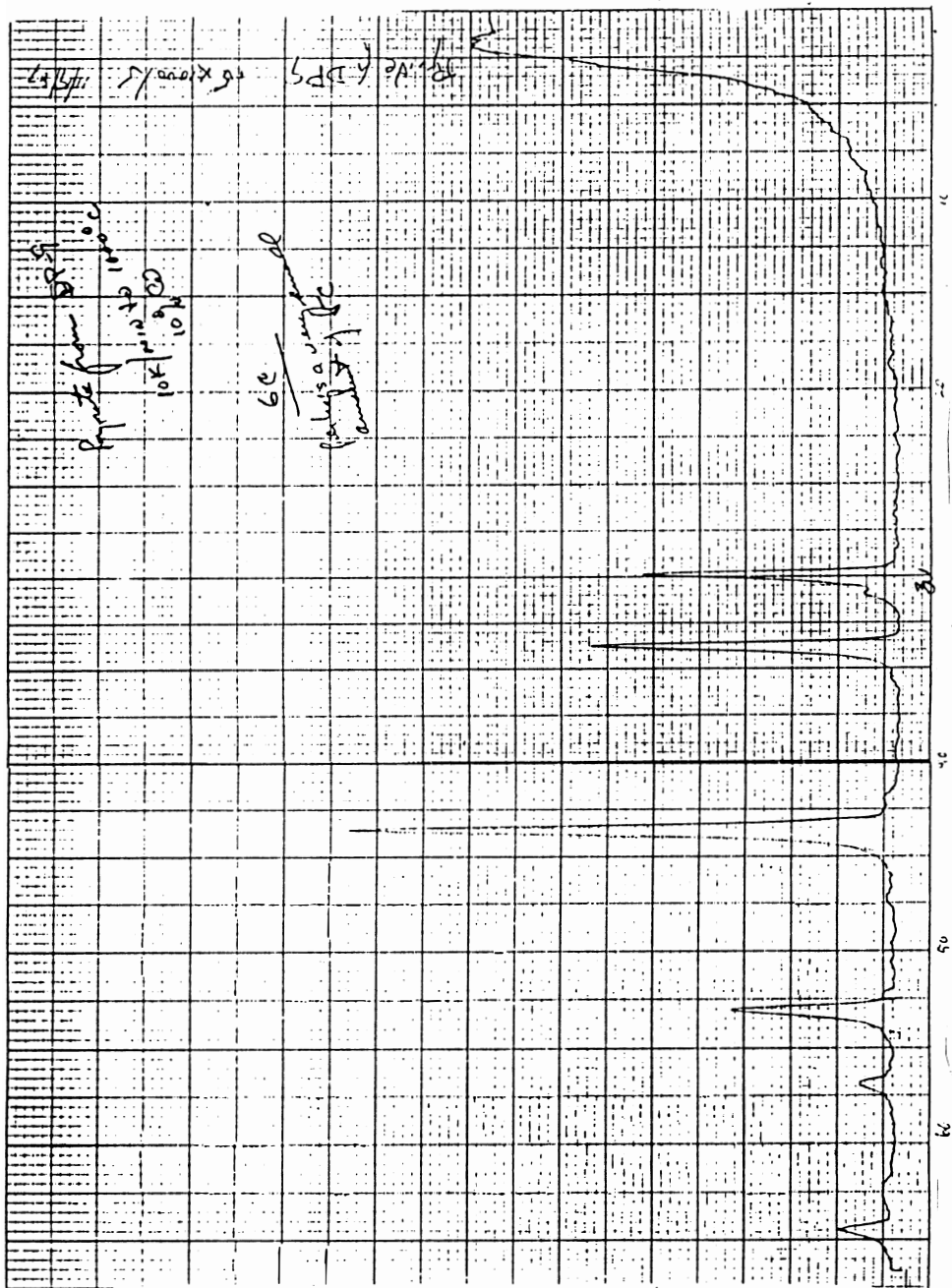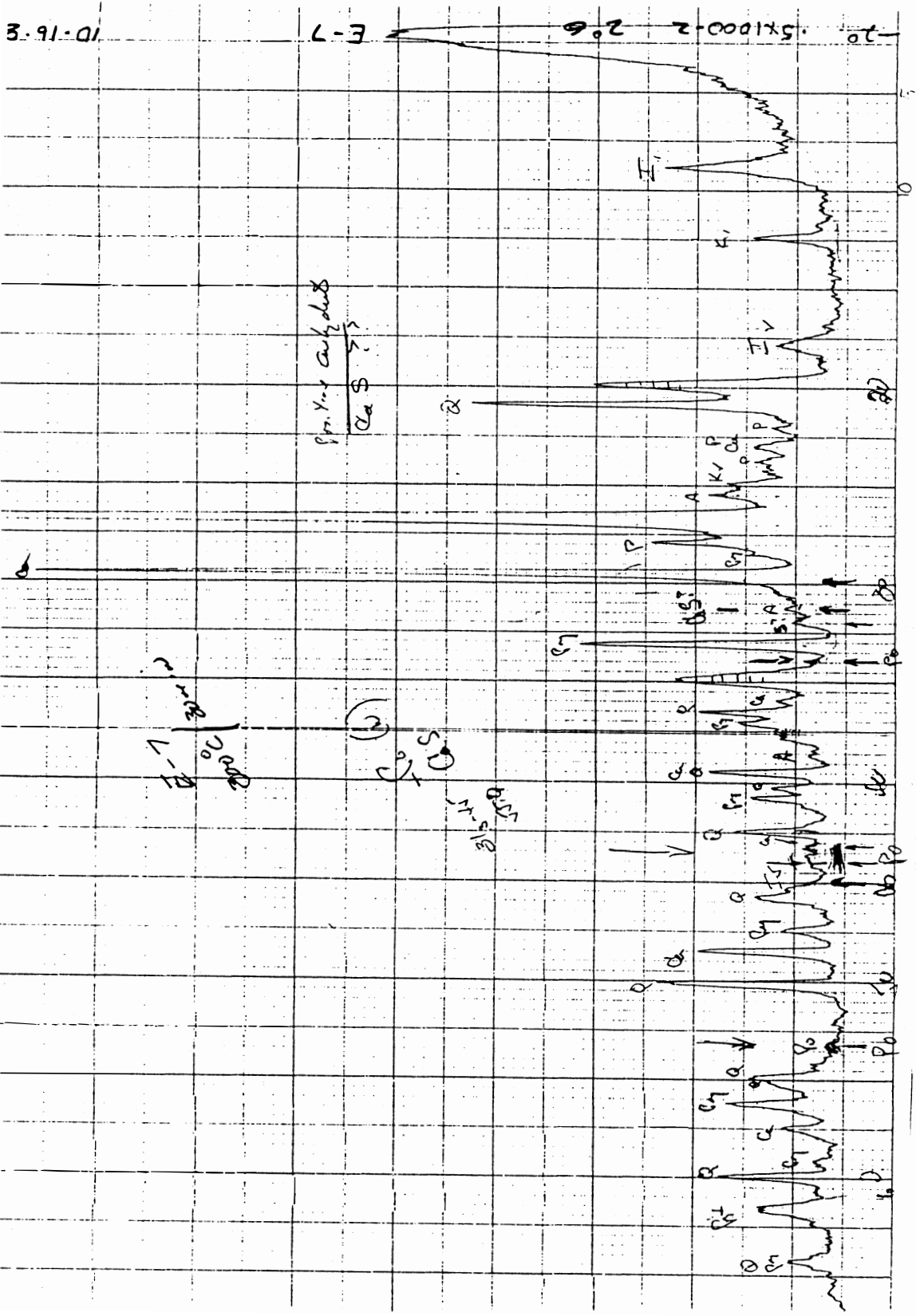
Figure 44: XRD recording for run DP-9

-93-
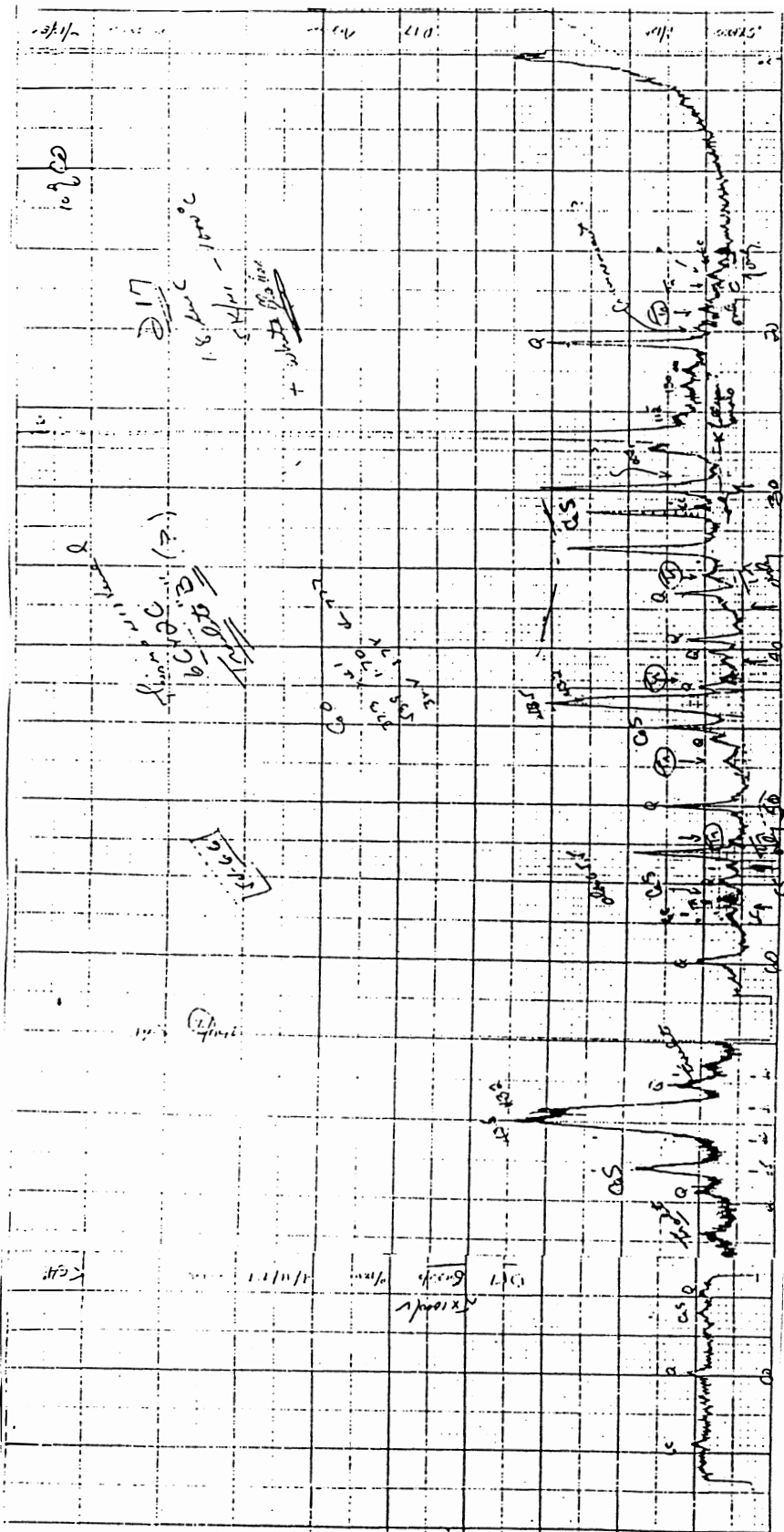
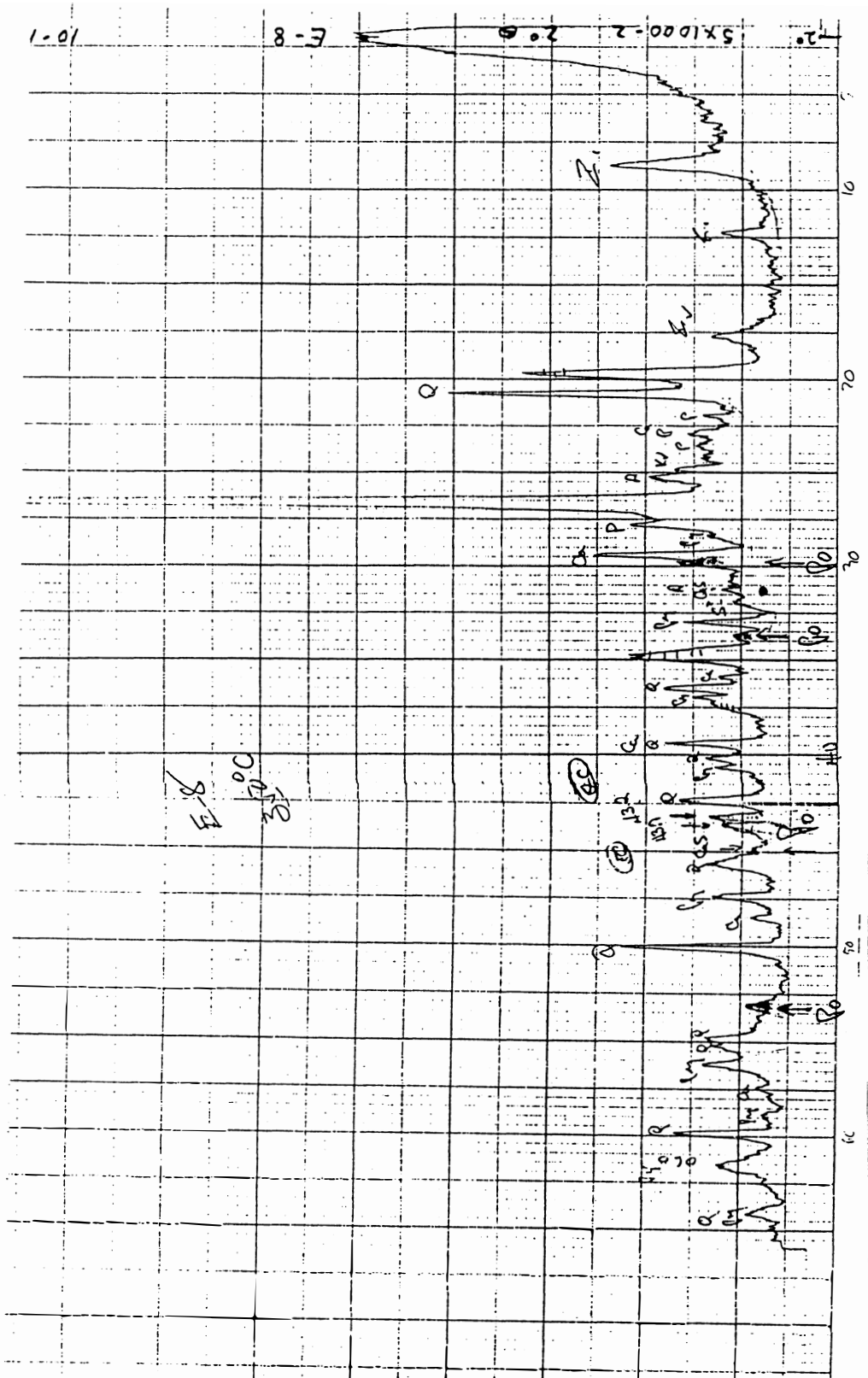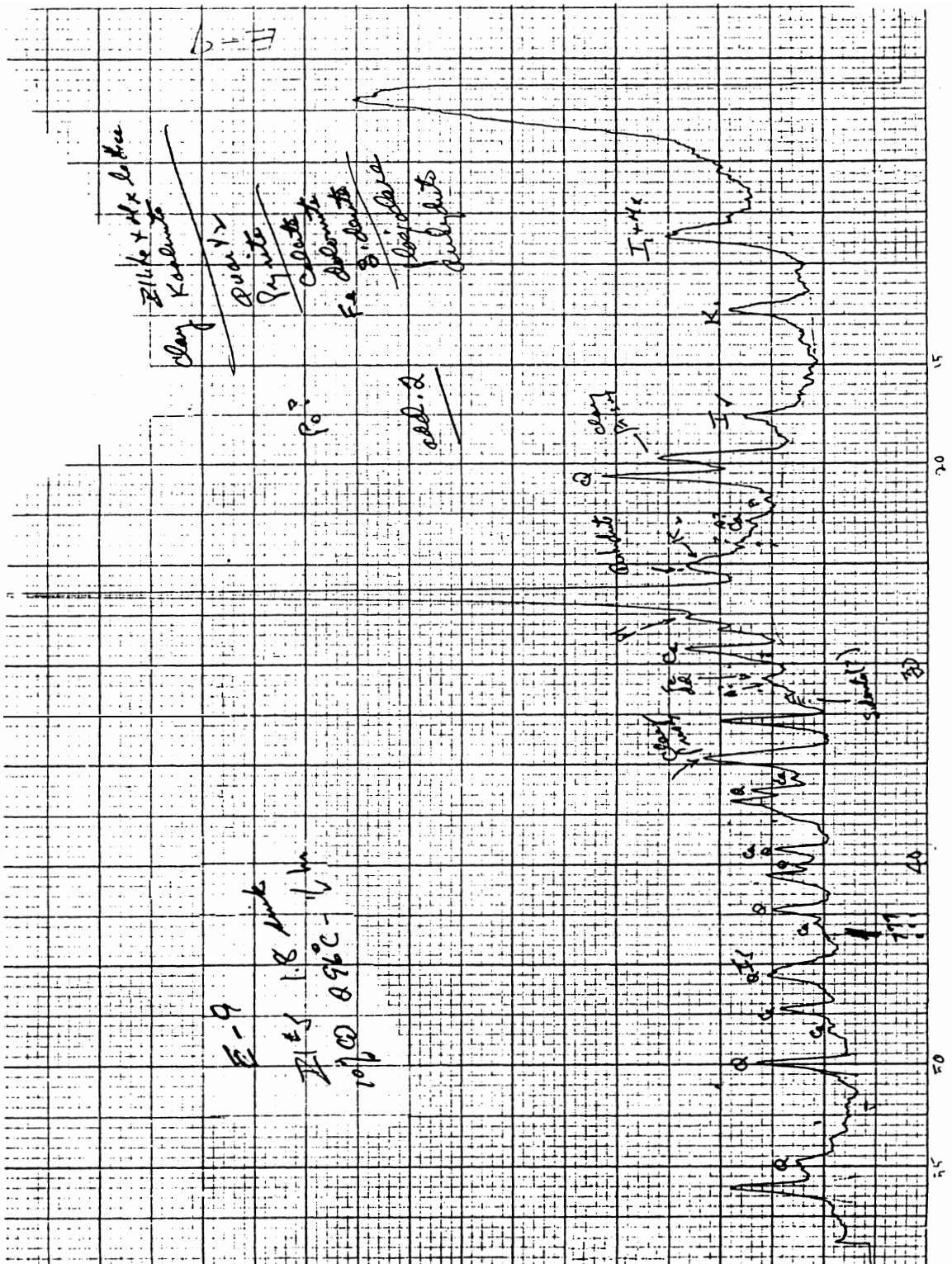Figure 45: XRD recording for run D-17
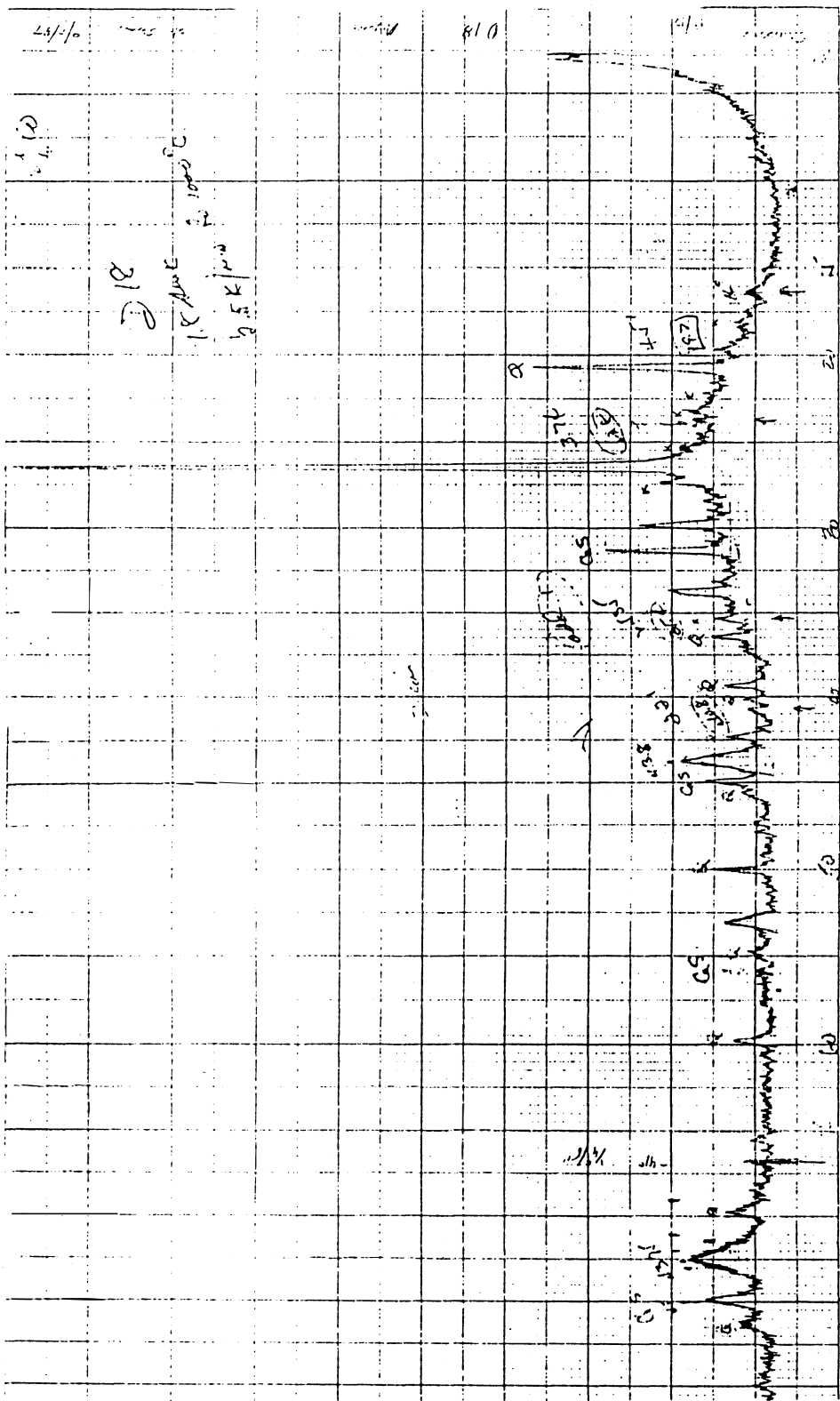
Figure 46: XRD recording for run D-18
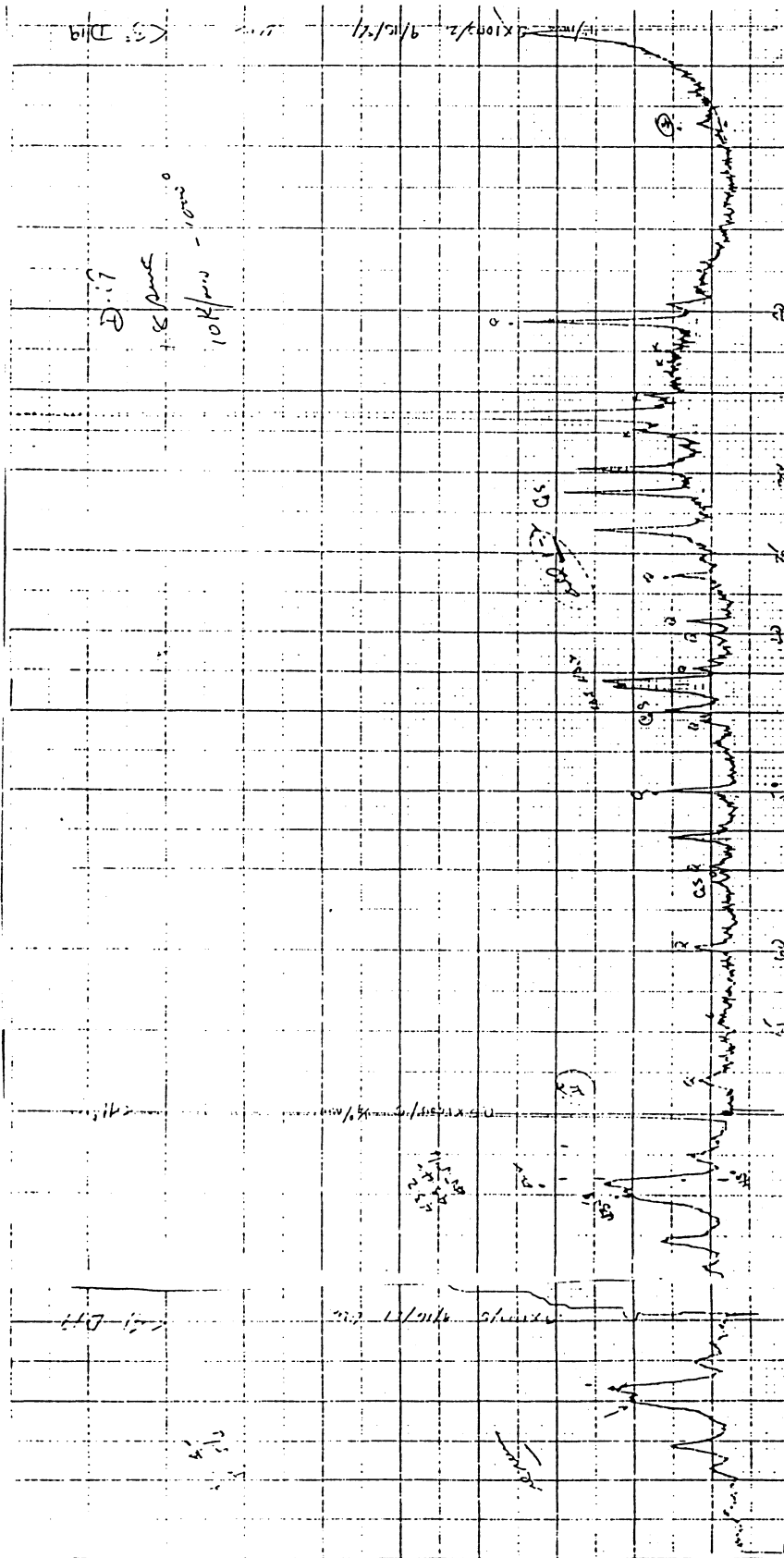
Figure 47: XRD recording for run D-19
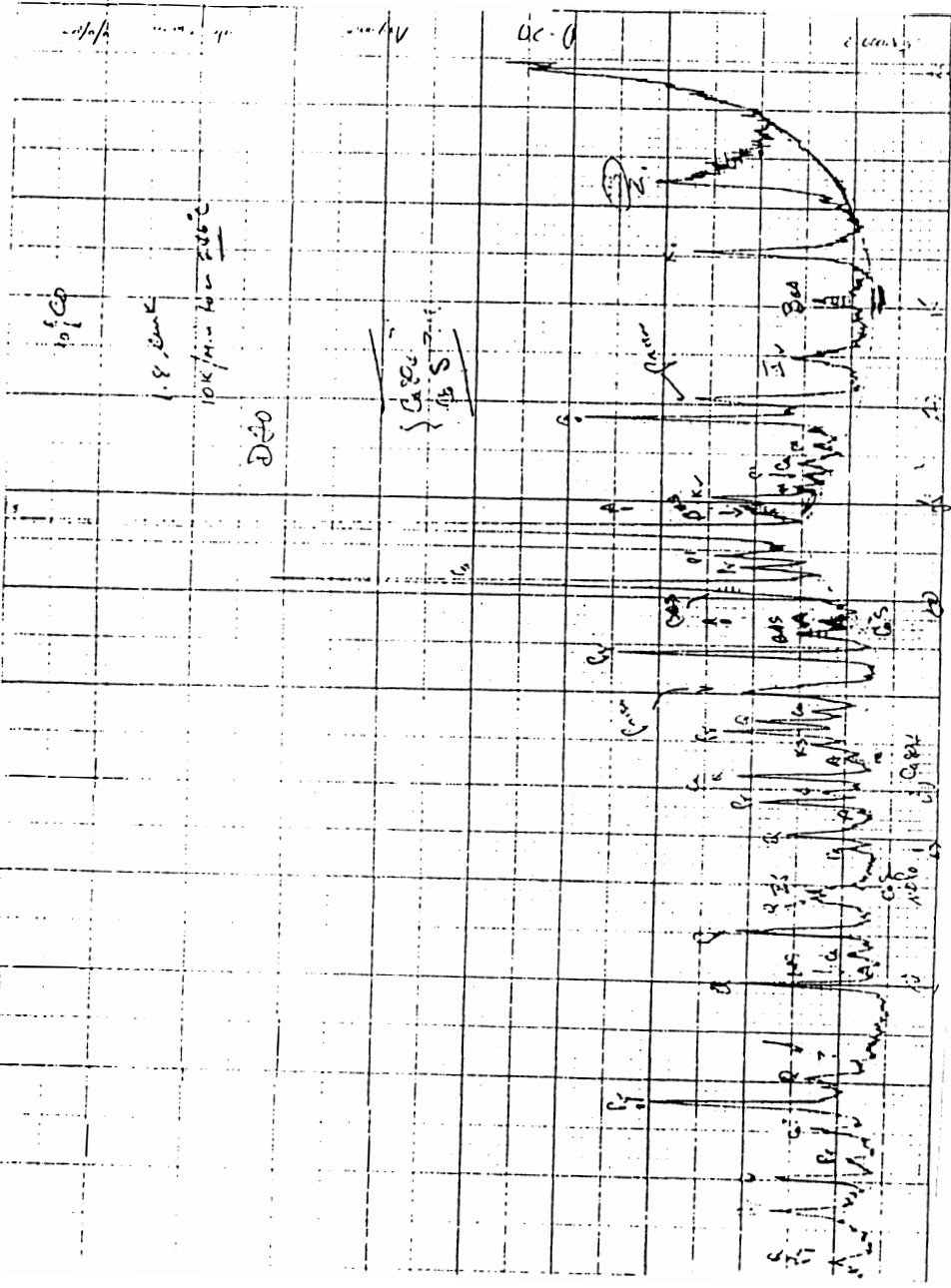
Figure 48: XRD recording for run D-20
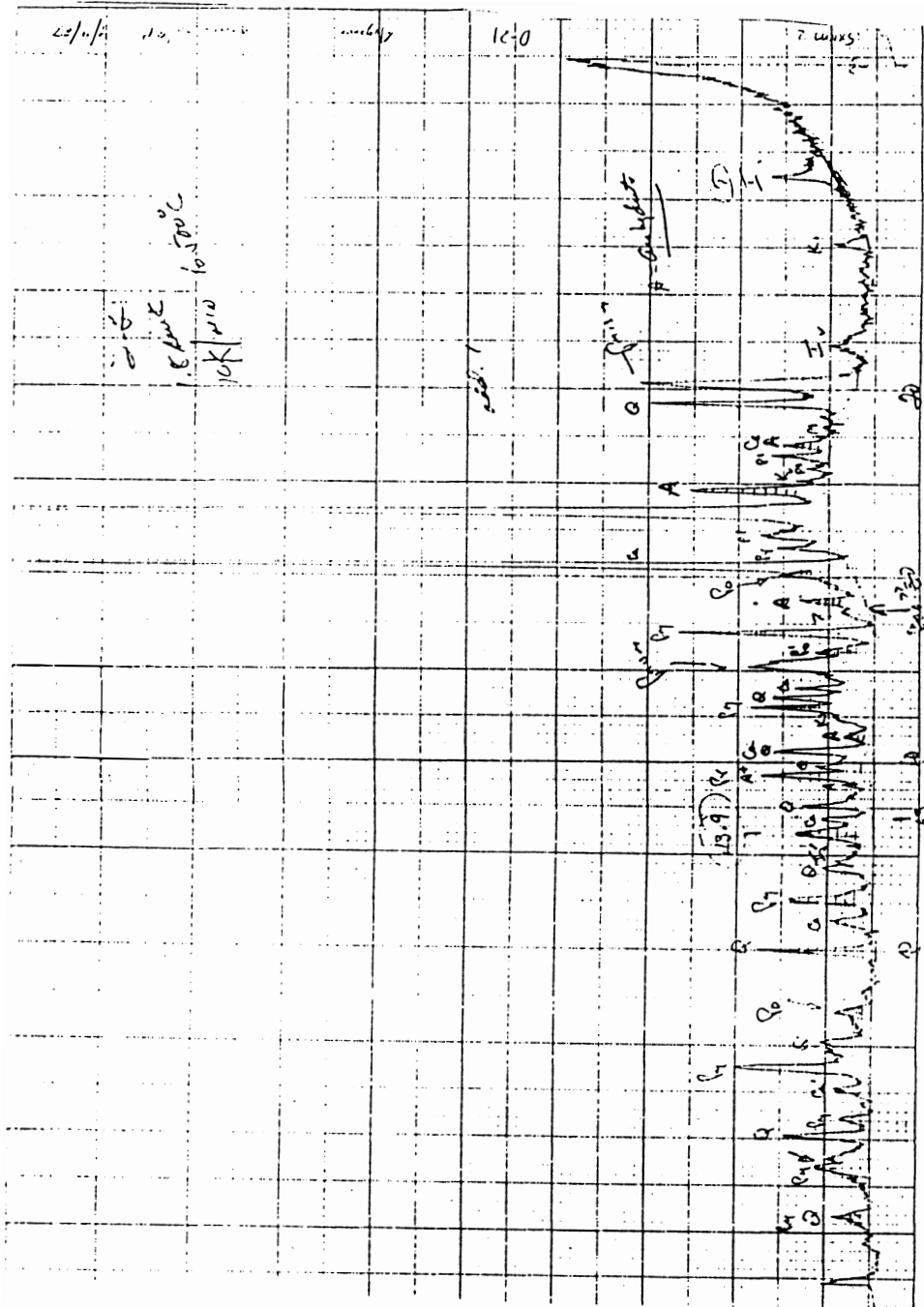
Figure 49: XRD recording for run D-21
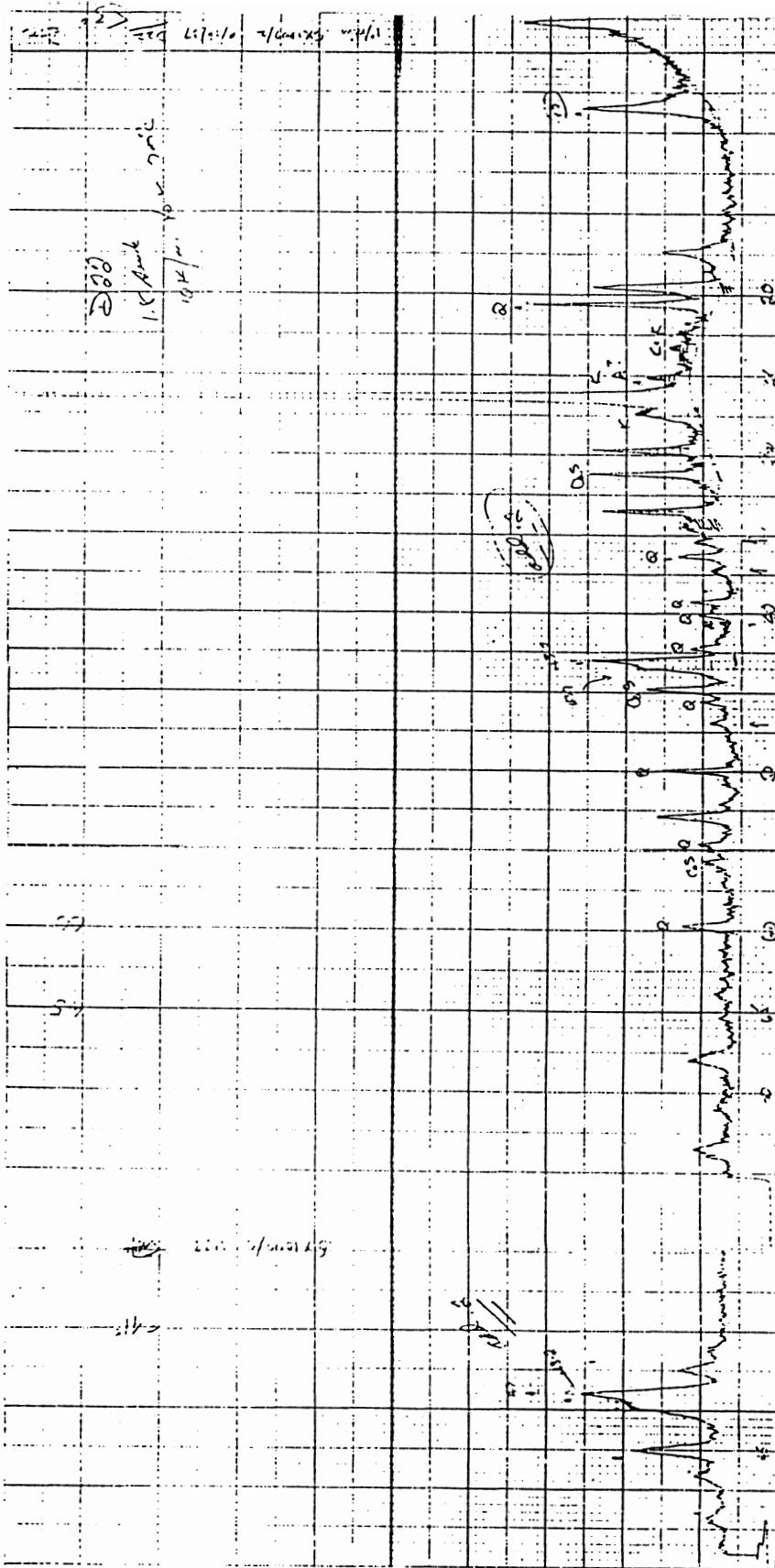
Figure 50: XRD recording for run D-22
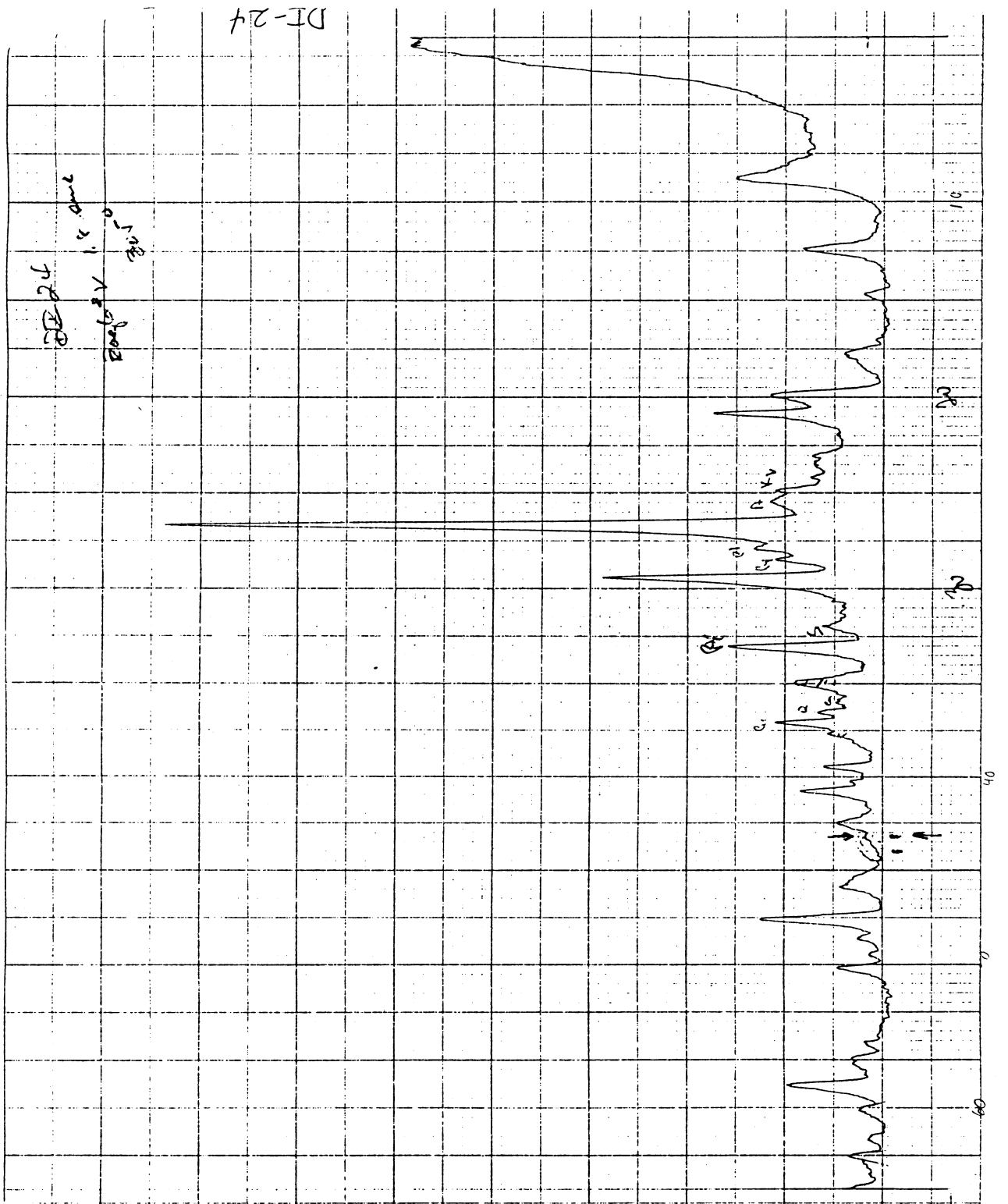
Figure 51: XRD recording for run D-24
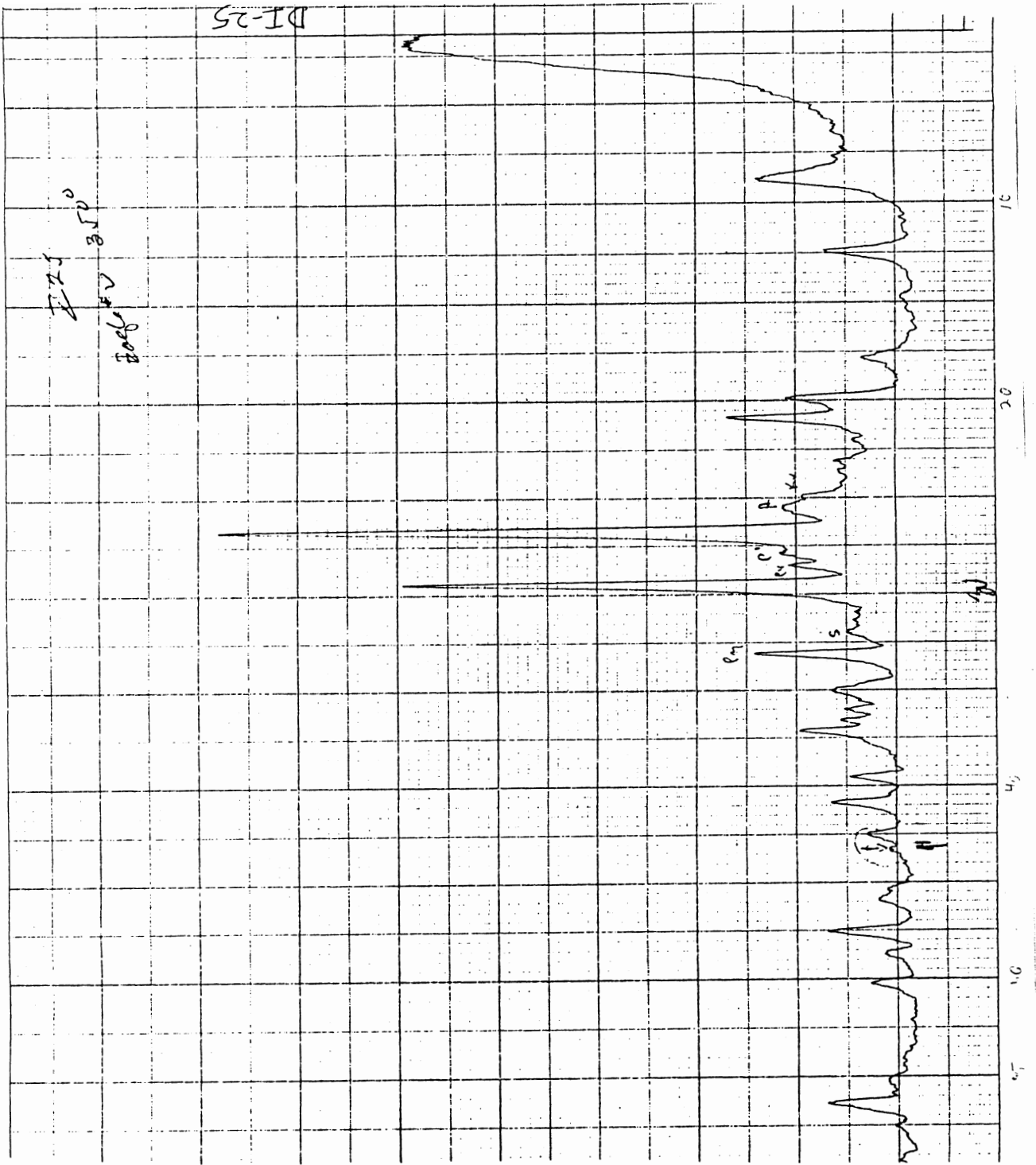
Figure 52: XRD recording for run D-25
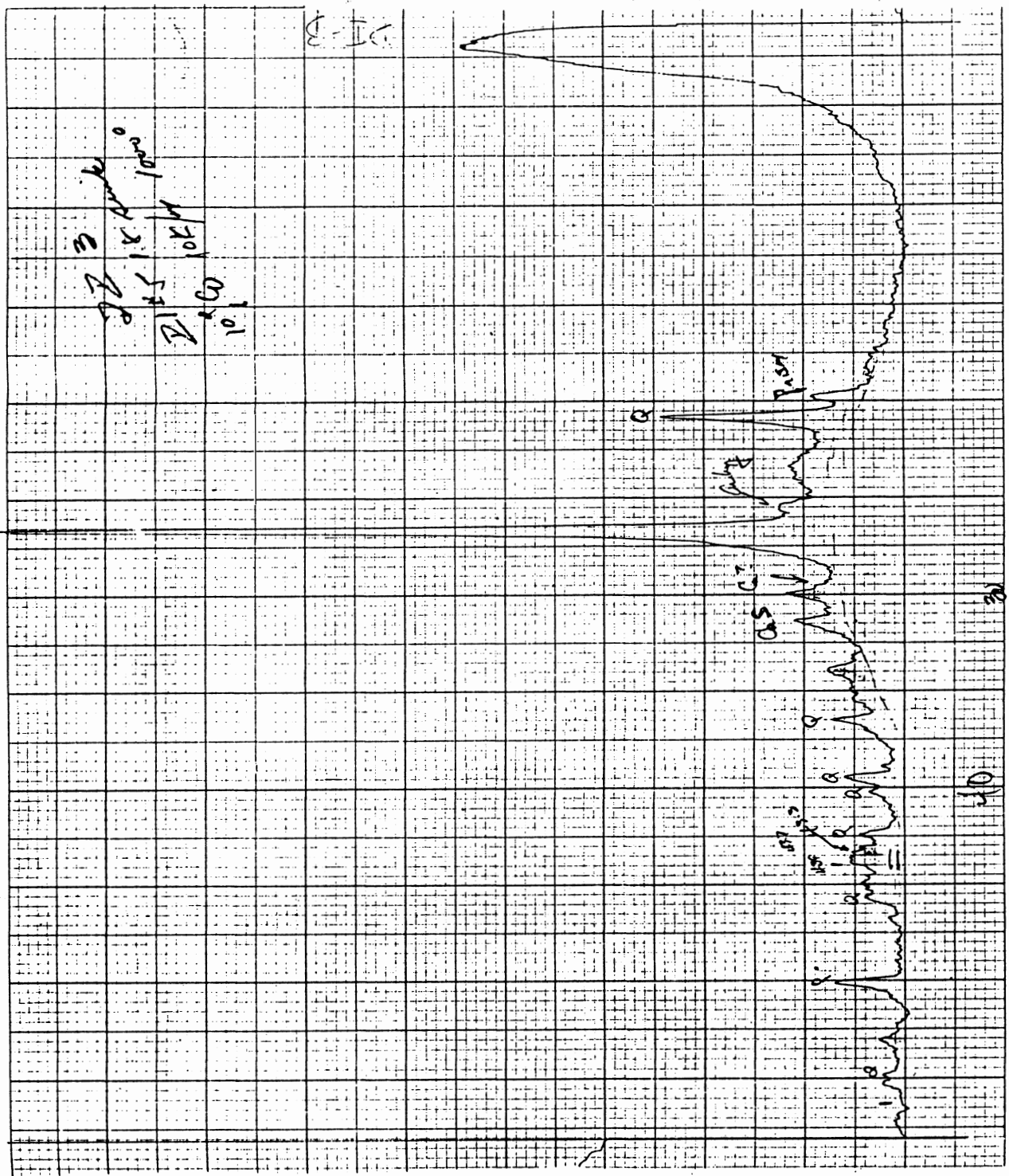
Figure 53: XRD recording for run DI-3
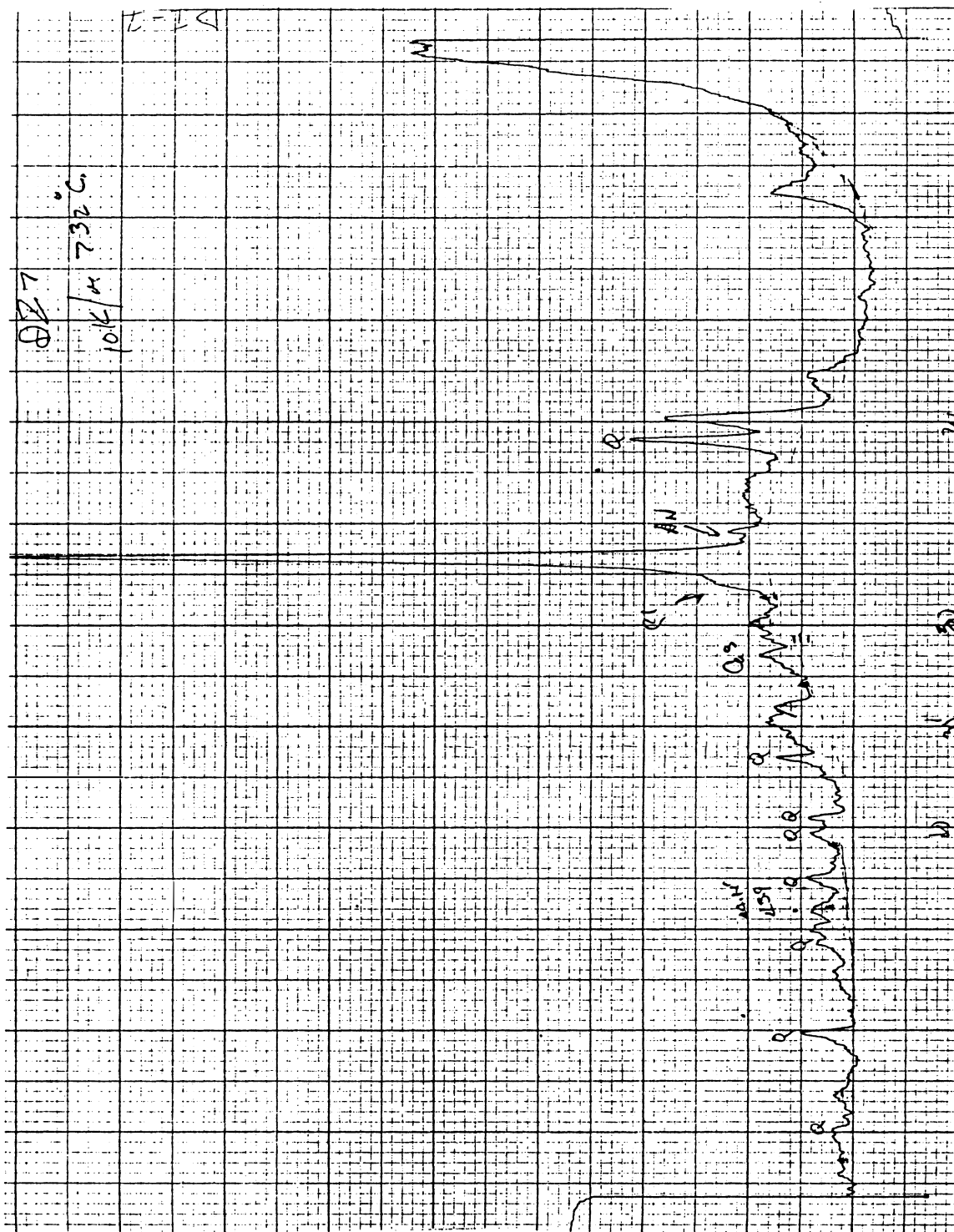
Figure 54: XRD recording for run DI-7
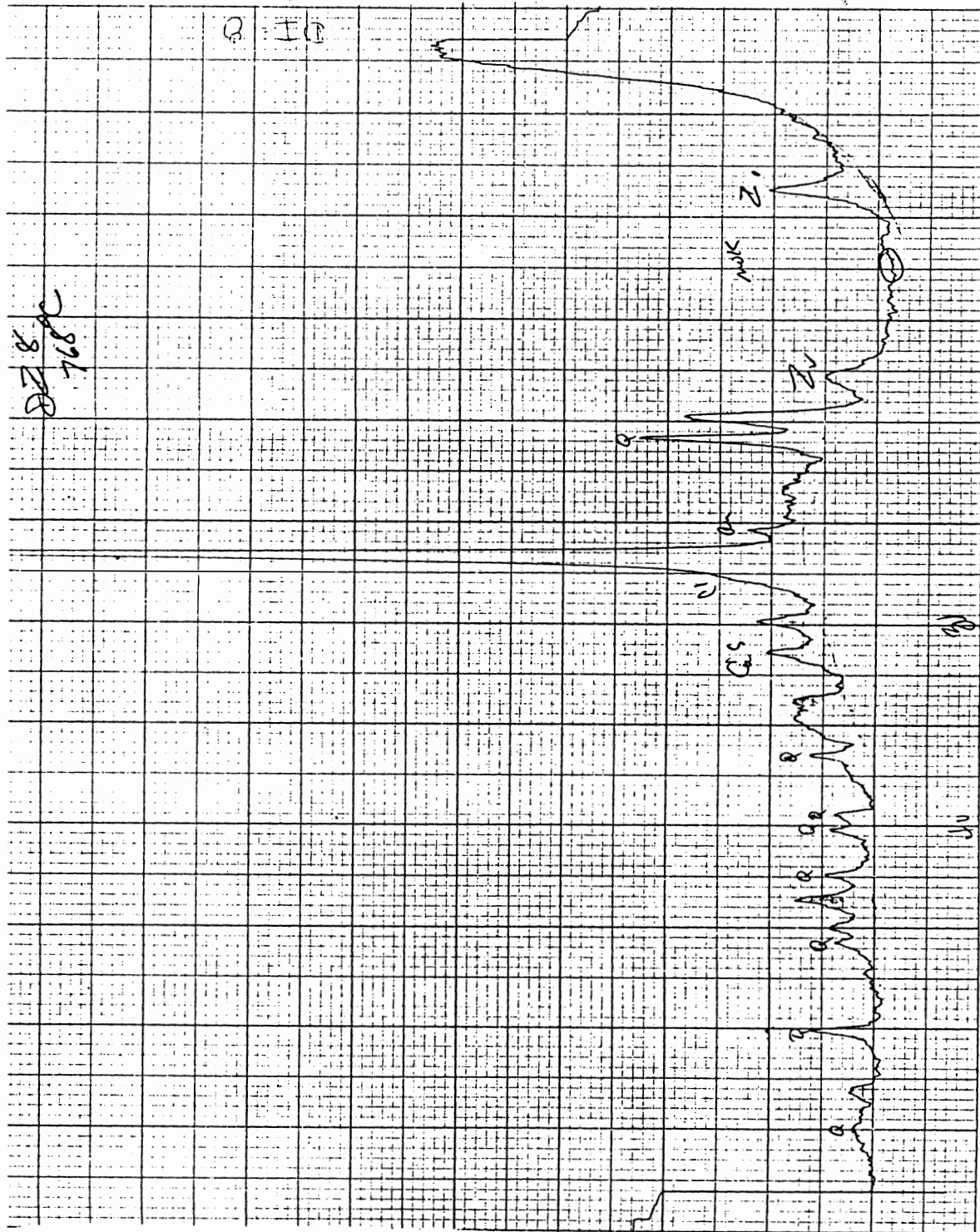
Figure 55: XRD recording for run DI-8
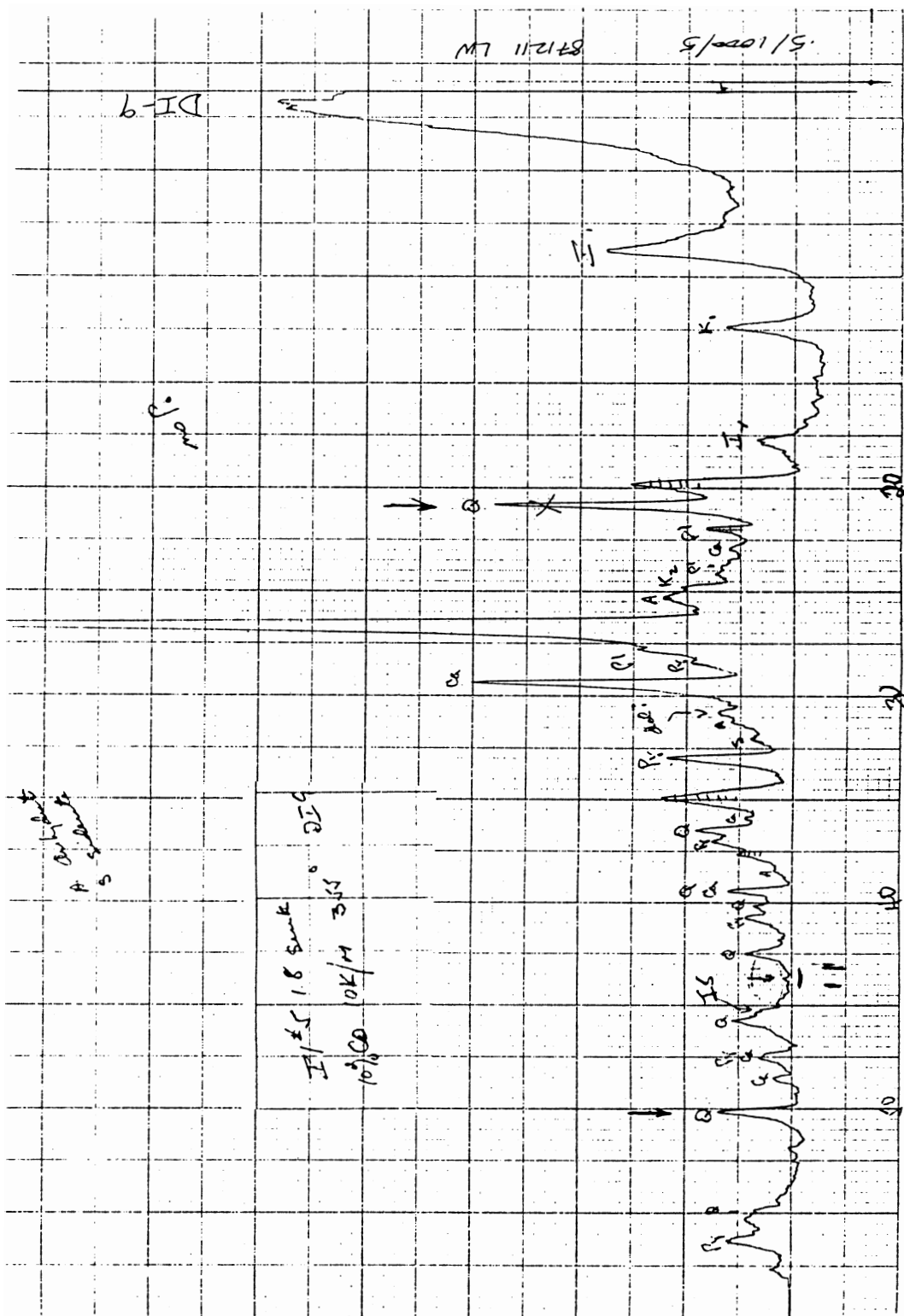
Figure 56: XRD recording for run DI-9

Figure 57: XRD recording for run DI-10

Figure 58: XRD recording for run E-1

Figure 59: XRD recording for run E-6

-108-

Figure 60: XRD recording for run E-7

Figure 61: XRD recording for run E-8
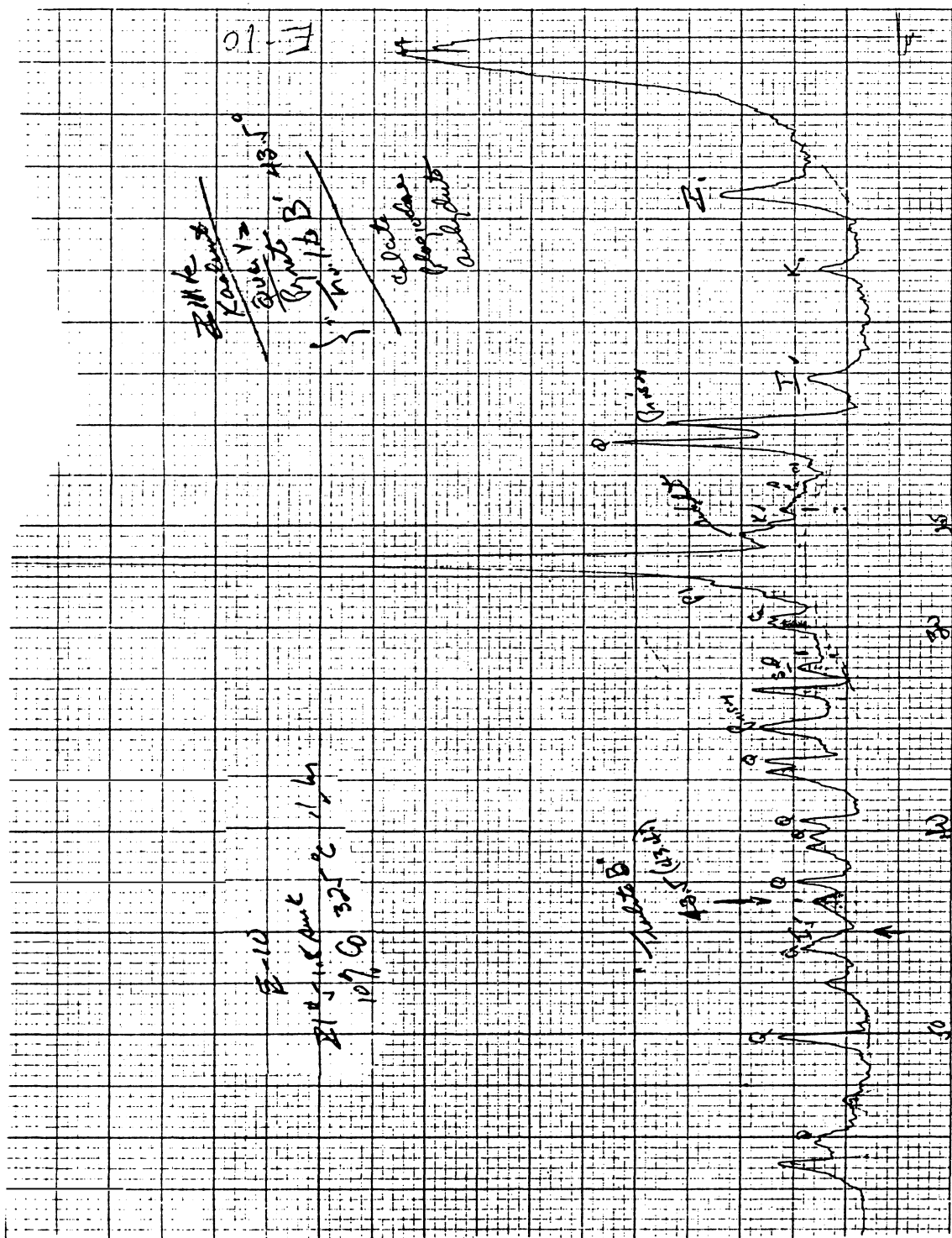
Figure 62: XRD recording for run E-9
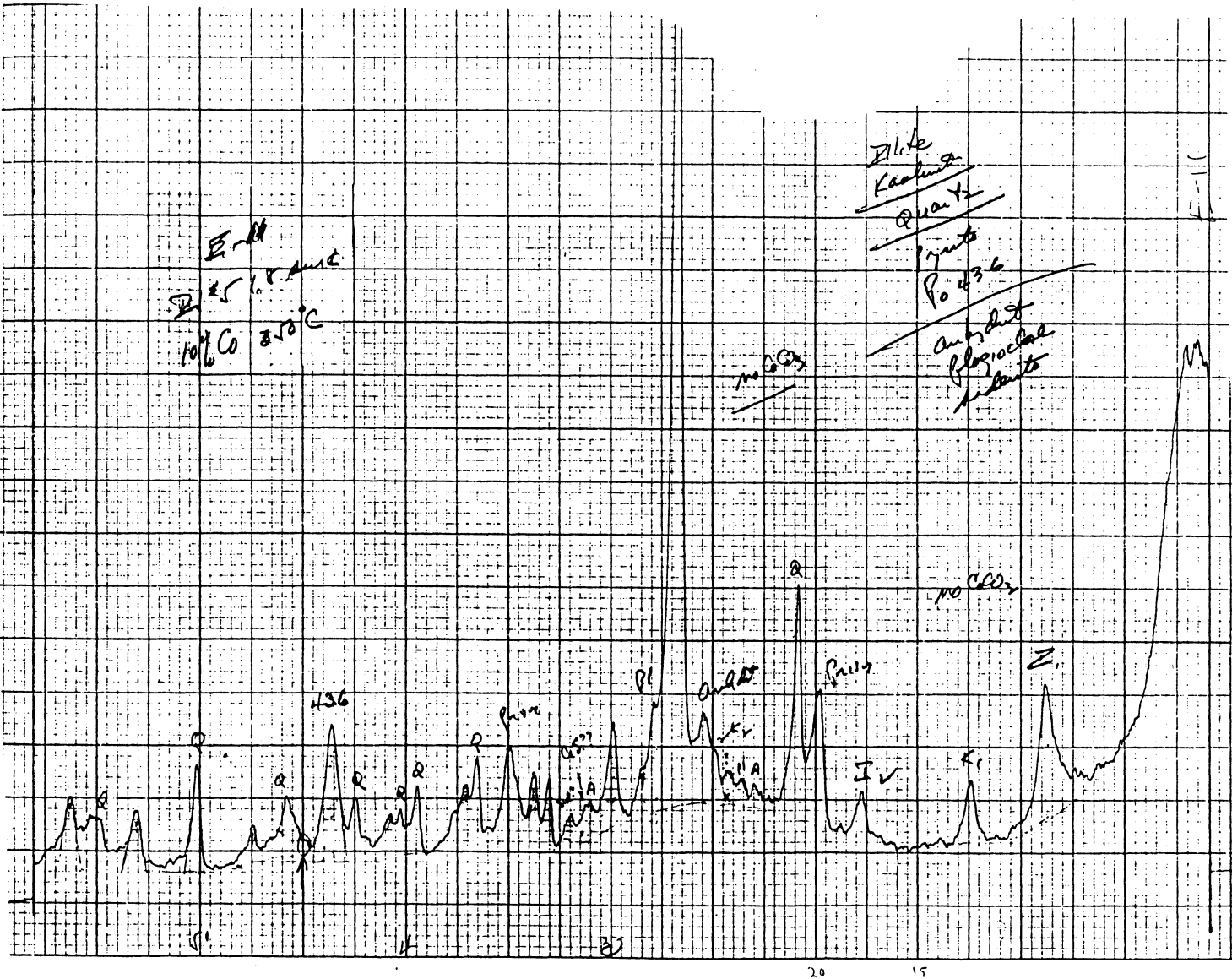
Figure 63: XRD recording for run E-10

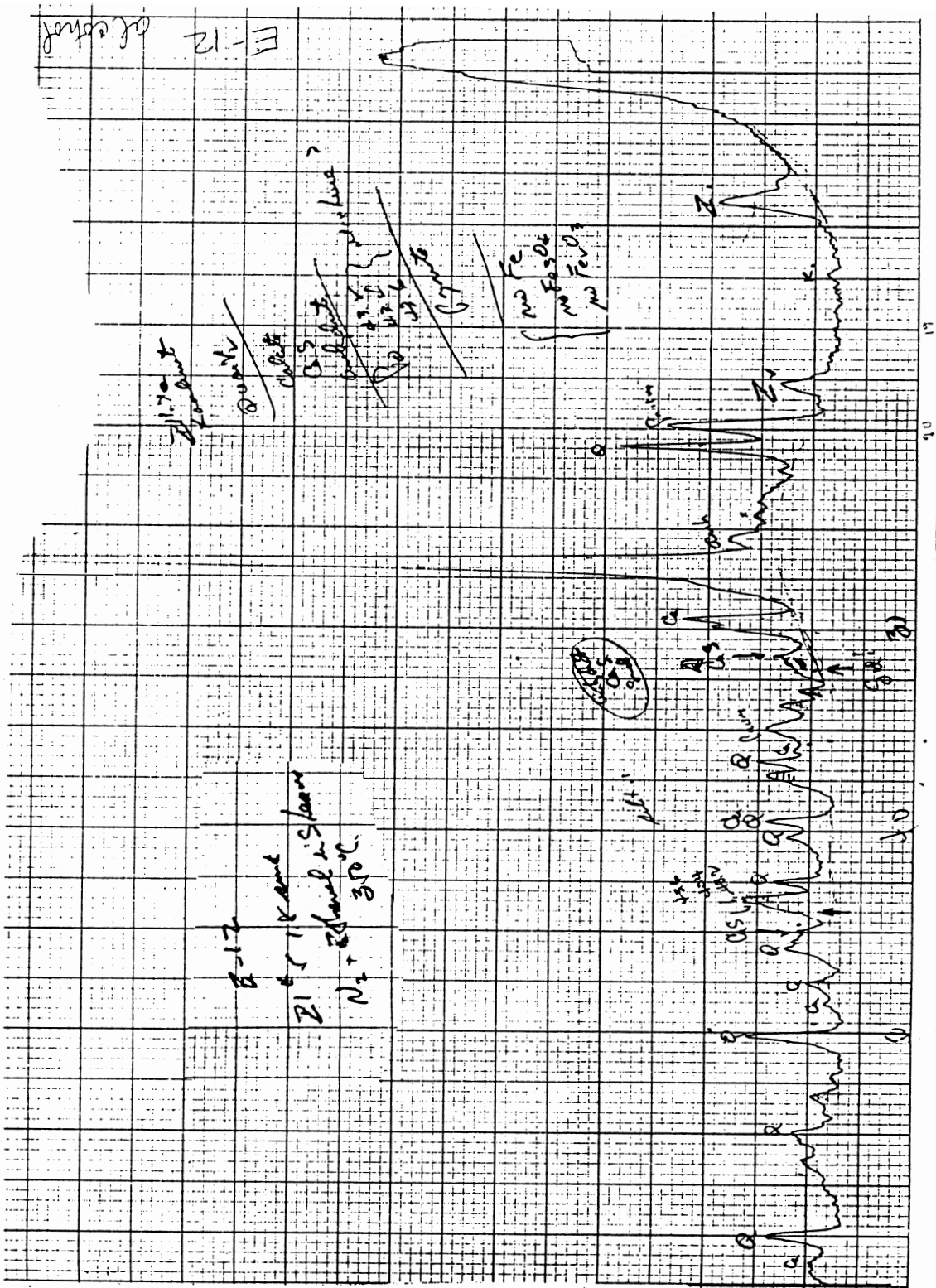Figure 64: XRD recording for run E-11

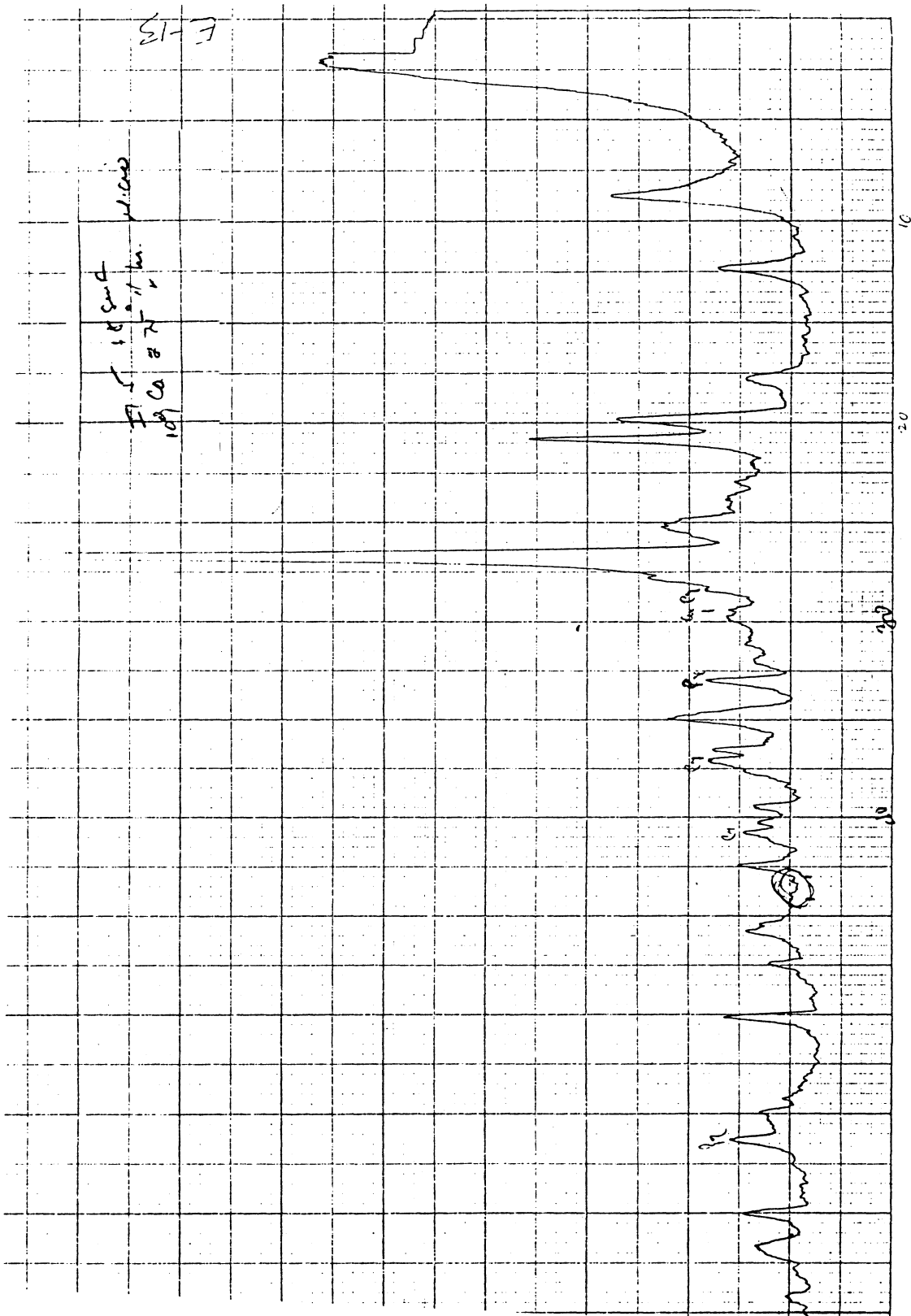Figure 65: XRD recording for run E-12
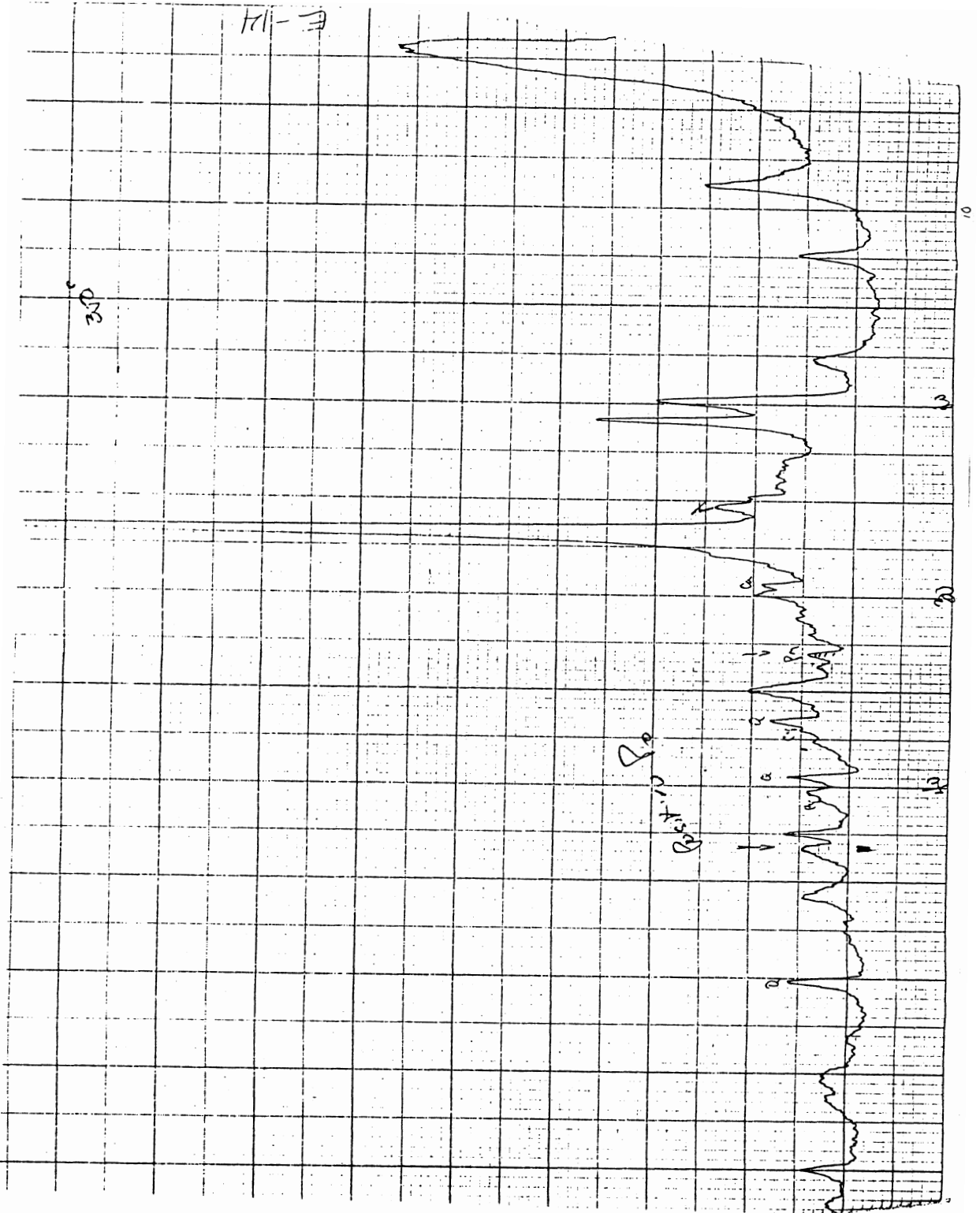
Figure 66: XRD recording for run E-13

Figure 67: XRD recording for run E-14
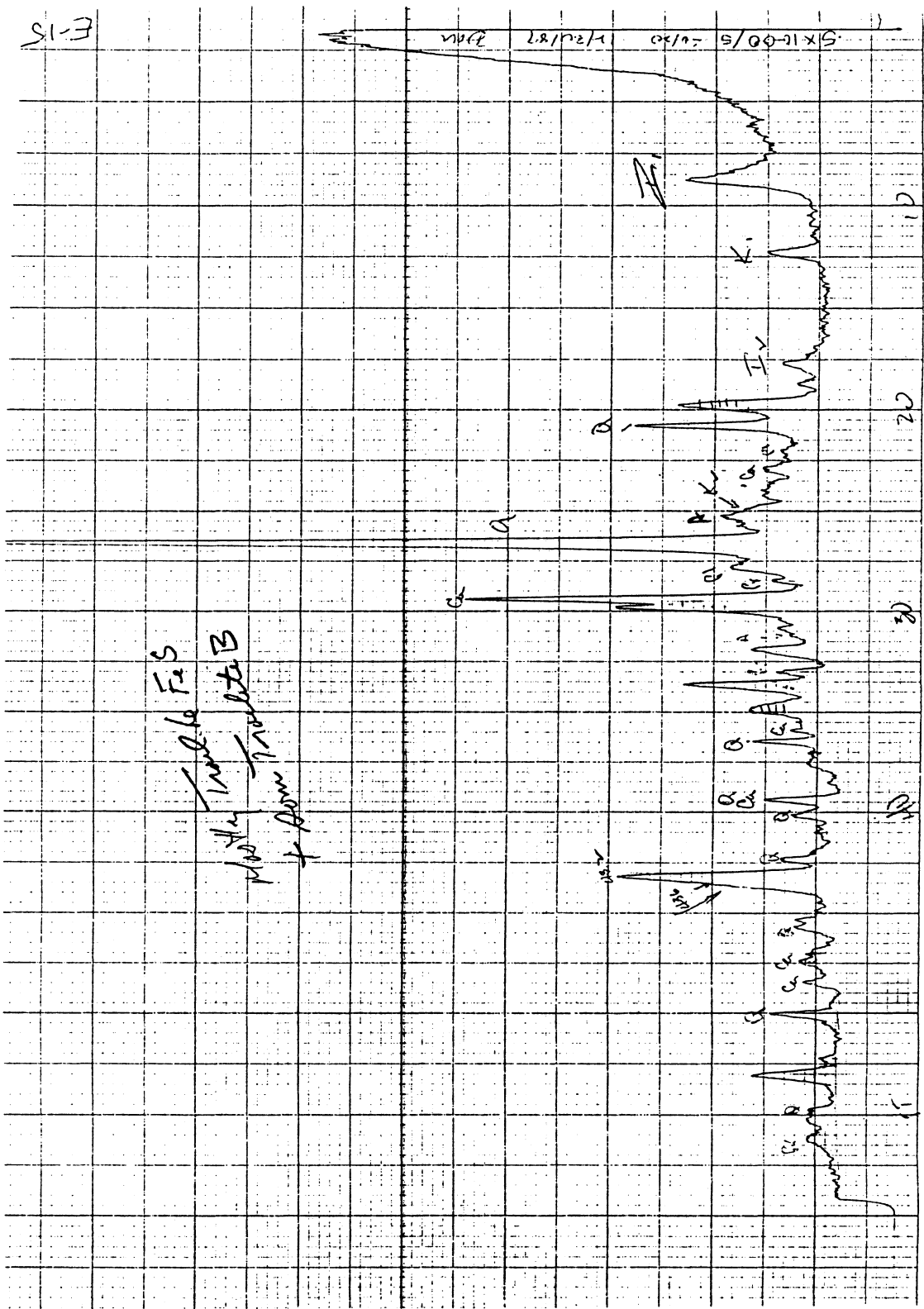
Figure 68: XRD recording for run E-15

Figure 69: XRD recording for run E-2
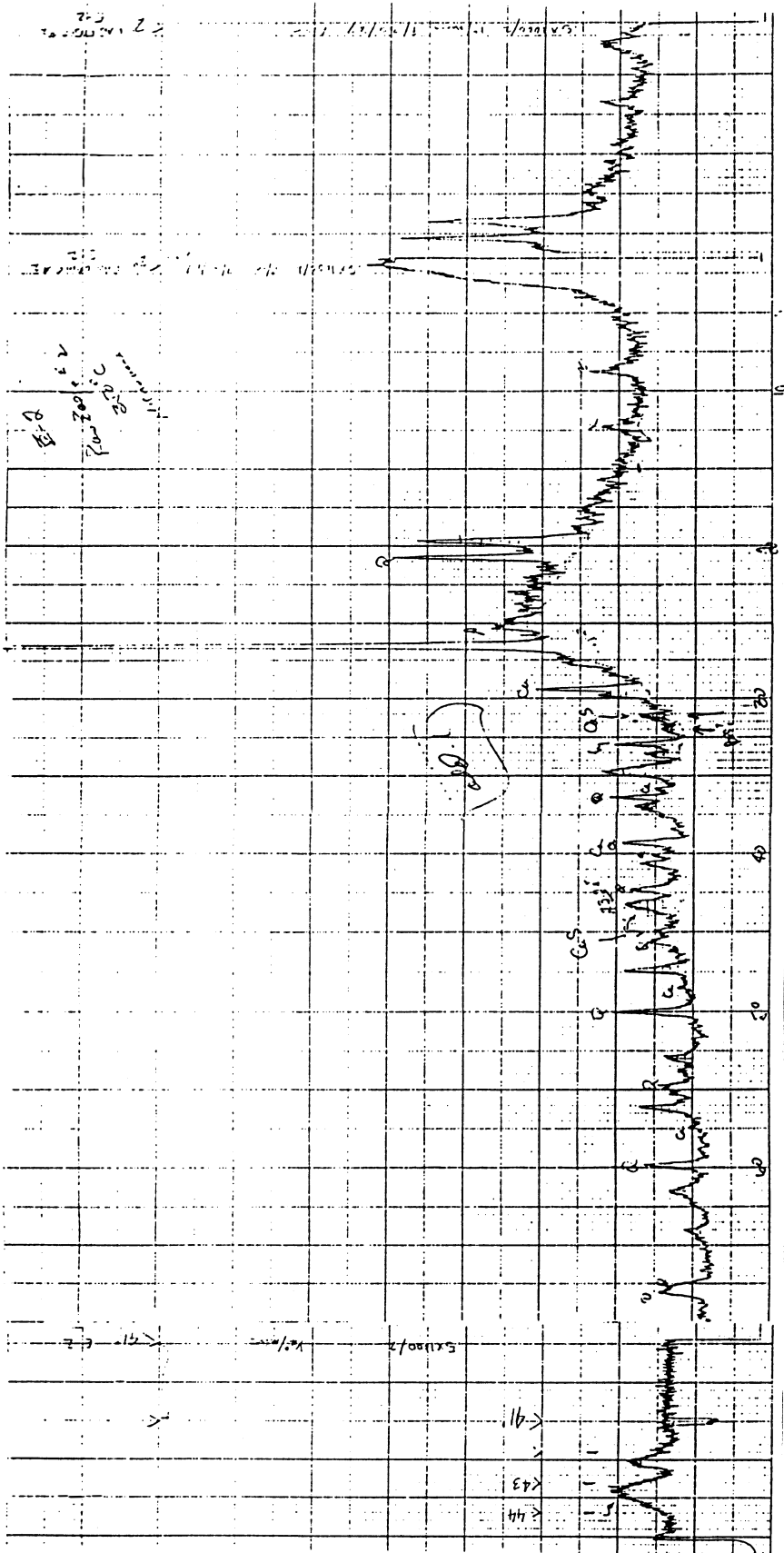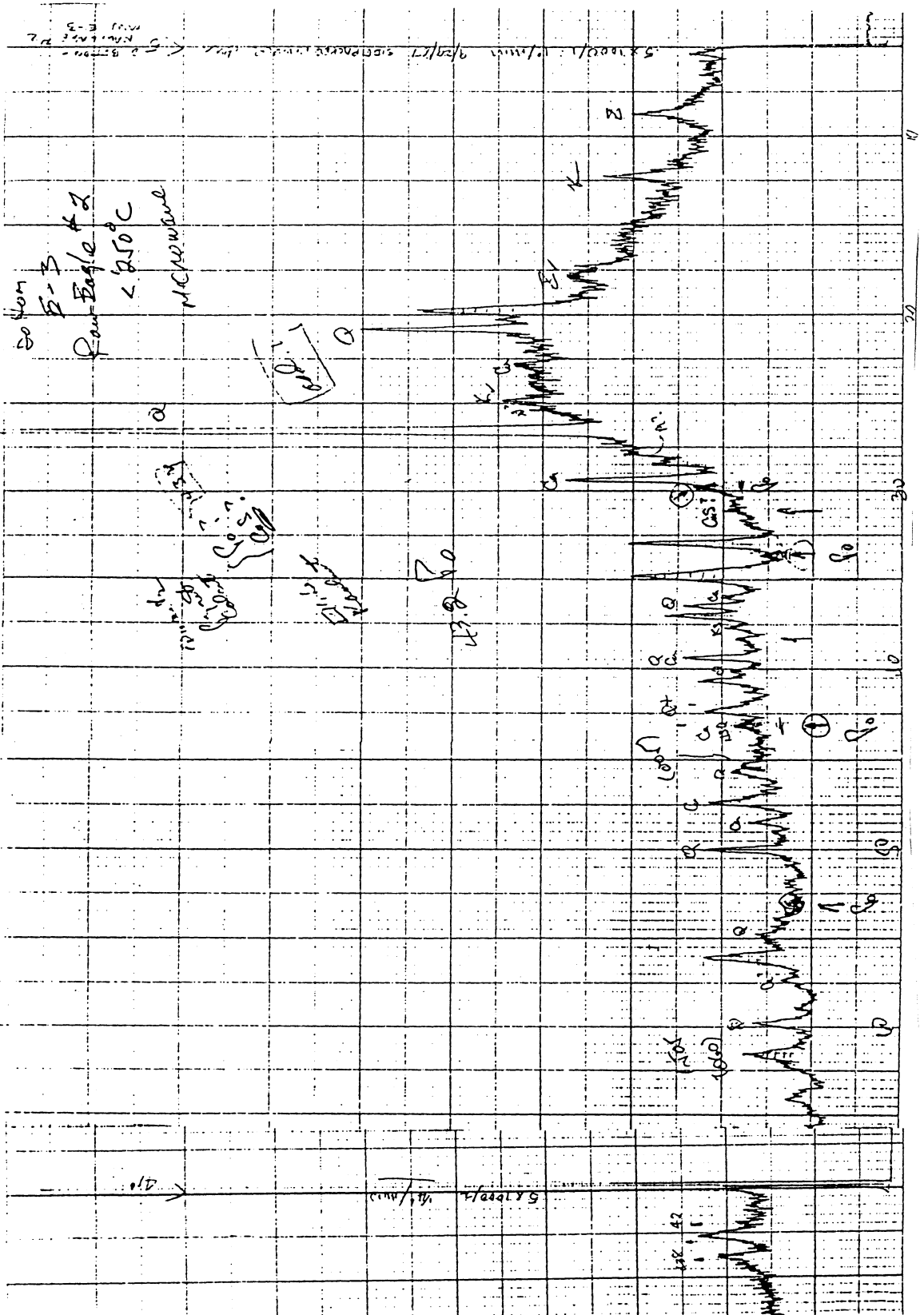
Figure 70: XRD recording for top part of run E-3

-119-

Figure 71: XRD recording for bottom part of run E-3

References

1) Wilfen, C.L. proj. dir. "Energy: Global Prospects 1985-2000";
   McGraw-Hill Book Co. : New York, 1977, Chap. 5, 167.

2) Junk, G.A.; Richard, J.J.; Avery, M.J.; Vick, R.D.;
   Norton, G.A. "Fossil Fuels Utilization: Environmental
   Concerns", 1st. ed.; 1986, Chap. 10, 109.

3) Liu, Y.A. ed. "Physical Cleaning of Coal"; Marcel Dekker,
   Inc. : New York, 1982, Chap. 3, 87.

4) Elsworth, S. "Acid Rain", 1st. ed.; Pluto Press: London,
   1984, 5.

5) Novakov, T.; Chang, S.G.; Harker, A.B. Science, 1974, 186,
   259.

6) Holt Jr., E.C.; Deurbouck, A.W. EPA Report #EPA-600/9-77-017
   Aug.,1977.

7) Attar, A. Fuel, 1978, 57, 201.

8) Majchrowicz, B.B.; Yperman, J.; Reggers, G.; Francois, J.P.;
   Gelan, J.; Martens, H.J.; Mullens, J.; VanPouck, L.L. Fuel
   Processing Tech., 1987, 15, 363.

9) Attar, A.; Corcoran, W.H. Ind. Eng. Chem., Prod. Res. Dev.,
   1977, 16 #2, 168.

10) Spiro, C.L.; Wong, J.; Lytle, F.W.; Greegor, R.B.;
    Maylotte, D.H.; Lamson, S.H. Science, 1984, 226, 48.

11) Khoury, D.L. ed. "Coal Cleaning Technology", 1st. ed.; Noyes
    Data Corp.: New Jersey, 1981, 67.

12) Attia, Y.A. "Fossil Fuels Utilization: Environmental
    Concerns", 1st. ed.: 1986, Chap. 2, 21.

13) Rai, C. "Fossil Fuels Utilization: Environmental Concerns", 1st ed.: 1986, Chap. 8, 86.

14) Shepard, M. EPRI Journal, 1987, Jun., 28.

15) Chandra, D.; Roy, P.; Mishra, A.K.; Chakrabart, J.N.; Sengupta, B. Fuel, 1979, 58, 549.

16) Kolm, H.; Oberteuffel, J.; Kelland, D. Sci. Am., 1975, 223 #5, 46.

17) Trindade, S.C.; Saddy, M.; Monteiro, J.L.F. IEEE Transcripts on Magnetics Mag-12, 1976, 335.

18) Webster, J.R.; Shiley, R.H.; Hughes, R.E.; Lapish, P.L.; Cowin, D.K.; Smith, G.V.; Hinckley, C.C.; Nishizawa, T.; Yoshida, N.; Wiltowski, T.; Wada, Y.; Saporoschenko, M. Proceedings of the Second Annual Pittsburgh Coal Conf., 1985, 138.

19) Webster, J.R.; Shiley, R.H.; Hughes, R.E.; Hinckley, C.C.; Smith, G.V.; Wiltowski, T. Proceedings of the Third Annual Pittsburg Coal Conference, 1986.

20) Webster, J.R.; Shiley, R.H.; Hughes, R.E.; Hinckley, C.C.; Smith, G.V.; Wiltowski, T. Fourth Annual National Conference, Alcohol Fuels, 1986.

21) Smith, G.V.; Hinckley, C.C.; Zahraa, O.; Nishizawa, T.; Saporoschenko, M.; Shiley, R.H. J.Catal., 1982, 78, 262.

22) Shiley, R.H.; Smith, G.V.; Hinckley, C.C.; Saporoschenko, M.; Hughes, R.E. "Desulfurization of Illinois Coal by In-Situ Preparation of Iron Sulfide Catalysts: Part III", final report, Aug., 1987.

23) O'Gorman, J.V.; Walker Jr., P.L. Fuel, 1973, 52, 71.

24) Coates, A.W.; Bright, N.F.H. Can. J. Chem., 1966, 44, 1191.

25) Powell, A.R. J. Ind. Eng. Chem., 1920, 12, 1069.

26) Groves, S.J.; Williamson, J.; Sanyal, A. Fuel, 1987, 66, 461.

27) Nickless, G. ed. "Inorganic Sulfur Chemistry"; Elsevier Publ.

28) Wiltowski, T.; Hinckley, C.C.; Smith, G.V.; Nishizawa, T.;
    Saporoschenko, M.; Shiley, R.H.; Webster, J.R. J. Solid
    State Chem., 1987, 71, 95.
    Co. : New York, 1968, Chap. 19, 715.

29) Morimoto, N.; Nakazawa, H.; Nishiguchi, K.; Tokonami, N.
    Science, 1970, 168, 964.

30) Arnold, R.G.; Reichen, L.E. Am. Mineral., 1962, 47, 105.

31) Tokonami, M.; Nishiguchi, K.; Morimoto, N. Am. Mineral.,
    1972, 57, 1066.

32) Buerger, M.J. Trans. Amer. Crystall. Assoc., 1971, 7, 1.

33) Donnay, J.D.H.; Kullerud, G.; Donnay, G. Trans. Amer.
    Crystall. Assoc., 1971, 7, 69.

34) Gruner, J.W. Amer. Mineral. 1929, 14, 227.

35) Bluhm, D.D.; Fanslow, G.E.; Beck-Montgomery, S.R. "Selective
    Magnetic Enhancement of Pyrite in Coal by Dielectric
    Heating", Report #IS-4766, Dec., 1982.

36) Vaughan, D.J.; Craig, J.R. "Mineral Chemistry of Metal
    Sulfides"; Cambridge Univ. Press : New York, 1978,
    Chap. 3, 93.

37) Giuntini, J.-C.; Zanchetta, J.-V.; Diaby, S. Fuel, 1987, 66,
    179.

38) Sproull, R.L.; Phillips, W.A. "Modern Physics, the quantum physics of atoms, solids, and nuclei", 3rd. ed.; John Wiley and Sons, Inc.: Toronto, 1980, 348.

39) Jacobs, I.S.; Zavitsanos, P.D.; Golden, J.A. J. Appl. Phys., 1987, 53(3), 2730.

40) Zavitsanos, P.D.; Golden, J.A.; Bleiler, K.W.; Jacobs, I.S. "Coal Desulfurization by a Microwave Process", Report # DOE/PC/30142-T1 through T7, Mar., 1981 to Mar., 1983.

41) Butts, J.R.; Lewis, J.E.; Steward, F.R. J. Microwave Power, 1983, 18(1), 37.

42) Briggs, W.E.; Lewis, J.E.; Tranquilla, J.M. J. Microwave Power, 1983, 18(1), 75.

43) Thorpe, A.N.; Senftle, F.E.; Alexander, C.; Dulong, F.T.; LaCount, R.B.; Friedman, S. Fuel, 1987, 66, 147.

44) Hughes, R.E. personal conference Dec. 23, 1987.

45) Prewitt, C.T.; Rajamani, V. "Sulfide Mineralogy, vol. 1"; Southern Printing Co.: Blacksburg, 1974, PR-1.

Daniel Cleaveland

Permanent Address

56 Hawthorne Road

Rock Island, Illinois 61201

(309) 788-1419

EDUCATION

M.S., March 1988, Eastern Illinois University,

Charleston,Illinois

Chemistry

Thesis: Coal Desulfurization using Pyrite Transformation through
         Microwave Heating

Areas of Interest: Physical, Spectroscopic, Instrumental

Post B.A., University of Iowa, Iowa City, Iowa, 1983-1985

Concentration: Chemistry

Post B.A., Augustana College, Rock Island, Illinois, 1982-1983

Concentration: Chemistry, Physics

B.A., May 1982, Knox College, Galesburg, Illinois

Physics

EXPERIENCE

Consultant for Illinois State Geological Survey (1987-1988).

Upgrading coal desulfurization process through use of dielectric

heating.

Resident Student Adviser (Summer 1986). Chemical Technology
Division, Argonne National Laboratory, Argonne, Illinois.
Experimentation in microwave assisted waste disposal.

PUBLICATIONS

Microwave-Assisted Chemical Process for Treatment of Hazardous
Waste, Annual Report, DOE/HWP-28

Oxidative Degradation of Trichloroethylene Adsorbed on Active
Carbons: Use of Microwave Energy", Environmental Science and
Technology, publication pending